

**REPUBLIC OF INDONESIA**  
**REPORT ON GEOLOGICAL SURVEY**  
**OF**  
**WEST KALIMANTAN**

PHASE III

JICA LIBRARY



1034432(3)

JANUARY 1982

**METAL MINING AGENCY OF JAPAN**  
**JAPAN INTERNATIONAL COOPERATION AGENCY**

14227

108

66.1

MPN

国際協力事業団	
船 84.9.13	108.
登録No. 09541	66.1
	MPN

## PREFACE

The Government of Japan, in response to a request extended by the Government of the Republic of Indonesia, agreed to conduct a metallic mineral exploration survey in West Kalimantan, and commissioned its implementation to the Japan International Cooperation Agency.

The Agency, taking into consideration the importance of the technical nature of this survey, sought the cooperation of the Metal Mining Agency of Japan in order to accomplish the proposed task.

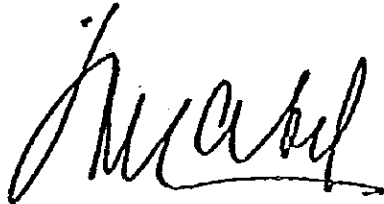
The Government of the Republic of Indonesia appointed the Directorate of Mineral Resources to execute the survey as the counterpart to the Japanese team. The survey is being carried out jointly by experts from both countries.

This year's work was the third phase of the program consisting of detailed geological survey, detailed geochemical survey and geophysical survey for metallic mineral exploration, based on the results of the prior phases.

This report hereby summarizes the results of the third phase of the survey, and will also form a portion of the final report that will be prepared with regard to the overall results.

We wish to take this opportunity to express our gratitude to all sides concerned in the execution of this survey.

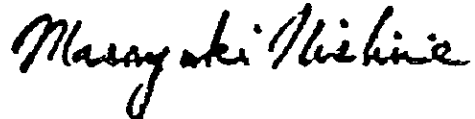
January, 1982.



**Prof. Dr. J.A. KATILI**  
Director General,  
Directorate General of Mines,  
Ministry of Mines and Energy,  
Republic of Indonesia.



**Kelsuke ARITA**  
President,  
Japan International  
Cooperation Agency,  
Japan.



**Masayuki NISHIE**  
President  
Metal Mining Agency of Japan,  
Japan.

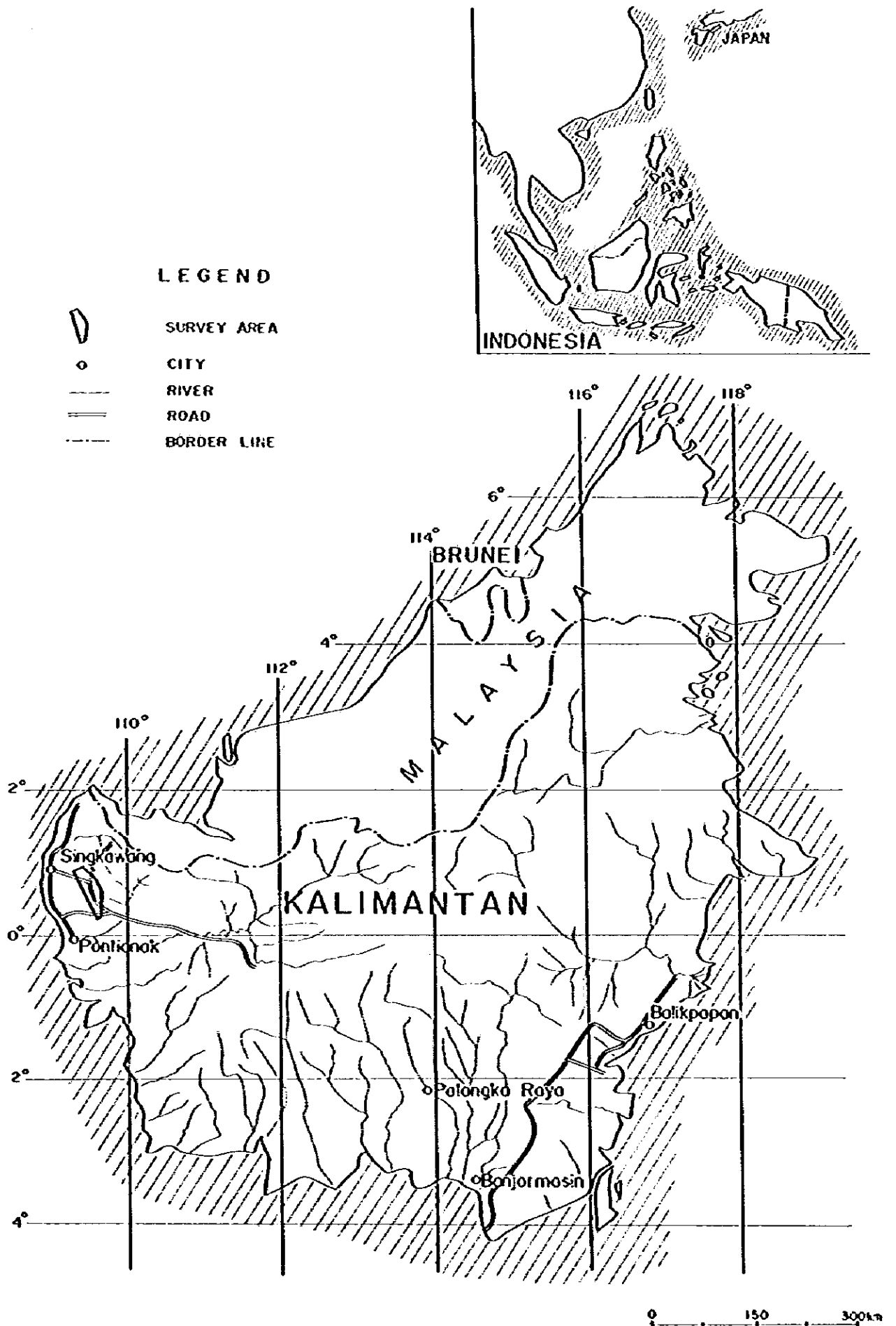


Fig 1-1 Location Map of Survey Area

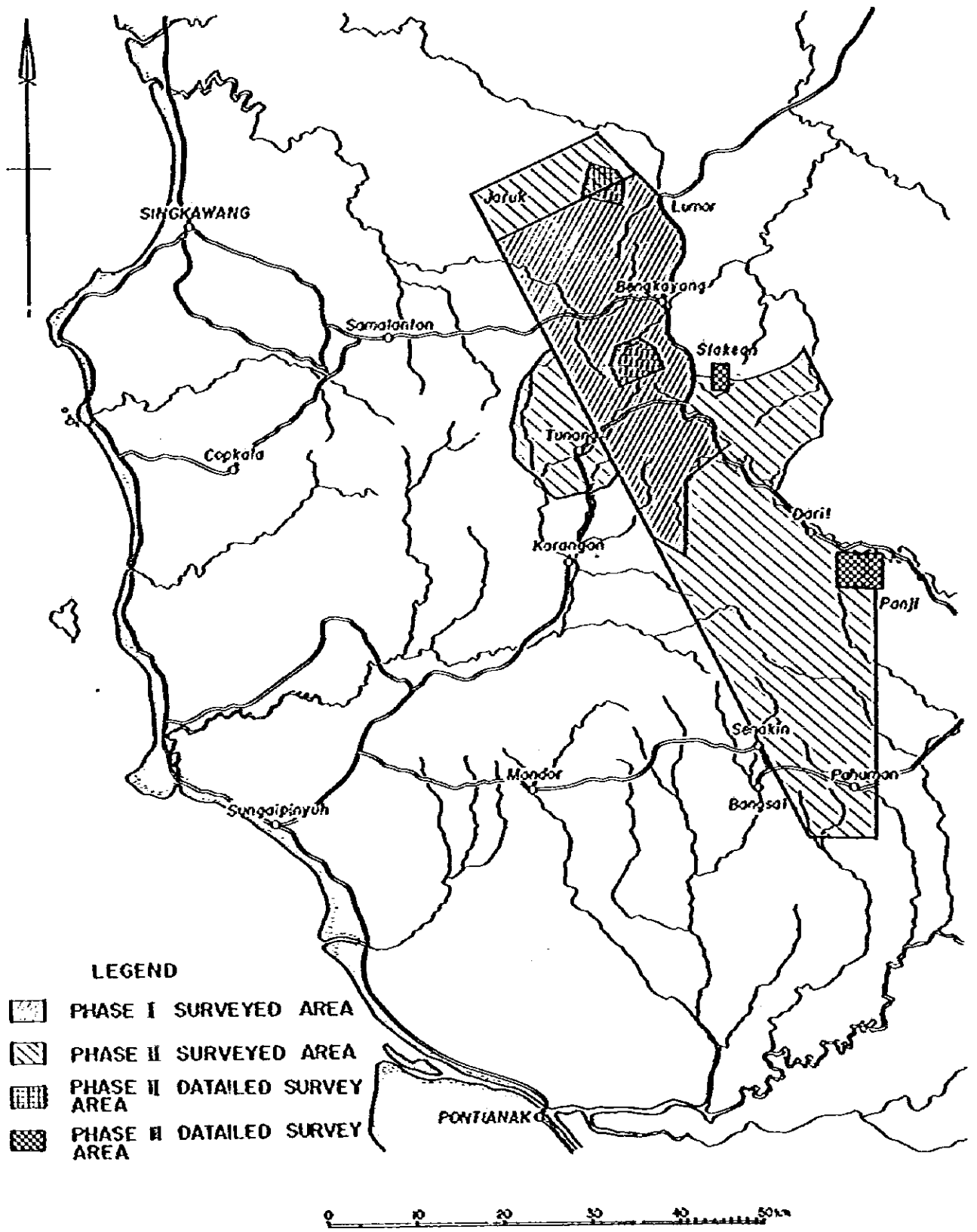


Fig 1-2 Map of Survey Area

## TABLE OF CONTENTS

	Page
PREFACE	
LOCATION MAP OF SURVEY AREA	
TABLE OF CONTENTS	
ABSTRACT	
PART I INTRODUCTION	
CHAPTER 1 DEVELOPMENT AFFAIR AND PURPOSE OF SURVEY .....	1
CHAPTER 2 OUTLINE OF THIRD PHASE INVESTIGATION .....	2
2-1 Detailed Geological and Geochemical Survey .....	2
2-1-1 Survey Purpose .....	2
2-1-2 Survey Area .....	2
2-1-3 Method and Amount of Survey .....	3
2-2 Geophysical Survey .....	4
2-2-1 Survey Purpose and Survey Area .....	4
2-2-2 Method and Amount of Survey .....	4
2-3 Survey Team and Schedule .....	5
2-3-1 Survey Schedule in Indonesia .....	5
2-3-2 Survey Team .....	5
CHAPTER 3 OUTLINE OF SURVEY AREA .....	6
3-1 location and Accessibility .....	6
3-2 Circumstances of Survey Area .....	8

## PART II GENERAL DISCUSSION AND CONCLUSIONS

CHAPTER 1 GENERAL DISCUSSION .....	9
1-1 Geological Location of Mineralization .....	9
1-2 Relationship among Geological Structures, Igneous Activities and Mineralizations .....	10
1-3 Relationship between Geochemical Survey Result and Mineralized Zones .....	11
1-4 Relationship between Geophysical Survey (IP Survey) Result and Mineralized Zone .....	12
1-5 General Discussions .....	12
CHAPTER 2 CONCLUSIONS AND FUTURE PROGRAM .....	13
2-1 Conclusions .....	13
2-2 Recommendation for Future Study .....	15

## PART III GEOLOGICAL AND GEOCHEMICAL SURVEYS

CHAPTER 1 GEOLOGICAL OUTLINE OF SURVEY AREA .....	16
1-1 Geology .....	16
1-1-1 Mesozoic Sedimentary, Volcanic and Pyroclastic Rocks .....	16
1-1-2 Mesozoic Cretaceous Granitic Rocks .....	16
1-1-3 Tertiary Dacite and Dacitic Pyroclastic Rocks.....	17
1-1-4 Tertiary Tonalite .....	17
1-2 Mineralization .....	17



	Page
CHAPTER 2 DETAILED SURVEY IN SELAKEAN AREA .....	18
2-1 Outline of Geology .....	18
2-2 Stratigraphy and Igneous Rocks .....	18
2-2-1 Jirak Andesite and Andesitic Tuff Formation .....	18
2-2-2 G. Raya Granodiorite .....	19
2-3 Geological Structure .....	20
2-4 Mineralization .....	20
2-4-1 Outline of Mineralization .....	20
2-4-2 Descriptions on Mineralizations .....	20
2-5 Geochemical Survey .....	22
2-5-1 Sampling .....	22
2-5-2 Statistical Data Processing of Analytical Data .....	23
2-5-3 Anomalous Areas .....	24
2-6 Characteristics of Selakean Mineralization .....	24
CHAPTER 3 PANJI AREA .....	25
3-1 Outline of Geology .....	25
3-2 Stratigraphy and Igneous Rocks .....	25
3-2-1 Belango Dacitic and (Quartz) Andesitic Tuff .....	25
3-2-2 G. Sebiawak Granodiorite .....	27
3-2-3 Other Igneous Rocks .....	28
3-2-4 Quaternary .....	29
3-3 Geological Structure .....	29
3-4 Mineralization .....	29

	Page
3-4-1 Outline of Mineralization .....	29
3-4-2 Descriptions on Mineralizations .....	30
3-4-3 Argillization Zone .....	33
3-5 Geochemical Survey .....	34
3-5-1 Sampling and the Number of Samples Collected .....	34
3-5-2 Statistical Processing and Interpretation of Analytical Data .....	34
3-5-3 Anomalous Areas .....	35
3-6 Characteristics of Panji Mineralization .....	36
CHAPTER 4 AGE DATING OF G. IBU GRANITIC ROCKS .....	37
4-1 G. Ibu Granitic Rocks .....	37
4-2 Chemical Compositions and Age of G. Ibu Granitic Rocks .....	38

#### PART IV GEOPHYSICAL SURVEY (IP METHOD)

CHAPTER 1 OUTLINE OF GEOPHYSICAL SURVEY .....	40
CHAPTER 2 IP METHOD .....	41
2-1 General .....	41
2-1-1 Principles of Measurement .....	41
2-1-2 Dipole-Dipole Method of Operation .....	41
2-1-3 IP Characteristics .....	42
2-2 Data Representation .....	44
2-2-1 Plotting of Results .....	44
2-2-2 Data Processing .....	44
2-2-3 Physical Properties of Rock Specimen .....	45
2-3 Method of Field Data Analyses .....	46

	Page
2-3-1 Qualitative Analyses .....	46
2-3-2 Quantitative Analyses .....	46
2-4 Instruments .....	47
2-4-1 Instruments Used for Geophysical Survey .....	47
2-4-2 Rock Specimen Testing Instrument .....	48
<b>CHAPTER 3 SURVEY RESULTS .....</b>	<b>48</b>
3-1 Results of Rock Specimen Tests .....	48
3-2 Results of IP Measurements .....	50
3-2-1 Plotted Maps .....	50
3-2-2 Statistical Conclusions .....	51
3-2-3 IP Anomalies .....	53
3-3 Simulation .....	55
3-3-1 Line C Models .....	56
3-3-2 Line J Models .....	58
3-4 Discussion .....	61
3-4-1 IP Properties of Rock .....	61
3-4-2 IP Results .....	62
3-4-3 Distribution of Anomalies .....	63
3-4-4 Consideration of Mineralization .....	63

## LIST OF FIGURES

- Fig. 1-1 Location Map of Survey Area
- Fig. 1-2 Map of Survey Area
- Fig. 3-1 Geological Map of West Kalimantan Project Area
- Fig. 3-2 Generalized Stratigraph of Survey Area
- Fig. 3-3 Schematic Geological Profile (Selakean Area)
- Fig. 3-4 Relationship of Two Fissures with Ore Mineral (Selakean Area)
- Fig. 3-5 Joint System in Jirak Formation (Selakean Area)
- Fig. 3-6 Location Map of Mineralization (Selakean Area)
- Fig. 3-7 Sketch Map of Selakean Ore Deposit (Selakean Area)
- Fig. 3-8 Sketch Map of Empawang Mineralization (Selakean Area)
- Fig. 3-9 Sketch Map of Entagak Mineralization (Selakean)
- Fig. 3-10 Histogram for Cu of Geochemical Analysis in Selakean Area
- Fig. 3-11 Histogram for Pb of Geochemical Analysis in Selakean Area
- Fig. 3-12 Cumulative Frequency Distribution for Cu and Pb of Geochemical Analysis in Selakean Area
- Fig. 3-13 Correlation of Geochemical Elements (Cu and Pb) in Selakean Area
- Fig. 3-14 Schematic Geological Profile (Panji Area)
- Fig. 3-15 Normative Q - Pl (Ab+An) - Or Diagram of Granitic Rocks in Project Area
- Fig. 3-16 Variation Diagram of Granitic Rocks in Project Area
- Fig. 3-17 Location Map of Mineralization and Geochemical Anomalies (Panji Area)
- Fig. 3-18 Sketch Map of Mineralization (East of Meraupaku) (Panji Area)
- Fig. 3-19 Sketch Map of Mineralization at West of S. Jenaham and S. Pitunan (Panji Area)
- Fig. 3-20 Histogram for Cu of Geochemical Analysis in Panji Area
- Fig. 3-21 Histogram for Mo of Geochemical Analysis in Panji Area
- Fig. 3-22 Cumulative Frequency Distribution for Cu and Mo of Geochemical Analysis in Panji Area
- Fig. 3-23 Correlation of Geochemical Elements (Cu and Mo) in Panji Area
- Fig. 3-24 Geological Map of G. Ibu Area
- Fig. 3-25 Absolute Age of Granitic Rocks in West Indonesia
- Fig. 3-26 Absolute Age of Granitic Rocks in West Kalimantan
- Fig. 3-27 Modal Qz - Pl - Kf1 Diagram of Granitic Rocks in G. Ibu Area

- Fig. 3-28 Modal Qz - Pl - Kf1 Diagram of Granitic Rocks in Project Area
- Fig. 4-1 IP Measurements of Dipole-dipole Configuration
- Fig. 4-2 Illustration of IP Measurements
- Fig. 4-3 Block Diagram of the Laboratory Measuring Apparatus
- Fig. 4-4 Flow Chart of IP Data Processing and Interpretation
- Fig. 4-5 FE-resistivity Correlation Diagram of Rock Samples
- Fig. 4-6 FE-pyrite Correlation Diagram of Rock Samples
- Fig. 4-7 Histograms of FE and AR
- Fig. 4-8 Cumulative Frequency Distributions of FE, AR and MF
- Fig. 4-9 Ranges and Mean Values of FE and AR
- Fig. 4-10 FE-AR Correlation Diagrams of IP Measurements
- Fig. 4-11 IP Pseudo-sections and Simulated Models for Line C
- Fig. 4-12 IP Pseudo-sections and Simulated Models for Line J
- Fig. 4-13 Results of Quantitative Analysis of IP Anomalies
- Fig. 4-14 Bird's-eye View of FE Values for n=1

#### LIST OF TABLES

- Table 3-1 List of Mineralized Zone and Chemical Analysis of Ore
- Table 3-2 Value of Mean Standard Deviation and Threshold in Selakean Area
- Table 3-3 Result of K - Ar Age Determination
- Table 3-4 Chemical Composition and Norm of Constitution Mineral of Granitic Rocks in Project Area
- Table 3-5 Value of Mean Standard Deviation and Threshold in Panji Area
- Table 3-6 Stratigraphic Correlation of West Kalimantan
- Table 4-1 Results of Rock Sample Tests
- Table 4-2 Ranges and Mean Values of IP Measurements
- Table 4-3 Correlation Coefficients between IP Measurements and Topography

#### LIST OF PLATES

- PL 3-1 Geological Map and Geological Profile of Detailed Survey Area (Selakean) (1/10,000)
- PL 3-2 Map of Relation between Geological Structure and Mineralization (Selakean) (1/10,000)
- PL 3-3 Contour Map of Geochemical Assay Value (Cu and Pb) in Selakean (1/10,000)
- PL 3-4 Location Map of Geochemical Samples (Selakean) (1/10,000)
- PL 3-5 Location Map of Rocks and Ore Samples Tested (Selakean) (1/10,000)
- PL 3-6 Geological Map and Geological Profile of Detailed Survey Area (Panji) (1/10,000)
- PL 3-7 Map of Relation between Geological Structure and Mineralization (Panji) (1/10,000)
- PL 3-8 Contour Map of Geochemical Assay Value (Cu and Mo) in Panji (1/10,000)
- PL 3-9 Location Map of Geochemical Samples (Panji) (1/10,000)
- PL 3-10 Location Map of Rocks and Ore Samples Tested (Panji) (1/10,000)
- PL 4-1 IP Lines and Locations of Rock Samples (1/10,000)
- PL 4-2 IP pseudo-sections Line A (1/5,000)
- PL 4-3 IP pseudo-sections Line B (1/5,000)
- PL 4-4 IP pseudo-sections Line C (1/5,000)
- PL 4-5 IP pseudo-sections Line D (1/5,000)
- PL 4-6 IP pseudo-sections Line E (1/5,000)
- PL 4-7 IP pseudo-sections Line F (1/5,000)
- PL 4-8 IP pseudo-sections Line G (1/5,000)
- PL 4-9 IP pseudo-sections Line H (1/5,000)
- PL 4-10 IP pseudo-sections Line I (1/5,000)
- PL 4-11 IP pseudo-sections Line J (1/5,000)
- PL 4-12 IP Plan Map Frequency Effect  $n=1$  (1/5,000)
- PL 4-13 IP Plan Map Frequency Effect  $n=3$  (1/5,000)
- PL 4-14 IP Plan Map Apparent Resistivity  $n=1$  (1/5,000)
- PL 4-15 IP Plan Map Apparent Resistivity  $n=3$  (1/5,000)
- PL 4-16 IP Plan Map Metal Factor  $n=1$  (1/5,000)
- PL 4-17 IP Plan Map Metal Factor  $n=3$  (1/5,000)
- PL 4-18 Map of Relations between Geological-geochemical Results and IP Results (1/10,000)

## **LIST OF APPENDICES**

- Appendix 1 List of Rock and Ore Sample Tested**
- Appendix 2 Microscopic Observation of Thin Section**
- Appendix 3 Microscopic Observation of Polished Specimen**
- Appendix 4 Microscopic Photographs of Thin Section**
- Appendix 5 Microscopic Photographs of Polished Specimen**
- Appendix 6 Chart and List of X Ray Diffractive Analysis of Clay Mineral**
- Appendix 7 Assay Result of Geochemical Samples**

#### REFERENCES (GEOLOGICAL AND GEOCHEMICAL SURVEY)

1. Aramaki S. et al (1972); Chemical Composition of Japanese Granites Part 2 Variation Trends and Average Composition. Jour. Geol. Soc. of Japan Vol. 78, No. 1, p. 39-49
2. Beemelen, R.W. Van (1949); The Geology of Indonesia. The Hague Netherland Gov. Printing Office.
3. Ben-Avraham, Z. (1978); The Evolution of Marginal Basin and Adjacent Shelves in East and South Asia Tectonophysics 45, 269-288
4. Direktorat Geologi (1970); Peta Geologi, Kalimantan Barat-Daja, 1:500,000.
5. Easton N.W. (1904); Geogische Uebersichtskarte Eines Teiles West-Borneo Jaab Hijn. Wetenschappelijke Gedelte, 509
6. Haile, N.S. (1968); Geosynclinal Theory and Organizational Pattern of the Northwest Borneo Geosyncline Quarterly Journal Geol. Soc, London 124 : 171-195
7. Haile N.S. McElhinny M.W., McDougall Ian (1977); Paleomagnetic Data and Radiometric Ages from the Cretaceous of West Kalimantan (Borneo) and Their Significance in Interpreting Regional Structure; Geological Society of London Quar. Jour. v. 133, 133-144
8. Hamilton W, (1978) Tectonic Map of the Indonesian Region United State Geological Survey
9. Hamilton W, (1978); Tectonics of the Indonesian Region USGS Prof. Paper 1078
10. Hutchison C.S. (1973); Tectonic Evolution of Sundaland: A Phanerozoic Synthesis Geol. Soc. Malaysia, Bulletin 6, July pp. 61-86
11. Hutchison C.S. (1975); Ophiolite in South Asia Bulletin of Geological Society of America, v. 86, 797-806
12. Ishihara, S. (1977); The Magnetite-series and Ilmenite-series Granitic Rocks, Mining Geology 27 number 145 293-305
13. Ishihara, S. et al (1980); Grainites and Sn-W Deposites of Peninsular Thailand, Mining Geology Special Issue No. 8
14. IUGS (1973); Plutonic Rocks, Classification and Nomenclature Recommended by the IUGS, Subcommittee on the Systematics of Igneous Rocks. Geotimes Oct. 1973



15. Katili, J.A. (1973); Geochronology of West Indonesia and its Implication on Late Tectonics  
Tectonophysics 19, 195-212
16. Katili J.A. (1973); Plate Tectonics and its Significance in the Search Mineral Deposits in Western Indonesia  
CCOP Technical Bulletin Volume 7
17. Katili J.A. (1981); Geology of South Asia with Particular Reference to the South China Sea  
Bull. of the Geological Research and Development Center of Indonesia No. 4 March 1981 1-12
18. Prime, H.N.A. et al (1975); Isotope Geochronology in the Indonesian Tin Belt  
Geol. Mijnbouw 54, 61-70
19. Pupilli M. (1973); Geological Evolution of South China Sea Area Tentative Reconstruction from Borderland Geology and Well Data Proceeding. Indonesian Petroleum Association, Second Annual Convention.
20. Rocksalagora, W. and Djumhani (1971); Metallic Mineral Deposits of Indonesia, XII Pacific Science Congress
21. Sato, T. (1967); Historical Geology (Jurassic) in Japanese, Asakura Shoten (Japanese)
22. Taylor D. and Hutchison C.C. (1978); Pattern of Mineralization in South Asia. Their Relationship to Broad Scale Geological Features and the Relevance of Plate Tectonics Concepts to their Understanding.  
Eleventh Commonwealth Mining and Metallurgical Congress.
23. Toton Suhanda Draft of final report on G. Ibu, West Kalimantan (CTA-19) Directorate of Mineral Resources Indonesia
24. Zeylan Van Eemichoven C.P.A. (1938); The Geology of the Central and Eastern of the Western Division of Borneo  
Jaarb. Mijn Ned-Indie 8-186

#### REFERENCES (GEOPHYSICAL SURVEY)

1. Hallof, P.G. (1967); The Use of Induced Polarization Measurements to Locate Massive Sulphide Mineralization in Environments in which EM Methods Fail, Mining and Groundwater Geophysics (edited by L.W. Morley), Economic Geology Report 26, Geological Survey of Canada, pp. 302-309
2. Katsube, T.J. (1977); Electrical Properties of Rocks, Induced Polarization for Exploration Geologists and Geophysicists, The University of Arizona, March 14-16, 1977
3. Madden, T.R. and Cantwell, T. (1967); Induced Polarization, a Review, Mining Geophysics, Vol. II, pp. 373-400
4. Pelton, W.H. (1977); Variable Frequency IP Case Histories 1955-1977 Dipole-dipole Pseudo-sections, Induced Polarization for Exploration Geologists and Geophysicists, The University of Arizona, March 14-16, 1977
5. Seigel, H.O. (1967); The Induced Polarization Method, Mining and Groundwater Geophysics (edited by L.W. Morley), Economic Report 26, Geological Survey of Canada, pp. 123-137
6. Sumner, J.S. (1976); Principles of Induced Polarization of Geophysical Exploration, Elsevier Scientific Publication Co., N.Y.
7. Sumner, J.S. (1979); The Induced-polarization Exploration Method, Geophysics and Geochemistry in Search for Metallic Ores (edited by Peter J. Hood), Economic Geology Report 31, Geological Survey of Canada, pp. 123-133

## ABSTRACT

The third phase detailed survey was conducted to cover 6 km<sup>2</sup> in Selakean area and 20 km<sup>2</sup> in Panji area which had been selected as promising mineralized areas in the second reconnaissance survey, consisting of the geological survey, geochemical survey with soil sampling and geophysical survey (IP Survey conducted in eastern Panji area), in order to attempt an elucidation on the existent condition, scale and grade of mineralizations in these two areas.

Selakean Mineralization is a gold bearing chalcopyrite-sphalerite-arsenopyrite ore deposit filled in a fissure which is considered to have been caused by the tectonic movement by the intrusion of G. Raya granodiorite, and it is a mesothermal ore deposit where exsolution dots of chalcopyrite in sphalerite are recognized. In the geochemical survey with soil sampling, the distribution range of copper anomaly overlaps the mineralized zone, while lead anomalous area is distributed somewhat apart.

In the main mineralized zone of Panji Mineralization, chalcopyrite and covellite disseminations are found, accompanying tourmaline. Pyrite dissemination is distributed outside these dissemination, resembling Banyu Mineralization which was surveyed in the second phase survey. In the geochemical survey, copper and molybdenum anomalous areas were found in the center (1.5 km EW and 2.0 km NS) of this mineralized zone. Also, in the geophysical survey (IP Survey), anomalies were found duplicated in these geochemical survey anomalous areas. The mineralizations are embedded in G. Seblawak granodiorite, which is 124 m.y. under the K-Ar absolute age dating, intruding in the Early Cretaceous period. Distribution of younger igneous rocks has not been confirmed in the geological survey as in Banyu Mineralization. However, younger igneous rocks are considered to exist and caused mineralizations.

G. Raya granodiorite and Sijanguk quartz diorite accompanying the copper and molybdenite mineralizations in G. Ibu area are both confirmed to be 30 m.y. under the K-Ar absolute age dating, and intruded in the Tertiary

Oligocene in age. It was confirmed again in the survey of this phase that copper, molybdenum, gold, mercury and antimony mineralizations distributed in West Kalimantan have been caused by younger igneous activities in the Early Tertiary to Middle Tertiary period.

## **PART I**

### **INTRODUCTION**

## CHAPTER 1 DEVELOPMENT AFFAIR AND PURPOSE OF SURVEY

The third phase of the collaboration survey for exploration of metallic mineral resources in West Kalimantan of the Republic of Indonesia was conducted under the following program.

- (1) The promising mineralized areas, Selakean and Panji, covering 26 km<sup>2</sup>, were selected out of the area of 1,000 km<sup>2</sup> surveyed during the second phase survey period. The investigation of mineralizations were conducted in detail, consisting of geological survey and geochemical survey with soil sampling, in order to explore the geology, geological structures, igneous activities, relationship among the mineralizations, scale and characteristics of mineralized zones in these areas.
- (2) Keeping pace with the geological and geochemical surveys, the geophysical survey (IP Survey) was conducted, in order to survey the mineralized condition of chalcopyrite dissemination area in granodiorite discovered in Panji area at the second phase survey. The survey was conducted in the northeastern region of Panji area over the area of 2.0 km N-S and 1.8 km E-W (20 km of survey line).

Six (6) experts (3 geologists for geological and geochemical surveys and 3 geophysicist for geophysical survey) from Japan (Metal Mining Agency of Japan) and twelve (12) counterparts (7 geologists for geological and geochemical surveys and 5 geophysicists for geophysical survey) from the Republic of Indonesia (Directorate of Mineral Resources, Ministry of Mines and Energy) were engaged in this field survey, commencing on June 8, 1981.

The field survey was completed on September 15, 1981 with the cooperation of governmental authorities in the province, cities, and villages of West Kalimantan, in addition to cooperation rendered by the Ministry of Mines and Energy and Directorate of Mineral Resources of the Republic of Indonesia.

The results of the field survey were interpreted and compiled into geological maps and geophysical survey results were interpreted by the geologists and geophysicists of both countries at the base camp in the field and Directorate of Mineral Resources in Bandung. Furthermore, after the rocks, ores and geochemical samples collected for the chemical analyses and laboratory test have been analyzed, examined and interpreted both in Japan and in the Republic of Indonesia, the final geological maps and the geochemical analysis maps were compiled. A simulated analytical interpretation of geophysical survey results was also conducted and its result was summarized in this report.

## CHAPTER 2 OUTLINE OF THIRD PHASE INVESTIGATION

### 2-1 Detailed Geological and Geochemical Surveys

#### 2-1-1 Survey Purpose

The third phase reconnaissance survey was conducted, consisting of geological survey and geochemical survey with soil sampling, in order to explore the geology, geological structures, igneous activities, relationship among the mineralizations and them, and scale, characteristics of mineralized zones in these areas.

#### 2-1-2 Survey Area

##### (1) Selakean area:

The massive gold and silver bearing chalcopyrite-sphalerite-arsenopyrite mineralized zones are distributed in this area of 6 km<sup>2</sup> where the detailed survey was conducted. The survey area is approximately located at Lat. 0°45'N and Long. 109°34'E.

##### (2) Panji area:

Chalcopyrite dissemination and tourmaline-quartz mineralization are noted in granodiorite in the area of 20 km<sup>2</sup> where the detailed survey was conducted. It is approximately located at Lat. 0°32'N and Long. 109°41'E.

### 2-1-3 Method and Amount of Survey

#### (1) Compilation of topographic maps:

The topographic maps of 1/5,000 in scale were compiled, using the aerial photographs of approximately 1/50,000 in scale provided by the Government of Indonesia, covering Selakean area of 20 km<sup>2</sup> and Panji area of 25 km<sup>2</sup> totaling to 45 km<sup>2</sup>. These maps were used for the detailed geological survey and geochemical and geophysical surveys, and further, as the original topographic maps to compile the geological maps of 1/10,000 in scale.

#### (2) Geological survey:

The detailed survey on geology, geological structure, igneous activities, mineralizations and alteration zones was carried out along the river and roads, using the topographic maps of 1/5,000 in scale. The survey area and survey route consisted of Selakean area of 6 km<sup>2</sup> and 37 km and Panji area of 20 km<sup>2</sup> and 142 km, totaling to 26 km<sup>2</sup> and 179 km.

Observation and analyses were made on the following samples collected through the geological survey; 44 samples for petrographic microscopic examination; 4 samples for ore microscopic examination, 10 samples for ore analysis (30 elements); 5 samples of igneous rocks for complete analysis; 3 samples of igneous rocks for determination of their absolute age (K-Ar method); and 7 samples for X-ray diffractive analysis.

#### (3) Geochemical survey:

Keeping pace with the geological survey, the geochemical survey of soil sampling was conducted for surveying mineralizations. Soil samples were collected from B-horizon consisting of brown ~ orange brown soil under the humus soil, selecting five (5) sampling points per km<sup>2</sup> where having no influence and no contamination from the rivers (mainly at ridges and summits) and one (1) sampling point per every 200-meter distance along the survey line of the geophysical survey (IP Survey) in Panji area. These soil samples collected



were dried in the sun shine at the camp, screened through an 80 mesh sieve and divided into two packs, one to Japan and the other to the Republic of Indonesia for chemical analyses in the laboratory.

The number of samples collected was, 31 samples in Selakean area, 196 samples in Panji area (of which 110 samples were collected along the IP survey line), totaling to 227 samples. Considering characteristics of mineralizations in each area, analyses of copper and lead were conducted as pathfinder elements for Selakean area and copper and molybdenum for Panji area, and used for interpreting anomalies in the geochemical survey.

## 2-2 Geophysical Survey

### 2-2-1 Survey Purpose and Survey Area

Geophysical survey (IP Method) was conducted to investigate the condition and scale of ore deposits in Panji chalcopyrite disseminations in granodiorite located by the second phase reconnaissance survey. The survey was conducted, selecting an area of 2 km S-N and 2 km E-W centering on Panji Mineralization, considering the copper and molybdenum anomalous areas by second phase reconnaissance geological and geochemical survey.

### 2-2-2 Method and Amount of Survey

The survey was conducted with the undermentioned specifications in ten survey lines totaling to 20 km in all, each extending 2 km S-N at intervals of 200 meters.

- (1) Apparent resistivity, frequency effect and metal factor were sought after through variable frequency method in a dipole-dipole array.
- (2) Electrode spacing was 100 meters with the electrode separation coefficient  $n=1, 2, 3$ .
- (3) More than 20 rock and ore samples were collected to measure resistivity and frequency effect to facilitate analysis of survey result.

Conspicuous IP anomalies were selected from the survey results for simulation analyses by electronic computer.

## 2-3 Survey Team and Schedule

### 2-3-1 Survey Schedule in Indonesia

The third phase survey was carried out in accordance with the following schedule.

Departure of Advance Party (Survey Team Leader) and Preparatory Work	June 8, 1981 to June 28, 1981
Departure of Geological Survey Team; Survey and Data Processing in Indonesia	June 29, 1981 to August 25, 1981
Departure of Geophysical Survey Team; Survey and Data Processing in Indonesia	July 8, 1981 to August 24, 1981
Return of Geophysical Survey Team to Japan	August 25, 1981
Return of Geological Survey Team to Japan	August 26, 1981
Data Processing in Indonesia and Return of Survey Team Leader to Japan	August 27, 1981 to September 15, 1981

### 2-3-2 Survey Team

#### (1) Planning and consultation:

Indonesia	Japan
Ir. Salman Padmanagara (D.M.R.)	Kyuzo Tadokoro (M.H.A.J.)
Ir. Hafny Moh. Noer ( " )	Shozo Sawaya ( " )
Ir. P.H. Silitonga ( " )	Kyoichi Koyama ( " )
Ir. Yaya Sunarya ( " )	Kenji Sawada ( " )
	Kazuhiko Uematsu ( " )

**(2) Survey members:**

<b>Indonesian Team</b>		<b>Japanese Team</b>
<b>(a) Leader</b>		<b>Leader:</b>
Ir. Yaya Sunarya (D.M.R.)		Sakae Ichihara (M.M.A.J.)
<b>(b) Geological Survey Party</b>		
Simpree Soeharto (D.M.R.)		Sakae Ichihara (M.M.A.J.)
Johnny R. Tampubolon ( " )		Terumi Ishikawa ( " )
Danny Z. Herman ( " )		Hirotsuka Nishimoto ( " )
Sukmana		
<b>(Assistant)</b>		
Moé Tamar (D.M.R.)		
M. Rachmat ( " )		
<b>(c) Geophysical Survey Party</b>		
Nanang Sunarya (D.M.R.)		Kenichi Nomura (M.M.A.J.)
Drs. Gusti Hidayat ( " )		Akihiko Chiba ( " )
Immanuel M.F. ( " )		Kazuhumi Yoshimura ( " )
Eddy Kurnia ( " )		
W. Soeparmin ( " )		

**(Note):** D.M.R. : Directorate of Mineral Resources  
M.M.A.J.: Metal Mining Agency of Japan

## **CHAPTER 3 OUTLINE OF SURVEY AREA**

### **3-1 Location and Accessibility**

The project area of the joint mineral exploration survey (1,500 km<sup>2</sup>) is situated in the northwestern region of the West Kalimantan Province, Republic of Indonesia, and surrounded approximately by the following latitudinal and longitudinal points:

North Latitude	0°56'	and	East Longitude	109°17'
"	1°00'	"	"	109°15'
"	0°38'	"	"	109°41'
"	0°15'	"	"	109°37'
"	0°17'	"	"	109°40'

The detail survey area of the phase is accessible from Pontianak, Capital of West Kalimantan Province, by two routes.

(a) The route to enter Selakean area (north route)

The north route starting from Pontianak, Capital of West Kalimantan Province, runs 145 km northward along the seaside road to Singkawang, the second biggest city in the same province, and reaches Bengkayang, the major location at the north part of the survey area, further 75 km eastward from Singkawang. Selakean area can be reached on foot in 3 km east of Teriak Village, located 10 km to the south east of Bengkayang.

(b) The route to enter Panji area (south route)

A paved road runs eastward up to Darit from Sungalpinyuh on Pontianak-Singkayang road, via Mandor, Pahuman and Sidas. Panji area can be reached on foot in 2 km south of Bagak Village (9 km southeast of Darit) on this road.

The major roads are first class roads, paved or gravelled, facilitating a passage even by a passenger car. However, the road between Bengkayang and Darit is still kept unpaved, hard in passing even by a four-wheel-driving car. Nothing but mountain roads and trails are dependable to the survey site from these major roads, through which the survey equipment, food and camping materials can only be transported by labor.

### 3-2 Circumstances of Survey Area

The detailed survey area in Panji and Selakean areas is generally characterized by a gently sloping mountain range with low land or plains of elevation ranging from 100 to 300 m above sea level (the highest mountain in Selakean is 424 m above sea level).

Owing to the high temperature with a high humidity, the plants have luxurantly grown; especially, the dense growing of bushes at the trace left after slashing-burning agriculture makes it difficult to enter into the field, except through the areas along a river or a road. The survey period of June to August is the dry season and the temperature is as high as 30° centigrade at daytime, but at night the temperature is so low in the mountains that it requires a sleeping bag at the camp.

## **PART II**

### **GENERAL DISCUSSION AND CONCLUSIONS**

## CHAPTER 1 GENERAL DISCUSSION

The third phase survey consisted of geological survey, geochemical survey and geophysical survey (IP Survey in Panji area) covering 26 km<sup>2</sup> over the Selakean and Panji mineralized zones, resulting in advanced knowledge on the relationships between the mineralized zones and geology, geological structures and igneous activities, as well as the situation of the mineral resources, in the survey area.

### 1-1 Geological Location of Mineralization

Along the northern edge of granodiorite batholith extending WNW for 500 km with maximum in extension with of 150 km in width from Central Kalimantan to West Kalimantan, intruding during Cretaceous age, copper, molybdenum, gold, lead and zinc mineralizations are distributed at several places. Namely, copper and molybdenum mineralization, gold mineralization, lead and zinc mineralization in Central Kalimantan and G. Ibu copper and molybdenum mineralization in West Kalimantan are well known. Also in this project area (1,500 km<sup>2</sup>) several mineralizations, i.e. Sirih and Takap copper and molybdenum mineralizations and Serantak gold and copper mineralization are similarly located along the marginal zone of granodiorite batholith.

Selakean chalcopyrite - sphalerite - arsenopyrite mineralization and Panji copper mineralization selected from the second phase reconnaissance survey result are located in the similar locations.

It has been made clear that mineralizations in this project area are distributed at the contact area of Jirak andesite and andesitic pyroclastic rock formation and Belango dacitic pyroclastic rock formation with granodiorite batholith, or at roof pendant area and being controlled by younger intrusive rocks (tonalite and dacite intruded during Tertiary age) and the tectonic line indicated by fault. But mineralization is poor where Cretaceous granodiorite is extensively distributed. It is considered that in areas where the inside of batholith is exposed due to erosion and thus mineralization is poor there.

## 1-2 Relationship Among Geological Structures, Igneous Activities and Mineralizations

Although Selakean Mineralization and Panji Mineralization are both distributed along the marginal edge of Cretaceous granodiorite batholithes, relationship among geological structures, igneous activities and mineralizations in these two areas are different and constructive to each other.

Selakean Mineralization is considered to be the mineralization resulting from fissures (NNE~SSW trend and NNW~SSE trend) made in Jirak andesite and andesitic pyroclastic rocks through intrusion of G. Raya granodiorite batholith and intrusive rocks. The mineralization is a hypo- ~ mesothermal deposit because of accompanying arsenopyrite and having exsolution texture of chalcopyrite in sphalerite. It is inferred that this mineralization has resulted from the intrusion of G. Raya granodiorite, since no other younger intrusive rocks are found in this area and distribution of geochemical anomalous area, alteration zones and mineralizations were limited to the contact area with G. Raya granodiorite.

Panji Mineralization is embedded in G. Sebiavak granodiorite and Belango (quartz) andesitic pyroclastic rock formation into which the former has intruded, with the distribution of pyrite dissemination outside and tourmaline chalcopyrite dissemination with or without tourmaline inside. Since exposure is bad, alteration is not clear. Mineralizations are sporadically distributed at an area of 2 km EW and 3 km NS, extending NNE~SSW direction.

While tectonic line extending NNE~SSW direction is inferred by including direction of younger intrusive and dyke rock (dolerite and dacite) and lineament through photo geological interpretation, in Panji area, copper and molybdenum anomalous areas found through the geochemical survey are also extending along this tectonic line and Panji Mineralization is considered to be controlled by the NNE~SSW structure line.



Panji Mineralization resembles Banyu Mineralization of which second phase detailed survey was conducted, as copper mineralization, accompanying tourmaline. The Banyu Mineralization is embedded in younger igneous rocks (Banyu tonalite) and it is considerable that the zone was formed by younger igneous activities. Although younger igneous rocks are hardly recognizable in the Panji area, the reason is probably these rocks have not been exposed sufficiently and latent existence of younger igneous is well considerable. G. Sebiawak granodiorite has been intruded during Early Cretaceous age of 124 m.y. under the K-Ar absolute age dating.

### 1-3 Relationship between Geochemical Survey Result and Mineralized Zones

The third phase geochemical surveys with soil sampling were conducted in Selakean area and Panji area with copper and lead as pathfinder elements anticipating copper, lead, zinc and arsenopyrite ore deposits and with copper and molybdenum as pathfinder elements anticipating copper and molybdenum ore deposits, respectively. As the result, anomalous areas were found in both areas where existence of mineralizations was anticipated.

In Selakean area, copper and lead anomalous areas were separately distributed, with copper anomalous area covered in the area where mineralizations is embedded in Jirak Formation adjacent to G. Raya granodiorite and lead anomalous area distributed surrounding copper anomalous area. Copper was more adaptive than lead as pathfinder element. However both copper and lead values were low, with the maximum anomalous value of 126 ppm of copper and 51 ppm of lead.

In Panji area, the 2nd class copper and molybdenum anomalous areas were recognized from the eastern part of old Panji Village to S. Tapis in scale of 1.5 km EW and 2 km NS. These anomalous areas consist of five anomalous areas (maximum 500 m × 500 m and minimum 200 m × 200 m), generally aligned in NNE~SSW direction and roughly speaking it is running along the general structural direction, as well as NNW~ESE direction. Besides, latent existence of the structural direction of NNW~ESE can be assumed. The maximum anomalous area contained Cu of 514 ppm and Mo of 123 ppm.

The anomalous area (geophysical survey line of C16~18 and D16~18) continuing from the mineralization in east of old Panji Village was the most noteworthy finding in the geochemical survey.

#### 1-4 Relationship between Geophysical Survey (IP Survey) Result and Mineralized Zone

The geophysical survey (IP Survey) was conducted along the total survey line of 20 km with 1.8 km EW and 2 km NS in the eastern region of geological and geochemical survey areas in Panji area, resulting in 7 locations of IP anomalous area which are inferred to be related to mineralization. Since the whole geophysical survey area is included in the geochemical survey anomalous area with the exception of some southeastern parts, no outstanding feature was observed in the distribution of FE anomalous area. However, since the direction of alignment of FE anomalous area discovered in the northern survey line (C16~18, D16~18) of the geophysical survey area is in the same direction as that of WNW~ENE direction in the northern geochemical survey area, it is considered to reflect one direction (structural direction?) of mineralization in Panji area. Especially, since FE anomalous area situated to the south of old Panji Village indicates the strongest FE anomaly of the above mentioned anomalous areas, and further it is adjacently situated to the south of mineralization in east of old Panji Village, it is considered the most promising anomaly in the geophysical survey.

#### 1-5 General Discussions

In Selakean area, while there are arsenopyrite veins accompanying chalcopyrite and sphalerite in Selakean Mineralization where old prospecting trenches are found, other mineralizations are small scale with low mineral content. Although a copper geochemical anomalous area was recognized overlapping mineralization at the contact area with G. Raya granodiorite through the geochemical survey, it is of low prospecting value since analytical value of copper is generally low.

In Panji area, there is a chalcopyrite disseminated zone east of old Panji Village where covellite is recognized as secondary mineral in addition to tourmaline mineralization. Through the geophysical survey (IP Survey) it was clarified that the anomalous area with  $FE > 6\%$   $AR < 500 \text{ ohm-m}$ , which is the best anomalous area (M-2 anomalous area) in this area is distributed in this southern area, where geochemical survey anomalous area is overlapped. In this area, in scale of 800 m NS and 500 m EW, copper (and molybdenum) dissemination ore deposits considered to exist, leaving room for future survey. Besides the above, M-3 and M-4 are anomaly areas are considered to be mineral deposit anomalies through geochemical, geophysical and geological survey results in Panji area, but since IP survey anomaly is weak and shallow compared to M-2 anomaly, they are not so strong as M-2 anomaly.

## CHAPTER 2 CONCLUSIONS AND FUTURE PROGRAM

### 2-1 Conclusions

The geological survey, geochemical survey (with soil sampling) and geophysical survey (IP Survey) were conducted in Selakean and Panji areas which were selected through the second phase reconnaissance survey in an attempt to interpret the relationship among geology, geological structures, igneous activities and mineralizations as well as distribution of mineralizations. The conclusions resulted from the third phase survey are as follows:

- (1) Mineralizations distributed in Selakean area are fissure filling ore deposits embedded in shear fissures resulted in Jirak Formation through G. Raya granodiorite intrusion. They are goldbearing chalcopyrite-sphalerite-arsenopyrite veins, judging from lumpy ores of Selakean ore vein which is the champion vein. Chalcopyrite is contained in sphalerite as exsolution dot and lamellae.
- (2) Panji area mineralization chiefly consists of chalcopyrite dissemination ore deposits accompanying tourmaline, and resembles Banyu Mineralization in the second phase survey. Several chalcopyrite

dissemination outcrops are distributed in the east of old Panji Village.

- (3) In Selakean area, a copper anomalous area was discovered mostly overlapping the mineralization through the geochemical survey, while a lead anomalous area is somewhat shifted and distributed slightly outside of G. Raya granodiorite. Their assay values are generally low. In Panji area, a copper-molybdenum anomalous area was discovered in the center of mineralized zone in the east of old Panji Village, generally extending toward the main structural line in this area. It also extends NNW~ESE direction and a latent existence of this structural line is also considered.
- (4) In the IP Survey, several anomalies were noted, of which anomalies (FE > 6% resistivity < 500 ohm-m) found in the IP lines C16~18 and D16~18 (indicated M2) are noticeable anomalies recognized in the area extended to the south of the mineralized zone in the east of old Panji Village.
- (5) The comprehensive study of mineralizations in these two areas based on the above survey results revealed that although there are mesothermal chalcopyrite, sphalerite and arsenopyrite ore deposits in Selakean area embedded in fissures resulted from the structural movement accompanying intrusion of G. Raya granodiorite, they are generally of low grade. In Panji area, several chalcopyrite disseminations accompanying tourmaline are found sporadically in a range of 2 km in the east-west direction and 3 km in the south-north direction. Further, it is overlapping geochemical and IP anomalies. Following survey is necessary in this area.
- (6) G. Seblawak granodiorite has been dated as 124 m.y. under the K-Ar absolute age dating, intruding in Early Cretaceous in age.  
Also, the dating resulted from granitic rocks accompanying the copper-molybdenite mineralization in G. Ibu area indicates 30 m.y. (Oligocene age). It was further confirmed that they are the same Tertiary igneous rocks as Banyu and Sirih tonalites (27~20 m.y.)

of this project area and that the copper-molybdenum mineralization in West Kalimantan area is due to younger igneous activities.

## 2-2 Recommendation for Future Study

As described above, the actual conditions of mineralized zones in Selakean and Panji areas were made clear. The future program and issues are described hereunder, based on these evaluations.

- (1) Selakean Mineralization is embedded on the side of Jirak Formation at the contact of Jirak Formation with G. Raya granodiorite. Since it was discovered also in the geochemical survey that a copper anomalous area is overlapping the mineralized zone, Selakean Mineralization was inferred to have resulted from the intrusion of G. Raya granodiorite, it is recommended that for the survey of mineralized zones in this area, a further survey be made of areas surrounding G. Raya granodiorite.
- (2) Panji Mineralization is a noticeable mineralized zone, judging from the IP anomaly recognized in the geophysical survey (IP Survey) survey line C16~18, D16~18 and geochemical survey anomaly (copper and molybdenum). It is desirable that existence (scale, shape and grade) of mineralization be confirmed through more prospecting and exploration works. Weak IP anomaly and geochemical survey anomaly were also found in several places, but according to IP Survey result, such anomalies are rather superficial and considered to be not so promising as the former.
- (3) As the result of K-Ar absolute age dating, granitic rocks (G. Raya granodiorite and quartz diorite according to T. Suhandu) related to the copper-molybdenite mineralization in G. Ibu granite distribution area were confirmed to be younger intrusive rocks intruding Tertiary Oligocene. As the result, it was further confirmed that the survey of ore deposits in West Kalimantan should be conducted taking notice of the existence of younger granite intrusive rocks.

**PART III**

**GEOLOGICAL AND GEOCHEMICAL SURVEYS**

## CHAPTER 1 GEOLOGICAL OUTLINE OF SURVEY AREA

The outline of geology, geological structures and mineralizations in the total survey area of 1,500 km<sup>2</sup> has been elucidated by the geological reconnaissance survey of the first and second phases is as described below. (Fig. 3-1, Fig. 3-2)

### 1-1 Geology

#### 1-1-1 Mesozoic Sedimentary, Volcanic and Pyroclastic Rocks

Upper Triassic-Lower Jurassic sedimentary rocks (Bengkayang Group) are extensively distributed from the north mountain region of G. Bwang-G. Mahmud up to the plains of Bengkayang-Sungaibetung. The Bengkayang Group has been divided from the top as following Formations.

Sungaibetung Formation: Alternated beds of sandstone, mudstone and siltstone

Riampelaya Formation : Sandstone

Kalung Formation : Black shale and fine sandstone

Banan Formation : Tuffaceous sandstone and sandstone

The ammonite fossils are found at the top horizon of Sungaibetung Formation, correlating with the lower Jurassic series.

Covering the Bengkayang Group unconformably, both Jirak Formation consisting of andesite and andesitic pyroclastic rocks and Belango Formation consisting of dacitic pyroclastic rocks are extensively distributed in the central and southern parts of the project area.

#### 1-1-2 Mesozoic Cretaceous Granitic Rocks

In the central and southern parts of this survey area, the G. Seblawak, G. Raya and G. Selantar granodiorites which have intruded into Bengkayang Group, Jirak Formation and Belango Formation are extensively distributed as a batholith, giving the contact metamorphism. The K-Ar absolute age dating dated as 114~95 m.y. for granodiorite and quartz diorite, resulting in an intrusion during Middle-Cretaceous age.

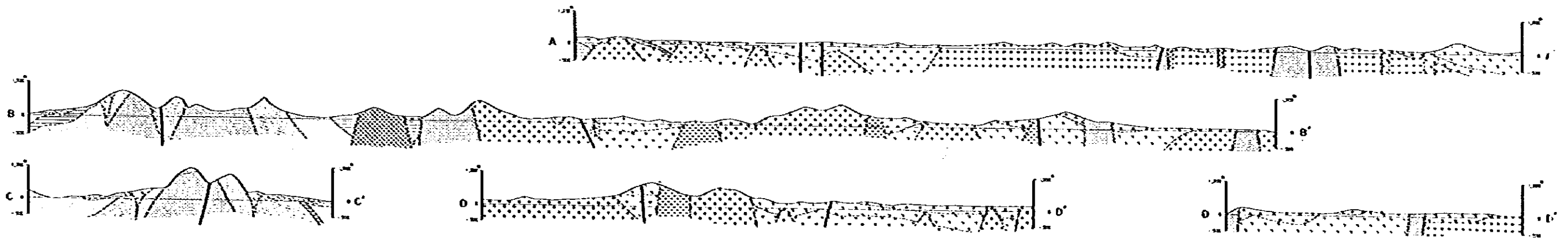
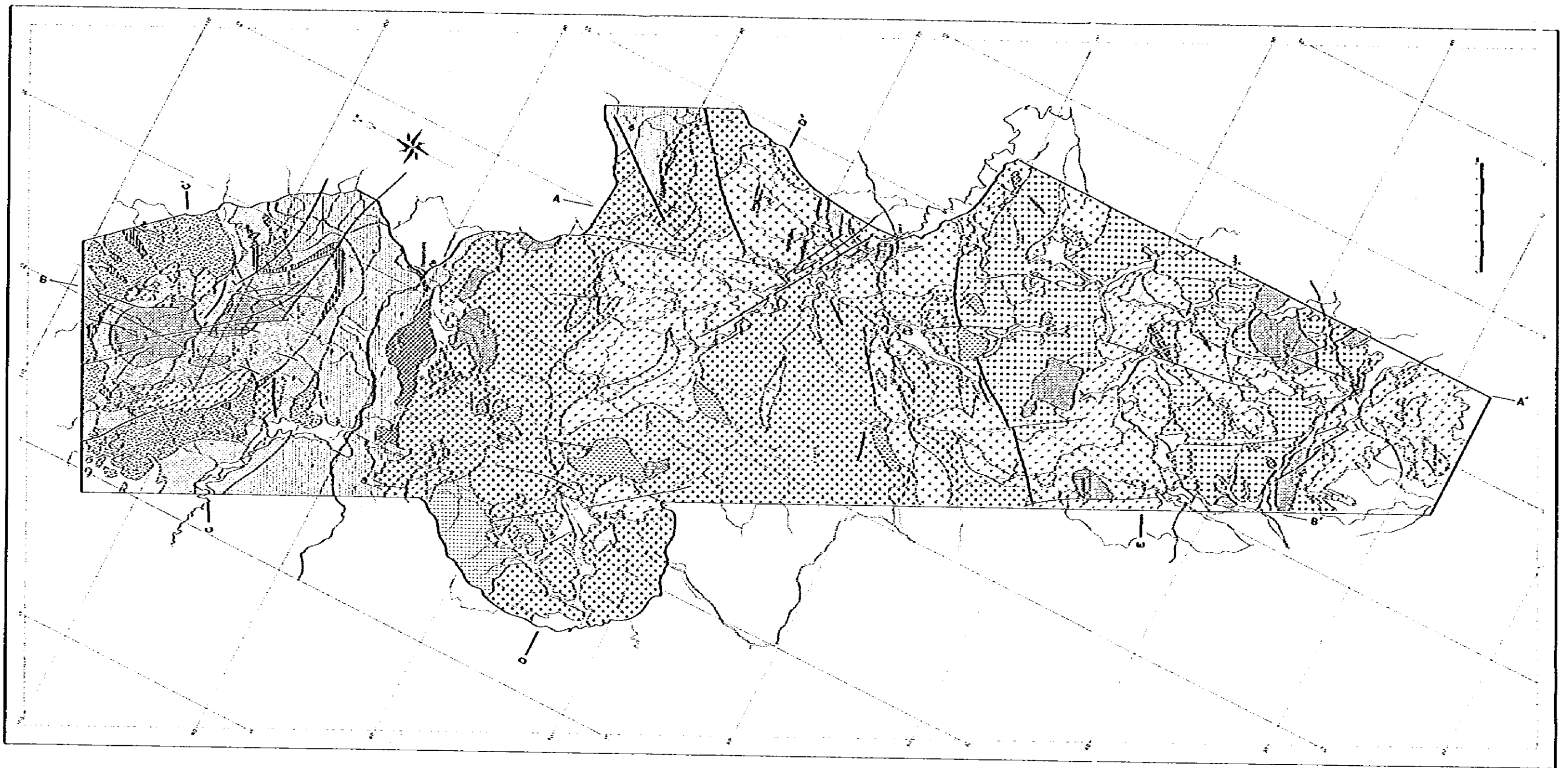


Fig. 3-1 Geological Map of West Kalimantan Project Area



# LEGEND

Quaternary		Gravel, Sand		
Tertiary	<p>Serantok Formation</p> <p> Dacitic pyroclastic rocks</p> <p> Serantok Dacite</p>	<p> Quartz porphyry 2</p> <p> Granodiorite 4</p> <p> Sirih, Bonyi Tonalite</p> <p> G.Ponandón Quartz gabbro, Dolerite</p>		
Cretaceous		<p> Tiong Quartz Diorite</p> <p> G.Selantar Granodiorite</p> <p> G.Roya Granodiorite</p> <p> G.Sebiwak Granodiorite</p>		
Triassic	<p>Belongo Formation</p> <p> Red Mudstone</p> <p> Andesitic rocks (Andesite lava, Andesitic tuff and tuff breccia)</p> <p> Dacitic rocks (Dacite, Dacitic tuff)</p>	<p>Jurassic</p> <p>Jirak Formation</p> <p> Red Mudstone</p> <p> Andesitic tuff and Tuff breccia</p> <p> Andesite lava</p>	<p>Bengkoyong Group</p> <p> Sungaibelung Formation</p> <p> Riampeloyo Formation</p> <p> Kelung Formation</p> <p> Banon Formation</p>	
		Fault		
		Anticlinal axis		
		Synclinal axis		

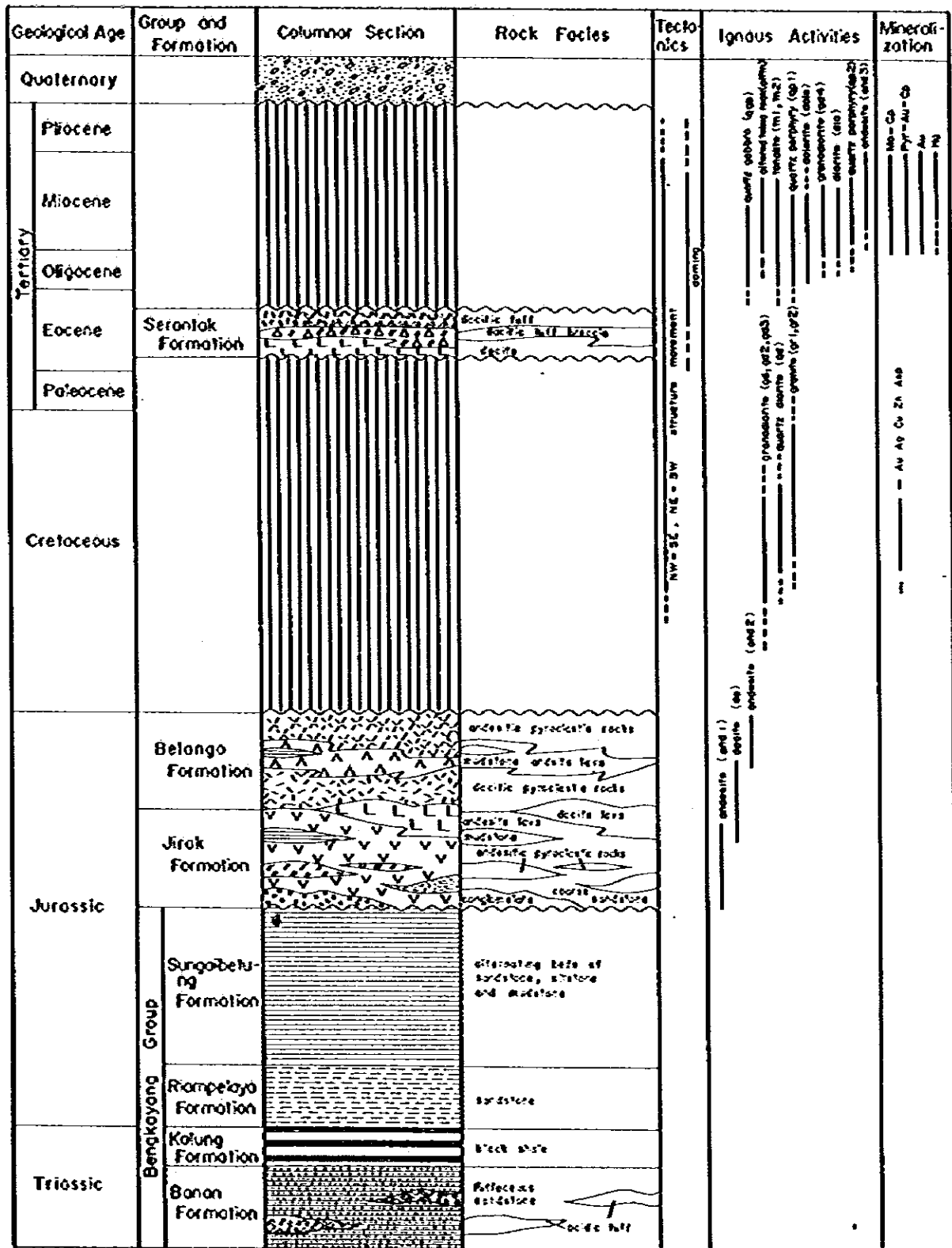


Fig. 3-2 Generalized Stratigraph of Survey Area

### 1-1-3 Tertiary Dacite and Dacitic Pyroclastic Rocks

The Serantak dacites and dacitic pyroclastic rocks are distributed around the mountain region of G. Bawang in the northern part of the survey area. The K-Ar absolute age dating indicates the dacites to be 50 m.y. intruding during Eocene age.

### 1-1-4 Tertiary Tonalite

The tonalites distributed at both the mountain region of G. Bawang-G. Mahmud and the area of S. Banyu intruded during the period from Oligocene in age to Early Miocene in age, judging from the K-Ar absolute age dating (27~20 m.y.) and its intrusion into the Serantak dacite. Gold, silver, copper and molybdenum mineralizations are found in and around the tonalites.

## 1-2 Mineralization

The following mineralizations were observed in the survey area through the reconnaissance survey and detailed survey.

- (1) Chalcopyrite molybdenite quartz vein (Sirih tonalite)
- (2) Mineralized zones consisting of tourmaline, chalcopyrite, molybdenite, pyrite and gold (area centering on Banyu tonalite)
- (3) Massive goldbearing pyrite pyrrhotite ore deposits (Banan Formation around Serantak dacite)
- (4) Gold and silver bearing chalcopyrite zincblende arsenopyrite ore vein (Jirack Andesite Formation)
- (5) Chalcopyrite disseminated zones (G. Sebiawak granodiorite)
- (6) Manganese ore deposits (Serantak pyroclastic rocks)

(Note) Items in parentheses show the country rock embedded ore deposit.

Besides the above, the pyrite disseminated zones accompanying silicification and argillization were discovered at many locations.

Many of these mineralizations are related to the younger igneous activities such as Serantak dacite, Sirih tonalite and Banyu tonalite.

## **CHAPTER 2 DETAILED SURVEY IN SELAKEAN AREA**

### **2-1 Outline of Geology**

In the eastern mountain side of G. Selakean (G. Jalu) in this detailed survey area, there are old trenches for the prospecting of gold, silver, chalcopyrite and sphalerite bearing arsenopyrite veins. Also, wide distribution of anomalous areas such as copper, molybdenum, zinc and lead have been found through geochemical survey with stream sediments performed in the second phase reconnaissance survey.

Geology in this area consists of Jirak andesite and andesitic tuffaceous stratum of the Mesozoic Jurassic system, into which Cretaceous G. Raya granodiorite has intruded. Intrusion of G. Raya granodiorite resulted in the contact alteration such as argillization, silicification, or pyrite dissemination. (Fig. 3-3)

### **2-2 Stratigraphy and Igneous Rocks**

#### **2-2-1 Jirak Andesite and Andesitic Tuff Formation**

The lower stratum abounds in andesitic tuffaceous rocks while the upper stratum abounds in andesitic rocks. In the andesite stratum, red andesitic tuffaceous rocks are intercalated, containing a lot of hematite. In the geological reconnaissance survey, the Jirak andesite and andesitic tuffaceous stratum are correlated with the Jurassic series, as they uncomfortably overlie the Sungaibetung Formation of the Bengkayang Group of the Lower Jurassic series and being intruded by G. Raya granodiorite during the Middle Cretaceous.

##### **(a) Andesitic tuff**

This Formation, which is distributed from G. Serawak to G. Jalu, has rock facies of dark green colored andesitic lapilli tuff and fine-grained sedimentary rocks. It partly consists of light yellow colored andesitic tuff accompanying a fine seam of black mudstone. Under microscopic, the stratum indicates strongly altered sandy andesitic tuff (RY-7) flow structure, and strongly sericitized

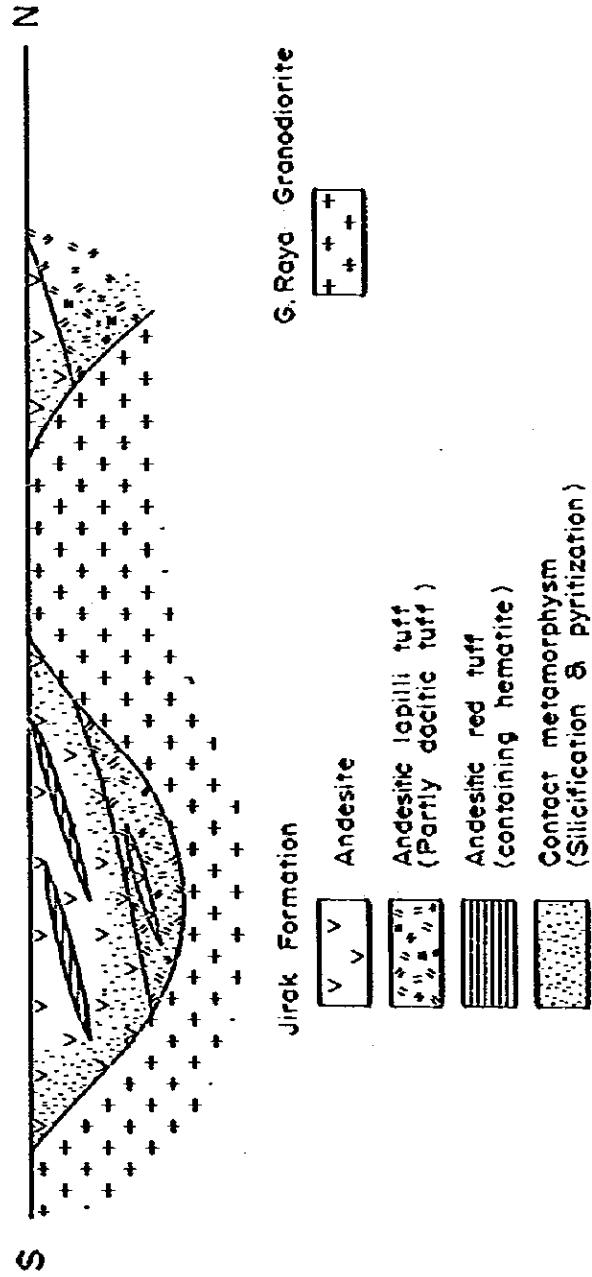


Fig. 3-3 Schematic Geological Profile (Selakcan Area)

andesitic tuff is observed. These alterations are considered to be due to contact alteration by G. Raya Granodiorite.

(b) Andesite

This rock is a dark green compact rock extensively distributed from G. Jalu to S. Empawang in the central and southern regions of the detailed survey area. Under microscope (RY-8) the result revealed that the rock is altered and consists of phenocryst of plagioclase and a small volume of hornblende on the ground mass of sericite and a small amount of quartz and plagioclase. Red andesitic tuffaceous stratum is intercalated where a large volume of hematite is contained in sericite and little kaolinized mineral. Red tuff and red sandy tuff with the similar hematite are intercalated in Jirak andesitic tuff and Belango dacitic tuff, which is considered to be sedimentation under oxidation condition on ground.

2-2-2 G. Raya Granodiorite

Granodiorite is distributed to the southern area of the downstream of S. Empawang in southwestern region of this detailed survey area, as a part of G. Raya granodiorite which is distributed as a batholith from Bengkayang to Darit in the reconnaissance survey area. Besides this, this rock has intruded into Jirak Formation as a granodiorite intrusive rock in the northeastern G. Batu Lumun and G. Serawak. This rock has a medium-grained holocrystalline granular texture, and under the microscope the result revealed that it is more or less tonalitic granodiorite with quartz, plagioclase, potashic feldspar and hornblende as its major constituent minerals, with a little quantity of sericite. Although some sericite occurs along the cleavage of plagioclase, this rock is generally fresh.

This rock is dated as  $114 \pm 6$  m.y. during Middle-Cretaceous age, resulting from the K-Ar absolute age dating of samples (81-RC64) collected in S. Empawang in the second phase reconnaissance survey.

## 2-3 Geological Structure

Jirak andesite Formation is massive and lack of bedding, but referring bedding of andesitic tuff on the lower Formation and hematite tuff stratum (generally striking  $N20^{\circ} \sim 80^{\circ}E$  and dipping  $15^{\circ} \sim 20^{\circ}S$ ), Jirak formation the considered to show monoclinic structure dipping south.

The rocks were not exposed well enough to confirm a fault through the geological survey. But, according to the photogeological interpretation, lineament striking  $N30^{\circ}E$  was interpreted from S. Nanggak to S. Batuparang which was inferred to be a fault. Mineralizations fills in the fissures (inferred to be a shear) of two systems, one striking  $N15^{\circ} \sim 30^{\circ}E$ , dipping  $75^{\circ}NW$  and the other striking  $N15^{\circ} \sim 30^{\circ}NW$ , dipping  $70^{\circ}NE$ . When they are considered conjugate sheares, the medium principal stress axis  $\sigma_2$  is  $N5^{\circ}E60^{\circ}NE$  as shown in the Fig. 3-4, inferred to be by the structural force pushing upward, resulting from G. Raya granodiorite intrusion.

Fig. 3-5 is the projection of mainly the joint pole, found in Jirak andesite and andesitic tuff found in this area, on Schmidt's net. The joint set is mainly  $N20^{\circ}E68^{\circ}NW$  trend, but some are  $N10^{\circ}E70^{\circ}SE$ ,  $N60^{\circ}W48^{\circ}SW$  trends.

## 2-4 Mineralization

### 2-4-1 Outline of Mineralization:

Gold and silver bearing chalcopyrite sphalerite arsenopyrite veins distributed on the east hill of G. Jalu are known ore deposits. Besides them, mineralizations are observed in altered clay zone and in the shear zone around G. Raya granodiorite. They are both accompanied by arsenopyrite. (Fig. 3-6)

### 2-4-2 Descriptions on Mineralization

#### (1) Selakean Mineralization

As reported in the second phase reconnaissance survey, there are many old trenches prospected in the past for gold, silver and

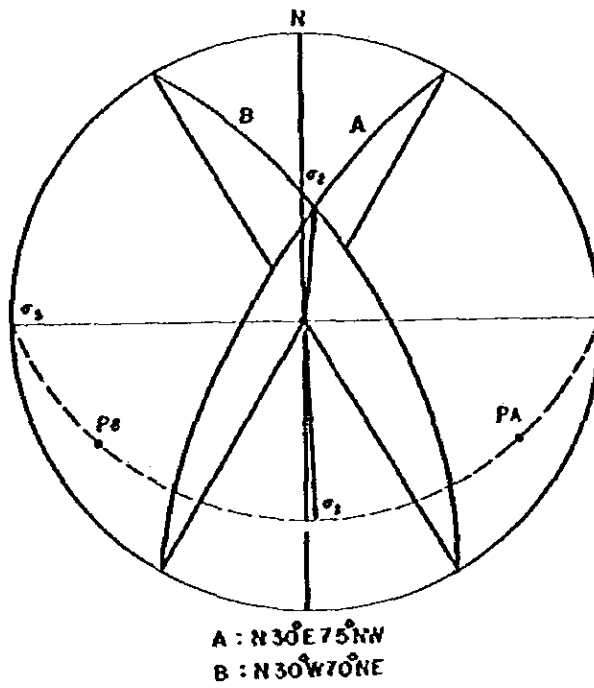


Fig. 3-4 Relationship of Two Fissures with Ore Mineral (Selakean Area)

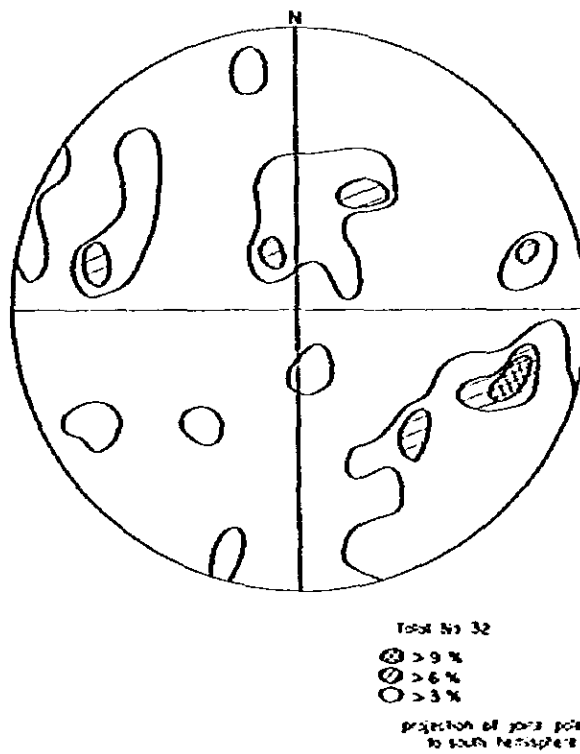


Fig. 3-5 Joint System in Jirak Formation (Selakean Area)







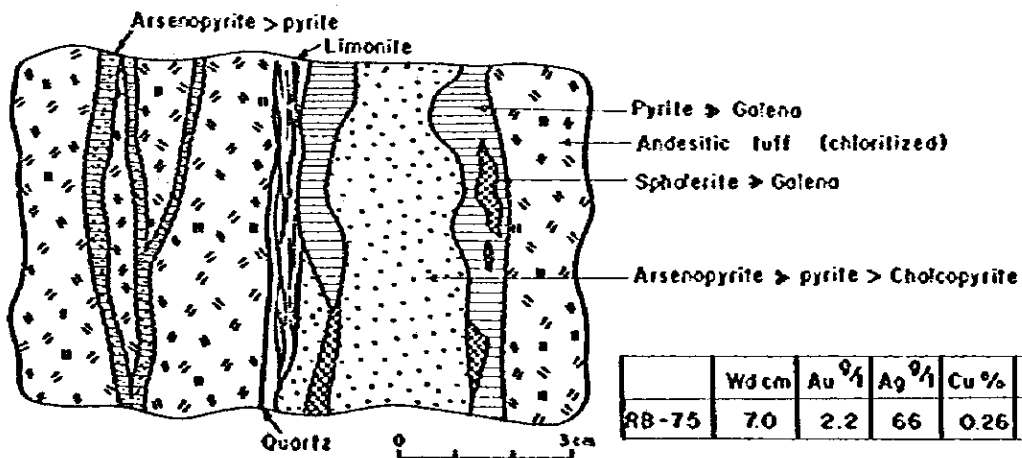
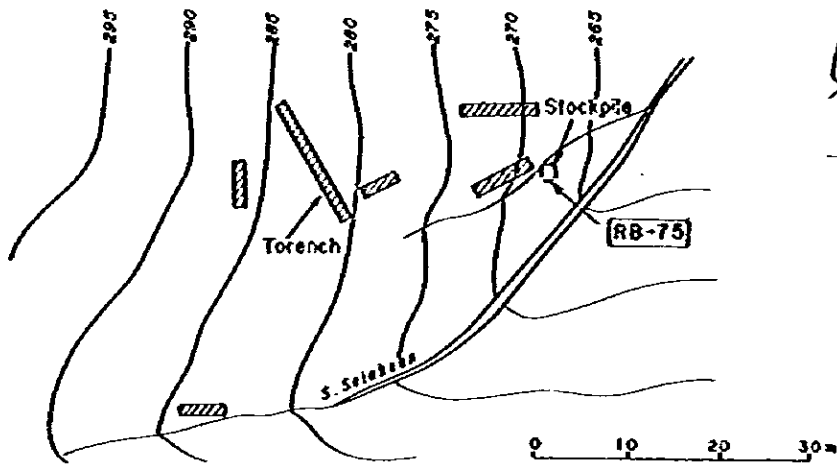
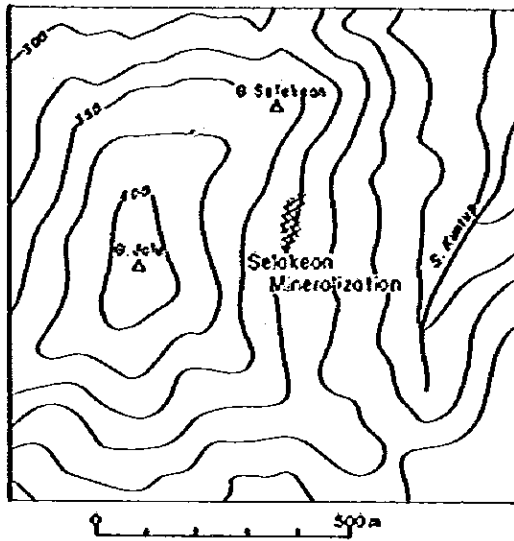
copper at east hill of G. Jalu in an area of 30 m × 40 m, but all are collapsed, and scales and mining conditions of the ore deposits are unknown. According to the microscopic observations of ore samples (RY-6) collected from lump ore, the ore chiefly consists of arsenopyrite, accompanying chalcopyrite and sphalerite and a little amount of covellite. Chalcopyrite is exsolved from sphalerite and existed as dots and lamellae. The assay result of lump ore was 7 cm in width, Au 2.2 g/t, Ag 66 g/t, Cu 0.26%, Zn 0.19% and Pb 0.04%. (Fig. 3-7)

(2) S. Empawang Mineralization:

In Jirak andesitic formation at the upperstream (150 meters above sea level) of the branching point of S. Empawang and S. Nanggak, five-meter wide shear zone with the strike of N30°E and the dip of 70NW was found, bearing pyrite scatter and small quartz veinlets. The grade of this mineralization is Au < 0.1 g/t, Ag 6 g/t, Cu 0.009%, Pb 0.01%, Zn 0.004% and As 0.002%. Slightly detected arsenic is considered to indicate the feature of mineralization in this area which accompanies arsenopyrite. (Fig. 3-8)

(3) S. Entagak Mineralization:

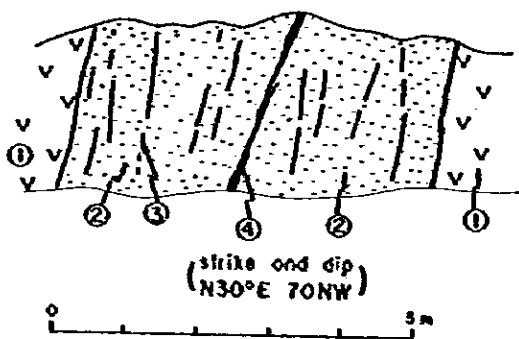
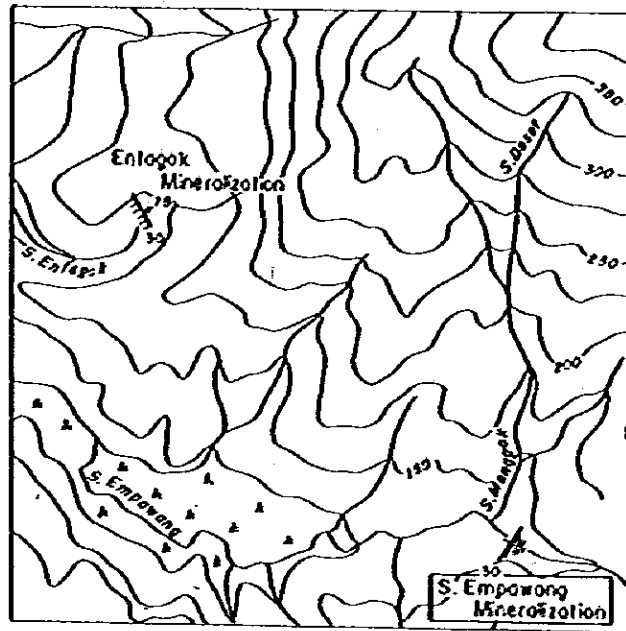
In the upperstream of S. Entagak (around 150 meters above the sea level), there is a grey clay exposure in which an altered zone was found with white clay veinlets in net. It strikes at N30°W with the dip at 75°NE. It was detected in the X-ray diffractive analysis that this clay, chiefly consisting of sericite and quartz, also contained peak of  $d = 5.64 \text{ \AA}$  (seem to be analcime) and peak of arsenopyrite. In addition to the above, in Jirak andesitic tuff at further upstream fissures with the strike of N30°W and the dip of 76NE are arranged in width for 2 meters at intervals of about 20 cm. Along this fissures, there is about 1 meter long and about 20 cm wide vein in lense. Grade of the ore is 20 cm in width, Au 0.1 g/t, Ag 14.8 g/t, Cu 0.16% and Pb 0.03%. (Fig. 3-9)



	Wd cm	Au <sup>g</sup> / <sub>t</sub>	Ag <sup>g</sup> / <sub>t</sub>	Cu %	Pb %	Zn %	Mo %
RB-75	7.0	2.2	66	0.26	0.04	0.19	<0.01

(from results of Survey in 1930)

Fig. 3-7 Sketch Map of Selakean Ore Deposit



- ① Jarak Andesite
- ② Argilized andesite
- ③ Quartz veinlet
- ④ Quartz vein in shear zone

RX-2 assay result

Au g/l	Ag g/l	Cu%	Pb%	Zn%	As%
<0.1	0.6	0.009	0.01	0.004	0.02

Grob sampling of 5m in width

Fig. 3-8 Sketch Map of Empawang Mineralization

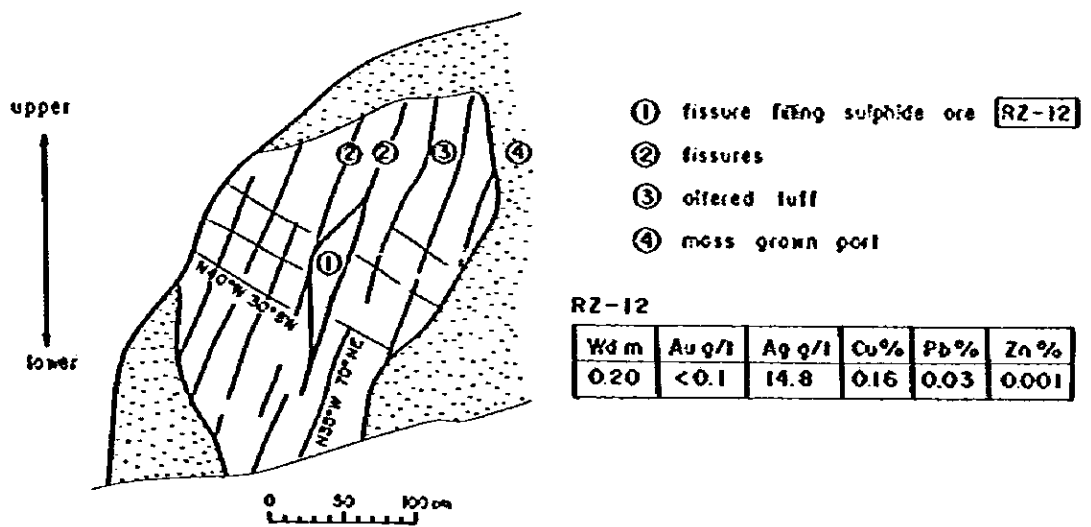
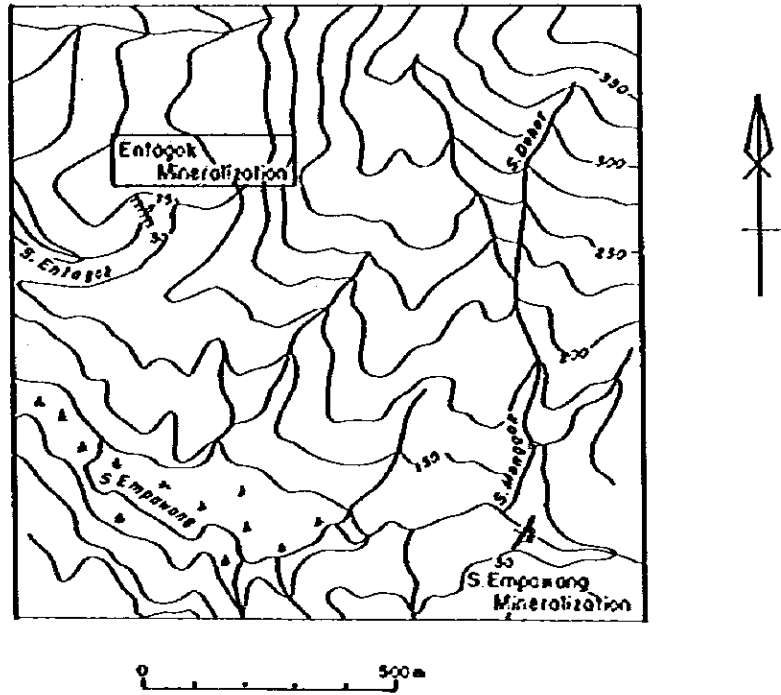


Fig. 3-9 Sketch Map of Entogok Mineralization

**(4) S. Melanci Alteration Zone:**

At upperstream of S. Melanci which is 500 meters north of S. Entagak Mineralization, green grey colored argillaceous alteration is exposed where a fissure with the strike of N30°W and the dip of 80SW is compactly developed, filled with white clay. The X-ray diffractive analysis (RZ-14) detected that in addition to a little quantity of chlorite, a large amount of laumontite are contained. Generally speaking, forming of laumontite and chlorite containing with Ca is considered to have been resulted from calcium rich rocks as andesite, etc. under the condition of neutral ~ Alkali hot water at comparatively low temperature of 100°C ~ 200°C. Sulphide mineralization such as arsenopyrite does not occur. Check analysis results in 50 cm in width Au < 0.1 g/t, Ag 0.5 g/t.

**(5) Serawak Mineralization:**

Old data described mineralization (Serawak ore deposit) in southern G. Serawak in northeastern region of survey area, together with Selakean Mineralization. But in this survey, only a small amount of pyrite scatter was confirmed at upperstream of S. Melansar in the contact of Jirak andesite and G. Raya granodiorite.

**(6) S. Belito Fracture Zone:**

A small, parallel fissures with the strike of N10°E and the dip of 50W is noted in a range of more than 2 meters on the andesite side of contact of G. Raya granodiorite with Jirak andesite at upperstream of S. Belito. Sulphide and other mineralizations are not strong.

## **2-5 Geochemical Survey**

### **2-5-1 Sampling**

Keeping pace with the geological survey, the geochemical survey with soil sampling was conducted to survey mineralizations. Sampling of soils for the geochemical survey was performed from B-horizon consisting of 30 cm ~ 50 cm deep brown ~ orange brown soil ensuring equal distance

distribution by selecting five (5) sampling points per km<sup>2</sup> in ridges and summits where having no influence and no contamination from the rivers. The number of collected samples was 31.

Considering the fact that the known ore deposit in this area was copper, zinc and lead-bearing veins and that copper and lead were effective pathfinder elements in the second phase reconnaissance survey, copper and lead were used as pathfinder elements.

#### 2-5-2 Statistical Data Processing of Analytical Data

Analyzed values were standardized through logarithmic conversion to prepare a histogram and cumulative frequency distribution and calculate correlation. Background and threshold values were sought to extract anomalous areas. Since the samples were collected almost at equal distance in the survey area, 5 samples at every 1 km<sup>2</sup>, threshold values ( $M+\sigma$ ,  $M+2\sigma$ ) obtained in statistical processing were referred to draw an equal analyzed value contour line in order to show the geochemical survey anomalous area.

The highest value of copper 126 ppm, its lowest value 24 ppm and the highest value of lead 51 ppm, its lowest value 17 ppm were divided into nine logarithmic groups of equal distance to prepare histogram and to calculate respective average values, standard deviations and threshold value (2) ( $M+\sigma$ ) and threshold value (1) ( $M+2\sigma$ ). (Fig. 3-10, 3-11)

Cumulative frequency distribution both for copper and lead became a straight line and classified as type 1 by C. Lepeltier method and frequency percent 2.5% is fixed as a threshold value (Fig. 3-12). Threshold values thus obtained are shown in Table 3-2. As the result, for analysis of Selakean area, reference was made to both analyzed values to seek for anomalous areas with the first class anomalous values as copper of 105 ppm and lead of 48 ppm and the second class anomalous values as copper of 70 ppm and lead of 36 ppm. Copper and lead are scarcely correlated, since their correlation coefficient is 0.212. (Fig. 3-13).



**Table 3-2 Value of Mean Standard Deviation and Threshold in Selakean Area**

Element	n pcs	M ppm	M + $\sigma$ ppm	M + 2 $\sigma$ ppm	Threshold value *ppm	Max ppm	Min ppm
Cu	31	50.0283	72.9622	106.4096	103.3710	126	24
Pb	31	28.3767	36.6666	47.3782	48.4546	51	17

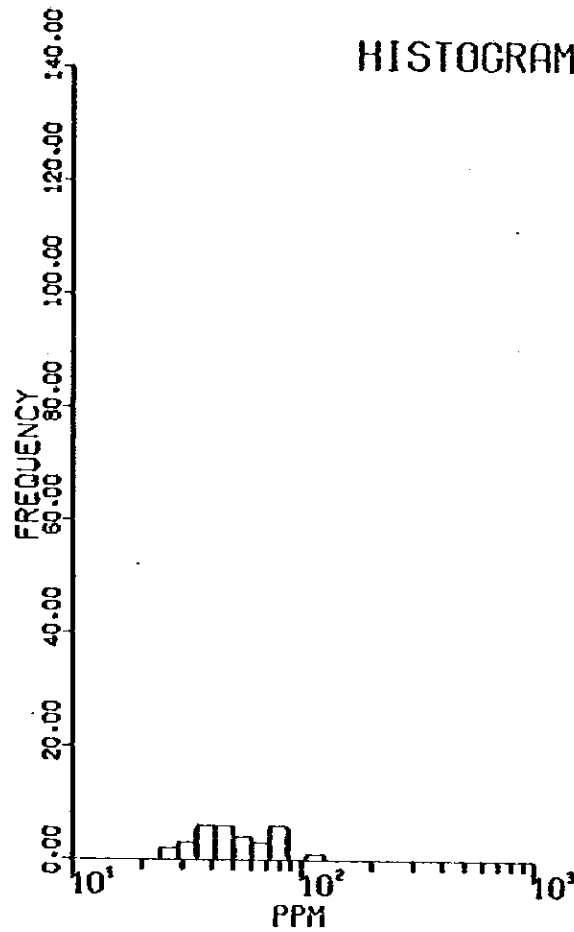
\* Threshold value based on bending point in graph cumulative frequency distribution.

### 2-5-3 Anomalous Areas

The distribution range of copper anomalous area (70 ppm of Cu) extends 1.5 km x 1.0 km, centering at S. Empawang, S. Nanggak and S. Sedayu approximately in the southwestern region of the survey area, and it is situated in Jirak andesite distribution area surrounded by batholithic G. Raya granodiorite and G. Batu Lumun granodiorite intrusive rock (Fig. 3-6). On the contrary, lead anomalous area is shifted about 500 m northward, not overlapping the copper anomalous area, and analyzed values are generally low. Considering G. Raya granodiorite as the center, the fact that copper is distributed on the side of granodiorite and lead is located rather outwardly may indicate that the anomalous areas are located on the mineralized location of copper and lead with granodiorite (could be zonal distribution?).

### 2-6 Characteristics of Selakean Mineralization

Mineralizations in Selakean area accompany arsenopyrite, ore deposits such as Selakean vein accompany sphalerite and chalcopyrite, and contains gold and silver. According to the microscopic observations of lump ore of Selakean vein, chalcopyrite occur in sphalerite as exsolution dot and lamerae. Exsolution of sphalerite and chalcopyrite is said to result in 550°C ~ 350°C (Schwartz 1931, Borchert 1934, Burger 1934) and with accompaniment of arsenopyrite, Selakean Mineralization is considered to be ore deposit of hypo-aethothermal type.



HISTOGRAM FOR Cu

Cu

N	CLASS LIMIT	FREQUENCY	CUMULATED FREQUENCY	CUMULATED FREQUENCY IN PER CENT
1	126.0000- 104.7980	1	1	3.23
2	104.7980- 87.1636	0	1	3.23
3	87.1636- 72.4966	6	7	22.58
4	72.4966- 60.2976	3	10	32.26
5	60.2976- 50.1513	4	14	45.16
6	50.1513- 41.7123	6	20	64.52
7	41.7123- 34.6934	6	26	83.87
8	34.6934- 28.8555	3	29	93.55
9	28.8555- 24.0000	2	31	100.00

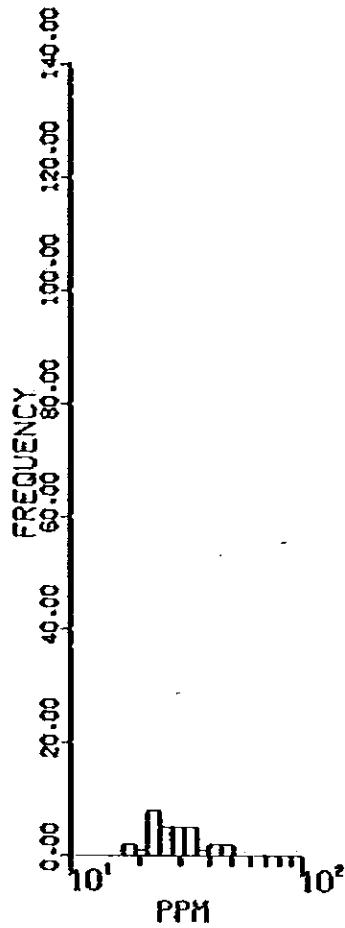
LOG INTERVAL= .8001770E-01

MEAN= .5002832E+02 STANDARD DEVIATION= .1638825E+00

THRESHOLD(1)= .1064096E+03 THRESHOLD(2)= .7296228E+02

Fig. 3-10 Histogram for Cu of Geochemical Analysis in Selakean Area

# HISTOGRAM FOR Pb



PB

N	CLASS LIMIT	FREQUENCY	CUMULATED FREQUENCY	CUMULATED FREQUENCY IN PER CENT
1	51.0000- 45.1395	2	2	6.45
2	45.1395- 39.9524	2	4	12.90
3	39.9524- 35.3614	1	5	16.13
4	35.3614- 31.2980	5	10	32.26
5	31.2980- 27.7015	5	15	48.39
6	27.7015- 24.5182	5	20	64.52
7	24.5182- 21.7008	8	28	90.32
8	21.7008- 19.2071	1	29	93.55
9	19.2071-	2	31	100.00

LOG INTERVAL= .5301347E-01

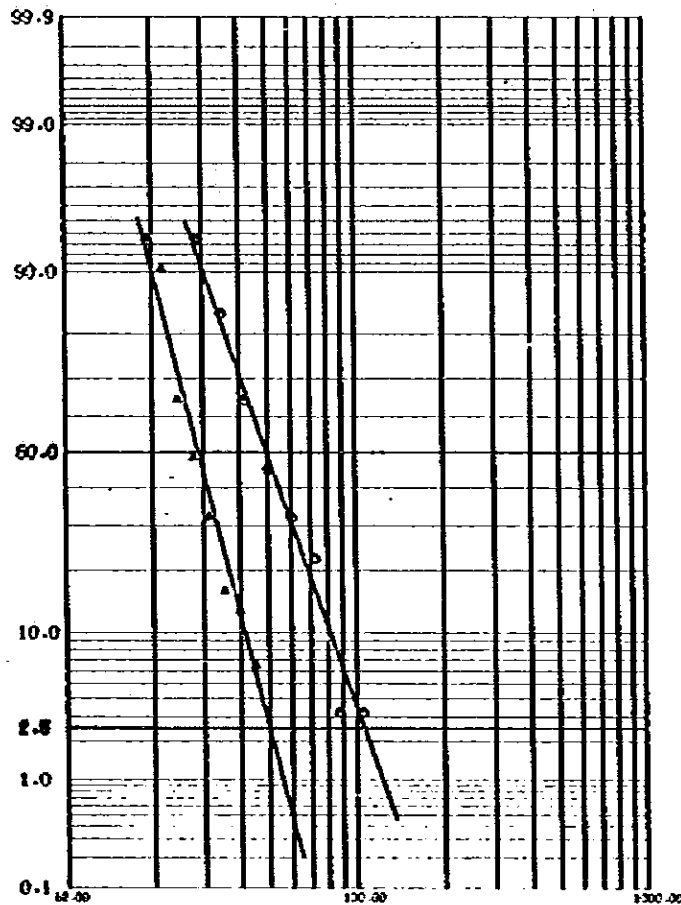
MEAN= .2837673E+02      STANDARD DEVIATION= .1113085E+00

THRESHOLD(1)= .4737828E+02      THRESHOLD(2)= .3666662E+02

Fig. 3-11 Histogram for Pb of Geochemical Analysis in Selakean Area

# CUMULATIVE FREQUENCY DISTRIBUTION

○ Cu  
▲ Pb



CU

Y=A+BX

N1= 1    N2= 8    A= .1841012E+03    B= -.3080776E+01  
 X= .5091561E+02    Y= .2724164E+02  
 X= .2296542E+02    Y= .1133499E+03

BACKGROUND= .4973713E+02  
 THRESHOLD= .1033710E+03    TYPE= 1

PB

Y=A+BX

N1= 1    N2= 8    A= .1735377E+03    B= -.4251116E+01  
 X= .3266238E+02    Y= .3468613E+02  
 X= .1414477E+02    Y= .1134066E+03

BACKGROUND= .2851593E+02  
 THRESHOLD= .4945466E+02    TYPE= 1

Fig. 3-12 Cumulative Frequency Distribution for Cu and Pb of Geochemical Analysis in Selakean Area

C.C. = 0.2120

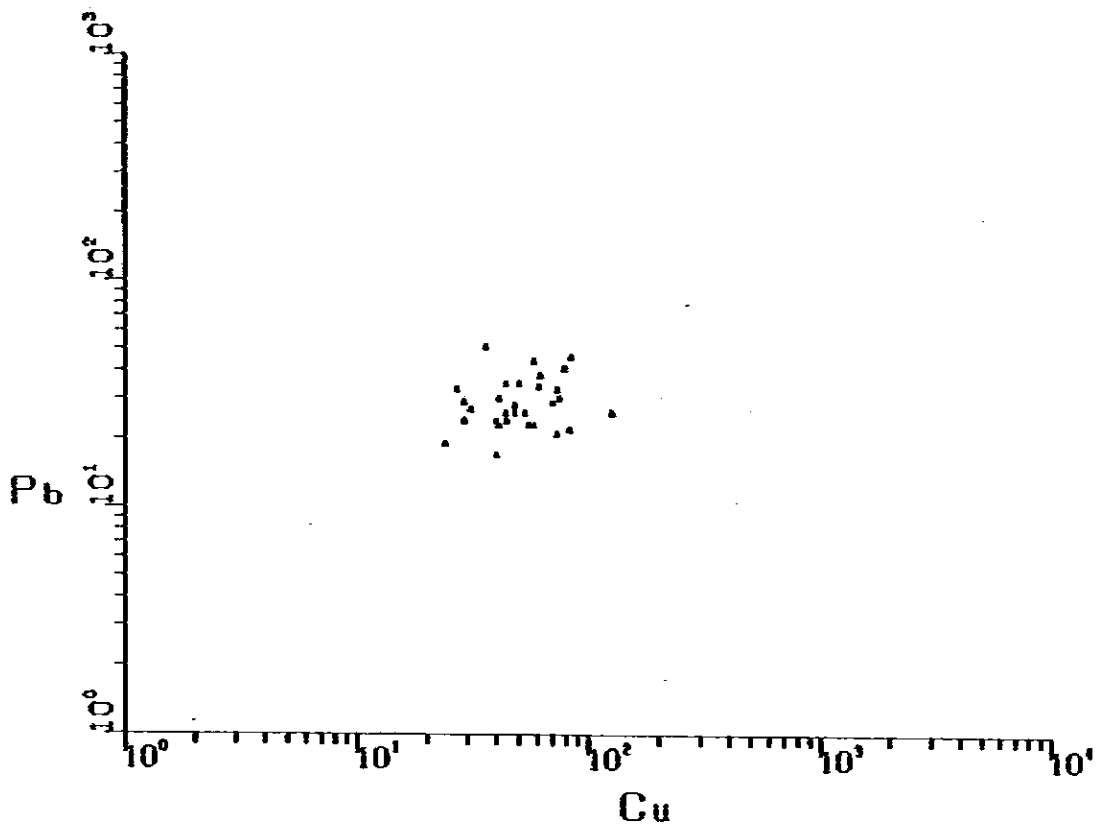


Fig. 3-13 Correlation of Geochemical Elements (Cu and Pb) in Selakean Area

Veins are formed in a fissure of two systems, one striking at  $N15^{\circ} \sim 30^{\circ}E$   $75^{\circ}NW$  and the other striking at  $N10^{\circ} \sim 30^{\circ}E$   $70^{\circ}NE$  and they are distributed in a triangle area (S. Entaggak, S. Mantagak, east hill of G. Julu and S. Melansar area) surrounded by batholith and G. Batu Lumun and G. Serawak intrusive rocks. Also, a copper anomalous area by the geochemical survey tends to show its distribution in these mineralized areas while a lead anomalous area tends to be rather outwardly distributed.

Under the fact, Selakean Mineralization is considered to have been formed by the intrusion of G. Raya granodiorite.

## CHAPTER 3 PANJI AREA

### 3-1 Outline of Geology

In the second phase reconnaissance survey, chalcopyrite dissemination ore was discovered in the branch of S. Jenaham approximately 2 km southeast of old Panji Village, and also tourmaline quartz vein boulders was found around old Panji Village. Also, through the geochemical reconnaissance survey of stream sediments, an anomalous area ranging  $3 \times 4$  km for copper and molybdenum was found, including Panji chalcopyrite dissemination.

The geology at this detailed survey area consists of Jurassic Belango dacitic ~ (quartz) andesitic tuff Formation and G. Sebiawak granodiorite which has intruded into this Formation. Quartz diorite, dolerite, dacitic porphyry have intruded into the above as stock and dyke rocks. (Fig. 3-14)

### 3-2 Stratigraphy and Igneous Rocks

#### 3-2-1 Belango Dacitic and (Quartz) Andesitic Tuff Formation

This stratum consists of dacitic tuff and (quartz) andesitic tuff, altered to sericite, hornfels and silicification through contact metamorphism as the result of intrusion of G. Sebiawak granodiorite, quartz diorite, etc. This Formation is upper than Jirak Formation and SungaiBetung Formation of Bengkayang Group and since it is intruded by Middle Cretaceous G. Raya granodiorite, this stratum is correlated with Jurassic series by the geological reconnaissance survey.

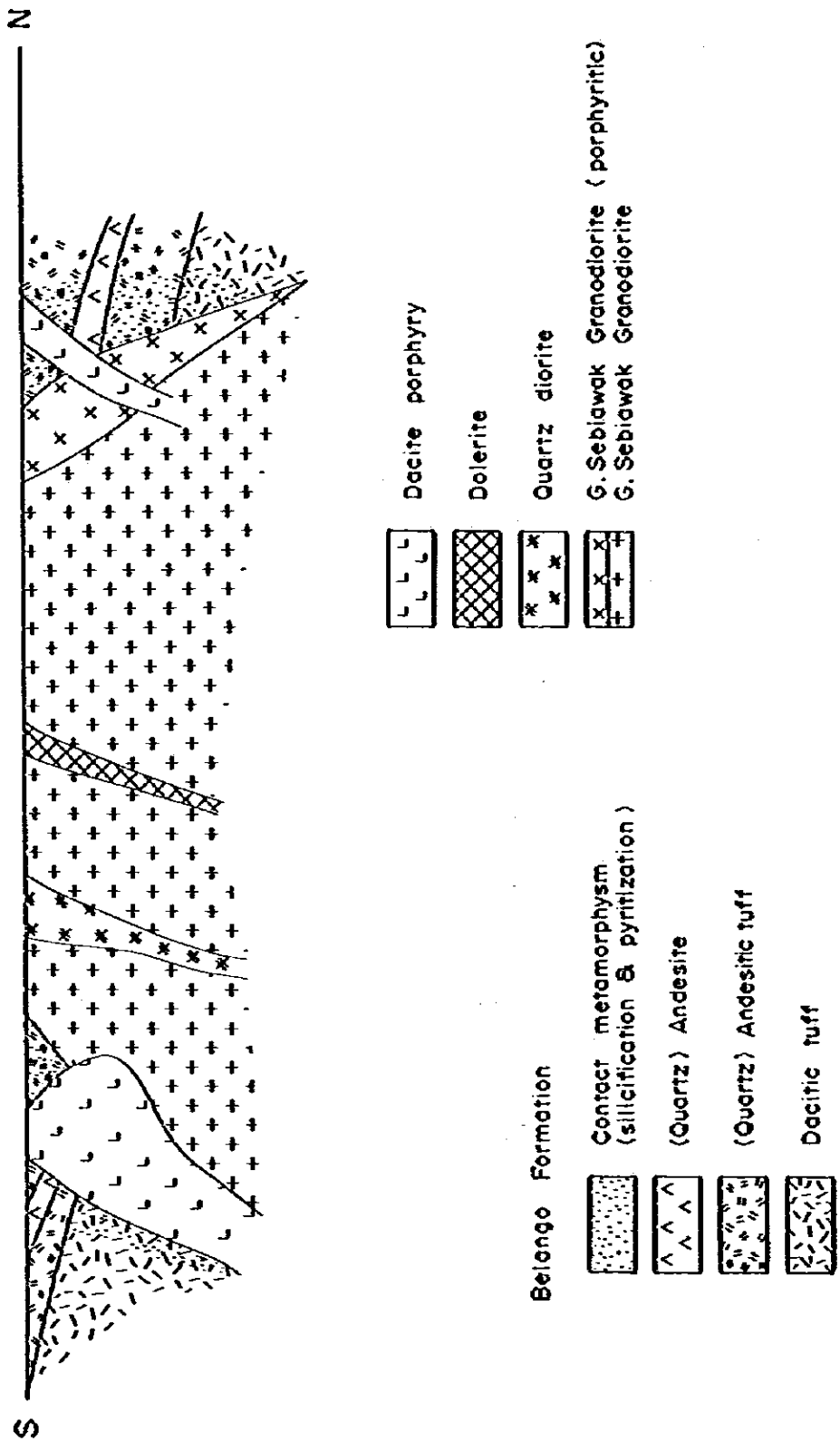


Fig. 3-14 Schematic Geological Profile (Panji Area)

(1) Dacitic tuff:

This rock is distributed in the southwestern region of this detailed survey area (eastern area of S. Merambadu). It is a light grey~grey colored hard rock, partly silicified due to mineralization. It accompanies many quartz veinlets. It is not clear stratigraphic relation between this stratum and andesitic tuff stratum because of their poor exposure. However, based on the second phase reconnaissance survey result and its distribution, this stratum is divided as lower stratum than andesitic tuff.

According to the microscopic observations (Rz-34), the result revealed that less than 1 mm quartz and plagioclase fragment, andesitic rock fragments are observable in the matrix portion consisting of quartz, plagioclase, chlorite, sericite, etc. Rocks subjected to strong hydrothermal alteration (Rz-35) consist of secondary alteration minerals of quartz and sericite, and original texture is unclear owing to that alteration.

(2) (Quartz) andesitic tuff:

It is a dark green~dark black green colored massive hard rock distributed along the southern and northern edges of the survey area, and although quartz grain cannot be observable at field survey with the naked eyes or with a loupe, but under microscope, the result revealed to have quartz or a quartz fragments in the matrix portion, and it was classified as (quartz) andesitic tuff. (Quartz) andesite, having a plagioclase phenocryst, is also intercalated in the (quartz) andesitic tuff stratum.

According to the microscopic observation, it is a lithic tuff, consisting of fragment of quartz, plagioclase and (quartz) andesite has a plagioclase phenocryst andesine with symmetrical extinction (angle of about  $28^\circ$ ) in the groundmass which consists of plagioclase, quartz and sericite. Secondary alteration minerals such as quartz, sericite, biotite, chlorite, etc. occur in both rocks, as hornfelsic alteration product by intrusion of G. Sebiawak granodiorite.



### 3-2-2 G. Sebiawak Granodiorite

#### (1) G. Sebiawak Granodiorite:

The sebiawak granodiorite is coarse to medium grained rock with color index of 5~10%, distributed from east to west covering most of the detailed survey area, having a porphyritic texture at the marginal contact portion with the Belango Formation near S. Koronang. In the second phase reconnaissance survey, this rock was found being widely distributed from southern Darit to the Pahuman area and had a feature of coarse-grained quartz being very conspicuous under weathering. For this reason the rock was distinguished from G. Raya granodiorite and was classified as the G. Raya granodiorite.

#### (2) Chemical compositions and age dating:

Chemical analyses were made on the two samples (Rx-53 and RZ-24) of G. Sebiawak granodiorite. Table 3-4 shows the analysis results since the first phase survey and the volumetric ratio of norm minerals calculated from such analytical results.

Through these analytical results, G. Sebiawak granodiorite contains SiO<sub>2</sub> ranging from 68% to 72%, slightly acidic and as plotted in the triangle diagram of quartz, plagioclase and potash feldspar on the basis of norm minerals (Fig. 3-15), this rock is divided into a group slightly near to granite rather than to G. Raya granodiorite. Furthermore, according to the results plotted in the variation diagram of each oxide and differentiation index (Fig. 3-16), this rock tends to coincide with the tendency of straight line as seen in variation line of granitic rocks in West Kalimantan, and classified into calc-alkali rock series belonging to the same granite group. K-Ar absolute age dating of Sebiawak granodiorite resulted in 124 ± 8 m.y. and they have intruded during Early Cretaceous in age, being slightly older than G. Raya granodiorite (Table 3-3).

Table 3-3 Result of K-Ar Age Determination

No.	Sample No.	Locality	Rock Name	Mineral or Rock	SecAr 40 Rad/9m x 10 <sup>-5</sup>	40 Rad% AR	K%	Aze(m.y.)
1	79RB-24	S. Bamua	Sirih Tonalite	Hornblende	0.213 0.223	48.3 48.9	2.80 2.79	20.0±1.0
2	79RB-52	S. Banyu	Banyu Tonalite	Hornblende	0.126 0.137	30.1 43.9	1.20 1.21	27.8±1.4
3	79RE-50	S. Sakung	Tiang Quartz Diorite	Hornblende	0.367 0.354	73.3 70.0	0.90 0.93	98.6±4.9
4	79RE-19	S. Bala	G. Raya Granodiorite	Hornblende	0.225 0.215	62.9 45.0	0.53 0.53	100.7±5.2
5	80RA-31	S. Molo	Serautak Dacite Porphyry	Whole rock	0.061 0.062	43.1 50.5	0.30 0.31	51.3±2.6
6	80RC-64	S. Empawang	G. Raya Granodiorite	Whole rock	0.702 0.722	86.9 89.7	1.56 1.56	114±6
7	80RD-45	Kp Parikap	" "	Whole rock	0.572 0.586	87.0 88.6	1.28 1.31	111±6
8	80RD-67	S. Serape	Tiang Quartz Diorite	Whole rock	0.267 0.280	66.7 70.5	0.72 0.72	95.1±4.8
9	80RF-52	G. Ganarabak	G. Raya Granodiorite	Whole rock	0.968 1.01	90.8 92.3	2.30 2.30	107±5
10	81RX-53	Panji	G. Sebiawak Granodiorite	Biotite	2.22 2.36	77.4 84.6	4.60 4.60	124±8
11	81QD-1	G. Ibu	Sijanguk	Biotite	0.624 0.626	67.1 61.1	5.22 5.31	30.3±1.5
12	81GD-1	G. Ibu	G. Raya Granodiorite *	Biotite	0.548 0.553	75.3 69.3	4.61 4.63	30.4±1.5

\* G. Raya Granodiorite of G. Ibu. (Different type of G. Raya Granodiorite in the Project Area)

Table 3-4 Chemical Composition and Norm of Constitution Mineral of Granitic Rocks in Project Area

Sample No.	79RR-19	79RR-20	80RC-64	80RC-67	80RD-65	80RE-32	80RE-51	80RY-52	79RQ-59	81RX-53	81R2-24
Rock Name	Gr. dio	Gr. dio	Gr. dio	Gr. dio	Gr. dio	Gr. dio	Gr. dio	Gr. dio	Gr. dio	Gr. dio	Gr. dio
Location	S. Pala	S. Sembawang	Kp. Perudu	Kp. Paritkep S. Depahan	North Kp. Emang	North Kp. Soliat	North Kp. Emang	G. Gamahabak	S. Secona	Panji	G. Kader (Napal)
SiO <sub>2</sub>	69.26	69.63	66.43	63.57	65.17	64.46	71.26	66.11	65.13	71.75	68.97
TiO <sub>2</sub>	0.41	0.40	0.50	0.56	0.63	0.60	0.33	0.42	0.57	0.42	0.48
Al <sub>2</sub> O <sub>3</sub>	14.26	14.14	15.86	16.11	15.08	14.08	14.17	14.69	14.34	13.41	14.36
Fe <sub>2</sub> O <sub>3</sub>	1.42	1.82	2.51	2.76	2.63	2.78	0.93	2.79	3.02	1.22	1.78
FeO	2.97	1.91	2.79	3.54	3.13	3.09	1.89	3.10	2.73	2.30	2.56
MnO	0.07	0.09	0.11	0.14	0.17	0.12	0.09	0.10	0.11	0.15	0.10
MgO	1.11	1.07	1.07	2.28	2.09	2.23	0.98	1.67	2.00	0.82	1.38
CaO	3.35	2.81	4.21	5.27	4.72	4.96	2.59	3.82	4.73	2.66	3.99
Na <sub>2</sub> O	3.56	3.95	3.51	3.14	3.25	3.22	3.54	3.21	2.79	3.75	3.39
K <sub>2</sub> O	2.40	2.42	1.98	1.59	2.01	2.24	2.88	2.99	1.85	2.03	1.60
P <sub>2</sub> O <sub>5</sub>	0.09	0.09	0.15	0.17	0.11	0.16	0.13	0.13	0.08	0.09	0.10
H <sub>2</sub> O(+)	1.17	1.27	0.65	0.46	0.70	0.82	0.72	0.88	2.26	0.95	0.88
H <sub>2</sub> O(-)	0.23	0.36	0.18	0.21	0.19	0.25	0.20	0.24	0.34	0.17	0.24
Total	99.70	99.96	99.95	99.80	99.83	99.61	99.71	99.95	99.95	99.62	99.83
q	29.6	29.3	27.18	23.39	24.89	23.48	31.94	24.79	28.0	34.30	31.62
or	13.9	14.5	11.69	9.40	11.85	13.24	17.03	17.64	11.1	12.02	9.46
ab	29.9	33.6	29.67	26.58	27.47	27.21	29.94	27.16	23.6	31.72	28.68
an	13.9	12.8	19.89	25.03	20.64	19.00	12.02	16.30	21.1	12.63	19.14
c	0.1	1.3	0.66	0.04	-	-	0.83	-	-	0.41	0.04
hc	-	-	-	-	-	1.92	-	0.75	0.6	-	-
wo	-	-	-	-	0.86	1.21	-	0.51	0.4	-	-
en	-	-	-	-	0.59	0.58	-	0.18	0.1	-	-
fs	-	-	-	-	0.20	4.34	-	3.64	4.6	-	-
en	2.8	1.2	2.66	5.67	4.61	2.03	2.44	2.69	1.7	2.04	3.43
fs	2.6	3.6	2.42	3.55	2.56	4.02	2.33	2.69	1.7	2.61	2.62
ma	2.1	2.6	3.63	4.01	3.82	4.02	1.34	4.05	4.4	1.76	2.57
il	0.8	0.8	0.96	1.06	1.20	1.14	0.62	0.80	1.1	0.80	0.91
ap	0.3	0.3	0.37	0.40	0.27	0.37	0.30	0.30	0.3	0.20	0.24
Total	98.0	99.0	99.13	99.13	98.96	98.54	98.79	98.81	97.0	98.49	98.71
qtz-ab	73.4	77.4	68.54	59.37	64.21	63.93	78.91	69.54	62.7	78.04	69.76
D.I.	74.9	78.2	69.14	59.89	64.98	64.48	79.87	70.37	64.6	79.24	70.67
Group	G. Raya	G. Raya	G. Raya	G. Raya	G. Raya	G. Raya	G. Raya	G. Raya	G. Raya	G. Seblauk	G. Seblauk
m.y.	103.7-5.2		114-16	111-16			107-15			124-8	

Abbreviation: Gr. dio: Granodiorite, Qz dio: Quartz diorite Ton: Tonalite, Qz Gab: Quartz gabbro, Gr: Granite.

Sample No.	79RE-30	79RE-32	79RE-50	80RD-67	80RE-5	79RB-24	79RD-52	79RD-72	79RD-28	QD-1	GD-1	80-NG-200	81-RY27
Rock Name	Gr	Gr	Qz dio	Qz dio	Qz dio	Ton	Ton	dac	Qz Cab	Qz dio	Gr. dio	ac. ff.	and ff.
Location	S. Pehen	S. Sembuan	S. Pehen	S. Soraps	Kp. Sempur anch	S. Banua	S. Banyu	S. Sarantak	G. Pandang	G. Ibu	G. Ibu	G. Sarantak	S. Kader2
Chemical Composition	SiO <sub>2</sub>	69.82	74.77	59.78	60.92	67.31	69.26	70.11	54.37	62.13	63.59	77.03	71.77
	TiO <sub>2</sub>	0.40	0.20	0.63	0.87	0.54	0.47	0.35	0.63	0.75	0.59	0.18	0.42
	Al <sub>2</sub> O <sub>3</sub>	13.53	13.03	16.03	15.77	15.80	15.45	13.94	18.69	16.84	16.09	7.80	12.77
	Fe <sub>2</sub> O <sub>3</sub>	1.80	1.62	2.81	3.41	2.18	1.66	2.16	1.21	2.87	2.44	2.04	2.08
	FeO	2.04	1.09	4.81	4.07	2.94	1.91	1.66	6.23	3.19	2.71	1.21	2.49
	MnO	0.06	0.06	0.08	0.16	0.14	0.06	0.05	0.05	0.13	0.11	0.06	0.05
	MgO	1.17	0.45	3.29	2.78	1.59	1.61	1.20	3.93	2.51	1.92	1.09	0.33
	CaO	1.80	2.14	6.92	3.95	5.20	3.99	2.63	7.59	5.36	4.63	6.58	7.03
	Na <sub>2</sub> O	4.02	4.23	3.00	3.46	3.93	4.19	3.78	3.78	3.89	3.96	1.40	1.41
	K <sub>2</sub> O	3.12	2.66	1.06	0.83	0.95	2.40	1.95	0.27	0.63	2.15	0.37	0.39
	P <sub>2</sub> O <sub>5</sub>	0.09	0.08	0.09	0.27	0.20	0.12	0.09	0.11	0.08	0.20	0.07	0.15
	H <sub>2</sub> O(+)	1.86	0.93	1.52	1.17	0.70	0.93	1.68	1.04	2.50	0.79	1.98	0.86
	H <sub>2</sub> O(-)	0.12	0.29	0.12	0.19	0.15	0.19	0.36	0.05	0.36	0.18	0.26	0.21
	Total	99.83	99.74	100.14	99.85	99.61	99.95	99.64	99.89	100.13	100.06	99.84	100.07
C.I.P.V. Note	q	28.5	36.9	18.0	20.50	24.91	30.2	29.3	5.8	19.09	19.48	55.76	47.30
	or	18.4	15.6	6.1	4.90	5.62	11.7	1.7	3.9	7.29	12.69	2.17	2.28
	ab	34.1	35.7	25.2	29.26	33.24	33.0	44.6	32.0	32.92	33.50	11.85	11.90
	an	9.1	7.5	27.3	25.06	22.67	17.8	12.2	32.0	24.84	19.78	13.91	27.39
	c	0.6	0.8	-	-	-	-	0.7	0.4	-	-	4.18	-
	he	-	-	-	-	-	-	-	-	-	-	-	-
	wo	-	-	2.6	1.13	0.77	0.5	-	-	1.9	0.19	0.91	3.44
	en	-	-	1.5	0.70	0.42	0.3	-	-	0.1	0.13	0.59	2.71
	fa	-	-	0.9	0.36	0.32	0.1	-	-	0.1	0.05	0.27	0.34
	en	2.9	1.1	6.7	6.21	3.53	3.7	3.0	3.3	9.6	4.12	4.19	0.05
	fa	1.7	0.9	4.5	3.15	2.64	1.5	0.5	4.1	9.4	2.41	1.92	0.17
	mag	2.5	2.3	4.2	4.95	3.17	2.3	3.2	2.1	1.9	4.16	3.54	3.01
	il	0.8	0.9	1.2	1.65	1.03	0.9	0.9	0.8	1.2	1.42	1.12	0.35
	ap	0.3	1.0	0.3	0.64	0.47	0.3	0.7	0.3	2.0	0.47	0.37	0.17
Total	97.9	98.1	98.5	98.51	98.79	99.5	98.0	98.8	99.9	99.09	98.36	97.84	98.91
qorwab	82.0	79.5	49.3	54.66	63.77	72.1	77.6	75.6	41.7	59.30	65.67	-	-
D.I.	82.7	81.0	50.1	55.48	64.55	72.5	79.5	79.2	41.7	59.84	66.76	-	-
Group	Granite	Granite	Tiang Q.D.	Tiang Q.D.	Tiang Q.D.	Birih Ton	Banyu Ton	Serantak	G. Pandan	G. S. Languk	G. Raya	Banan F	Belango F
mg			98.624.9	9554.8	9554.8	20±1.0	27.8±1.4	51.3±2.6	30.3±1.5	30.3±1.5	30.4±1.5		

\* strong hornfelsic alteration.

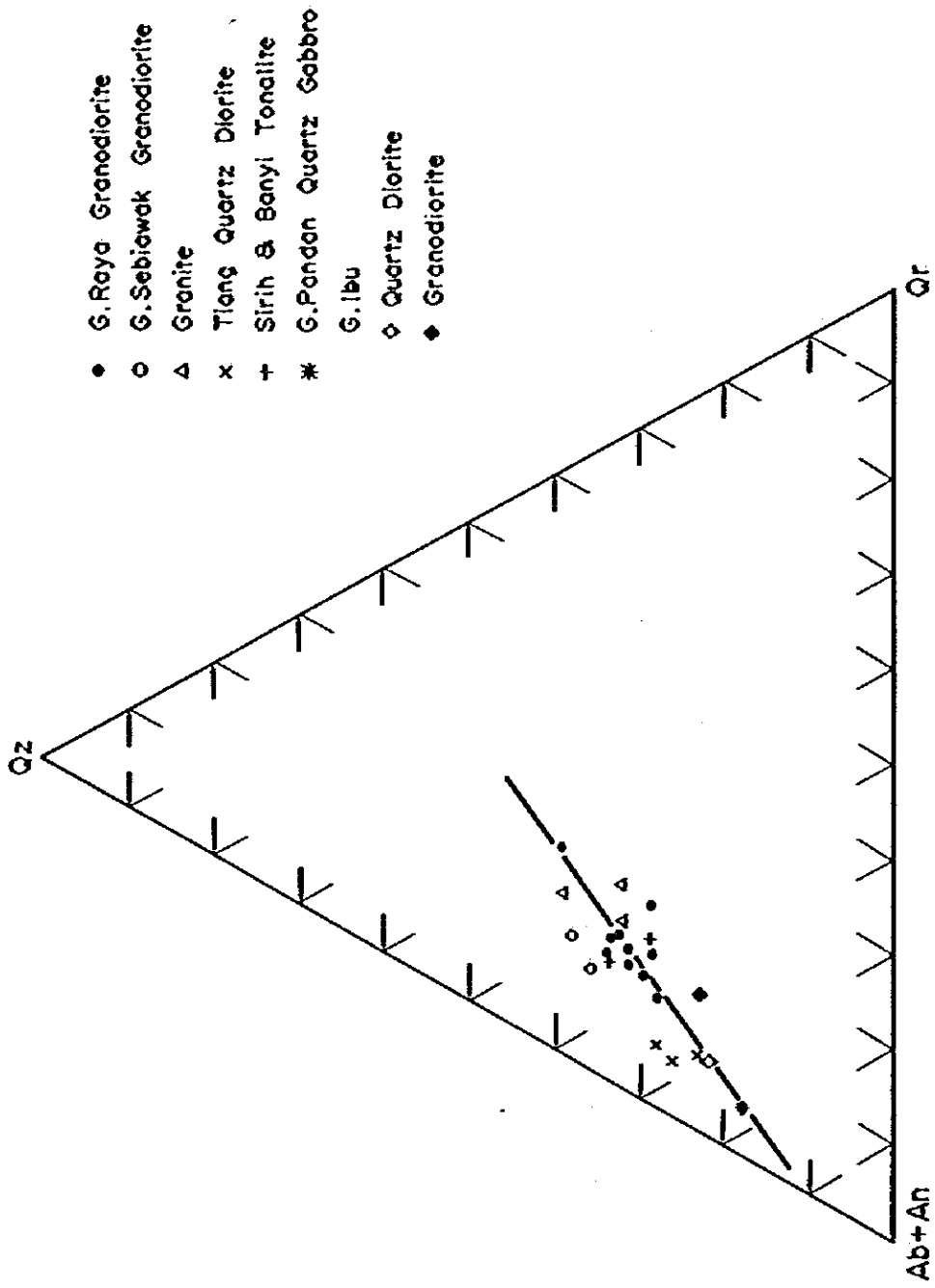


FIG. 3-15 Normative Q - Pl (Ab+An) - Or Diagram of Granitic Rocks in Project Area

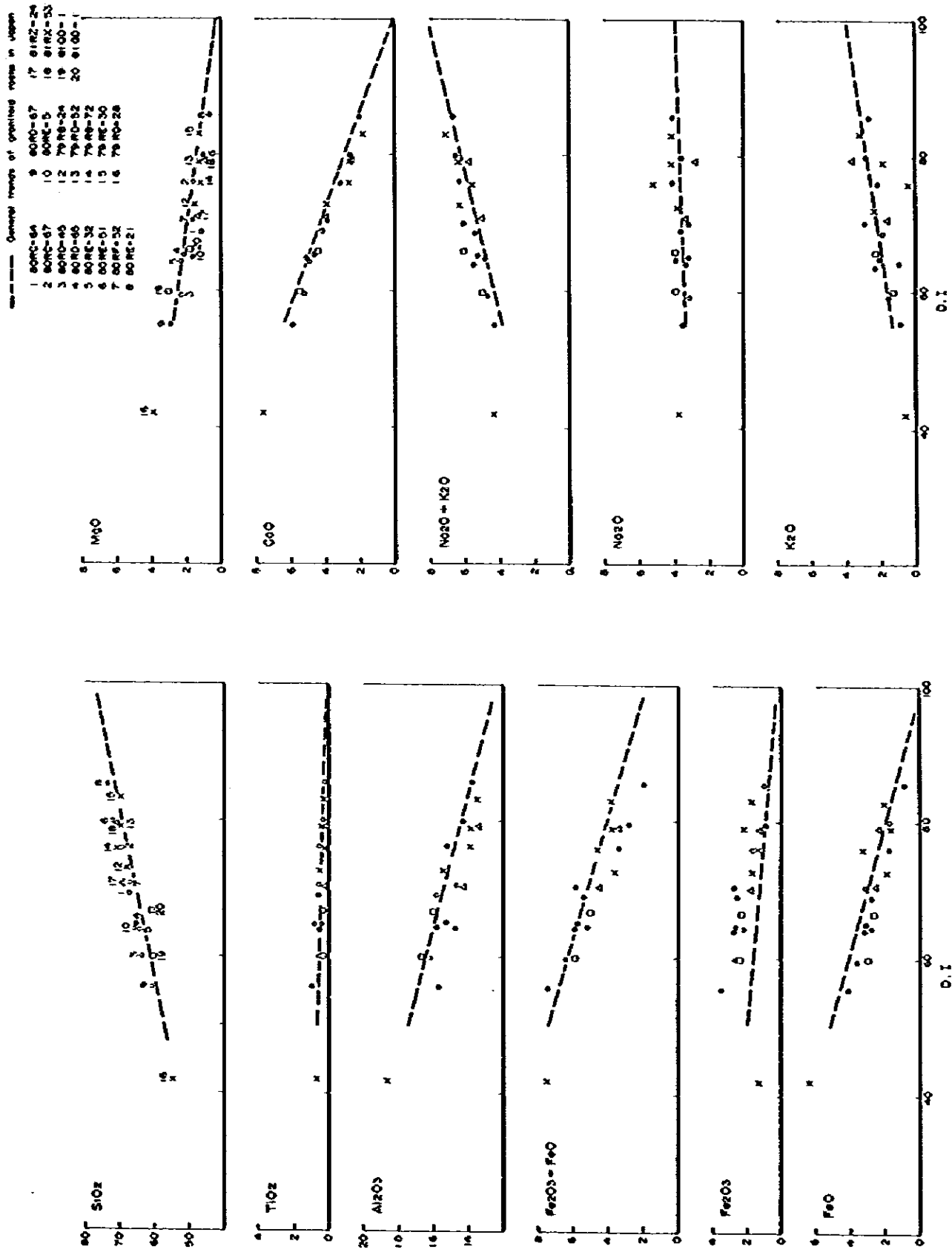


Fig. 3-16 Variation Diagram of Granitic Rocks in Project Area

### 3-2-3 Other Igneous Rocks

#### (1) Quartz diorite:

While G. Sebiawak granodiorite contains fine-grained melanocratic and holocrystalline autolith, boulders and outcrops of quartz diorite are extensively distributed in S. Sikap and S. Menjalin. Since their lithology and rock facies resemble Tiang quartz diorite, having a color index of 30 in dark grey with a equigranular texture, these rocks were classified into quartz diorite dyke and intrusive stock. According to the microscopic observations (Rx-37, Rz-51), the result revealed that this rock is a fine-grained holocrystalline and comparatively fresh, consisting of quartz, plagioclase, green-brown hornblende and a little quantity of biotite.

#### (2) Dolerite dykes:

Dolerite dykes, having a dark green color with a medium granular texture, are distributed in the branching point of S. Jenaham and S. Baba and S. Tapis, having the strikes at NNE ~ SSW. The constituent minerals are plagioclase, hornblende, pyroxene and a minor quantity of biotite, including a very few of quartz. The rocks show a dolerite texture.

Dolerite is interpreted as a clear continuous lineament, through photogeological interpretation. Distribution of dolerite dyke extensions was found in the second phase survey and the extensions were tracked 10 km. In view of all these facts, it is a dyke intruded into a long elongated NNE ~ SSW tectonic line.

#### (3) Dacitic porphyry and granodiorite porphyry:

At the upperstream of S. Merambadu branch in the southwestern region of the survey area and S. Menjalin in the northern region, dacitic porphyry with plagioclase and quartz phenocryst is distributed as a dyke or intrusive rock.

The rock distributed in S. Menjalin is granodiorite porphyry, consisting of phenocryst of a large volume of quartz, hornblende and

potassium feldspar and a little quantity of biotite and groundmass of quartz hornblende and biotite. (Rx-33)

The rock distributed in the branch of S. Merambadu is dacitic porphyry having quartz and hornblende phenocryst on a quartz hornblende groundmass. These porphyries are classified into Serantac type dacitic porphyry since their rock facies resemble this type.

### 3-2-4 Quaternary

Inconsolidated sediments, consisting of gravel, sand and silt, are distributed in the river basins of main rivers such as S. Jenaham, S. Bayung and S. Napal.

### 3-3 Geological Structure

Because rock exposures were bad in this survey area, geological structure such as faults and folds were not identified. However, some lineaments were interpreted in aerophotographs.

The most conspicuous lineament is dolerite dyke and dacite intrusive NNE ~ SSW trend lineament. Especially, the lineament which runs along a dolerite dyke, also continues to the north and south outsides of the survey area, and it is considered to be a conspicuous tectonic line.

The joint trend of S. Sebiawak granodiorite was projected on the Schmidt's net, resulting in N65°W 70°NW, N40°E 70°SE, N12°W 83°NE and a low dip of N75°W 12°NE, N48°W 48SW.

### 3-4 Mineralization

#### 3-4-1 Outline of Mineralization

Since the rock exposure was poor in the detailed survey area, it was difficult to clarify the total situation of the mineralizations through the geological survey. Confirmed mineralizations including information of mineralized rock boulders and weak mineralized outcrops are shown in the map (Fig. 3-17). These mineralizations can be roughly classified into the following two types in the area.





### LEGEND

Volcanic and Sedimentary rocks		Igneous rocks
	Quartzite	
	Tuffery	
	Granodiorite (G. Sebick)	
	Belongs Formation	

	Mountain
	Pyrite dissemination
	Tourmaline
	Chalcopyrite
	Silicification
	Copper anomaly
	Molybdenum anomaly
	Boundary of Metamorphism
	Lineament

Fig. 3-17 Location Map of Mineralization and Geochemical Anomalies (Panji Area)

**(1) Tourmaline-chalcopyrite mineralization:**

This is Panji Mineralization, accompanying tourmaline, chalcopyrite and pyrite, embedded in G. Sebiawak granodiorite and Belango Formation, extending at the eastern and southeastern parts of old Panji Village.

**(2) (Pyrite) silification zone:**

Silification zone and argillized zone are found near the contact area of Belango andesitic tuff and G. Sebiawak granodiorite, accompanying minor pyrite dissemination. Silification is found in S. Kolonang, S. Koro and southwestern region.

Besides, there are several argillized zones in Panji area, having kaoline mineral as the main constituent clay partly accompanying gibbsite.

**3-4-2 Descriptions on Mineralizations**

**(1) Tourmaline chalcopyrite mineralization:**

In the areas (S. Jenaham, S. Pemate ~ S. Tajir) of EW 1.5 km and SN 2.0 km in the eastern and southeastern parts of old Panji Village, several tourmaline, quartz and chalcopyrite mineralizations are distributed. The main mineralizations are described below (PL 3-7, Fig. 3-17).

**(a) Outcrop RY-39**

A small outcrop is located at 500 m east of old Panji Village. Under microscope, the result revealed to accompany chalcopyrite dissemination (less than 4 mm in grain size) with tourmaline and quartz as its main constituent gangue mineral. Fine grain covellite occurs around chalcopyrite. The analysis of check samples resulted in Au 0.1 g/t, Ag 9.4 g/t, Cu 0.39% and Mo 0.09%.

**(b) Outcrop Rx-59**

A small outcrop is found in the eastern branch of S. Napal (800 m northeast of old Panji Village), consisting of quartz and tourmaline, chalcopyrite and pyrite (1~2 mm in size) dissemi-

nations are observed. Fine covellites are also observable. Check sample analysis resulted in Au < 0.1 g/t, Ag 0.4 g/t and Cu 0.015%.

(c) Outcrop Rx-53

Magnetite and chalcopyrite disseminations were confirmed, having 2.5 m wide outcrop in G. Sebiawak granodiorite exposing in the branch of S. Jenaham (1.2 km southwest of old Panji Village). This mineralization was found in the second phase reconnaissance survey (80 RO-29) and check sample analysis resulted in Au 0.2 g/t, Ag < 0.2 g/t, Cu 0.08% and Mo 0.01% of 2.5 m in width.

Besides, there are small outcrops and boulders with small amount of chalcopyrite disseminations as well as tourmaline mineralization outcrops and boulders as shown in PL3-7 and Fig. 3-17.

In S. Menjalin area in the western area of old Panji and in the south of S. Bayung in the south eastern part of old Panji, pyrite disseminations are extensively detected in G. Sebiawak granodiorite and Belango andesitic tuff.

Judging from the above distribution of mineralizations, Panji Mineralization is generally considered to zone of tourmaline-chalcopyrite mineralization inside and pyrite dissemination outside. Conspicuous alteration zone was not confirmed due to poor exposure.

(2) (Pyrite) silification zone:

(a) S. Koro silification zone

Belango andesitic tuff silification zone is distributed in S. Koro dam cutting. According to the microscopic observations (Rx-23), the result revealed to consist of a large volume of sericite and quartz and a little quantity of chlorite, with plagioclase phenocryst completely altered into clay. Quartz

veinlets are recognized in completed alteration rock. But, check sample analysis resulted in a low ore grade of Au < 0.1 g/t, Ag 0.2 g/t and Cu 0.001%.

(b) S. Koronang clay zone

At the upperstream of northwestern region of the survey area, there is a mineralization zone where Belango andesitic tuff shows a strong argillization. Although the X-ray diffractive analysis (RY-21) detected sericite and some kaoline as clay minerals, sericite is polytype 2  $H_1$ , which shows characteristic peaks between  $d = 4.47 \text{ \AA} \sim 2.99 \text{ \AA}$ . But, mineralization is weak and check sample analysis resulted in Au < 0.1 g/t and Ag < 0.1 g/t.

(c) North Pempadang Perahe silification zone

This silification zone situated in the branch of S. Kerampak in the southwestern end of the survey area is a mineralization where Belango Formation dacitic tuff has been silified. Under microscope (RZ-31, 34, 35), the result revealed to have altered secondary minerals such as quartz, sericite, etc. Especially lithology of sample RZ-35 is completely altered, turning into sericite and clay mineral (kaoline mineral).

This silification zone contains 10 cm wide quartz vein, accompanying white clay. The analysis result shows, however, gold and silver contents are very scarce as shown below.

(Fig. 3-18)

	Vein Width	Au g/t	Ag g/t
RZ-31	2 cm	< 0.1	0.4
RZ-32	7 cm	< 0.1	0.2

### 3-4-3 Argillization Zone

White argillized zone is found in three places along S. Jenaham and one place in the northern area of old Panji Village.

- (a) Outcrop RZ-42 (East of the branching point of S. Jenaham and S. Began)

The X-ray diffractive analysis detected that it chiefly consists of kaoline mineral, accompanying some sericite and quartz. Crystallinity of kaoline is discussed on peak between  $d = 4.48 \text{ \AA} \sim 4.13 \text{ \AA}$  in X-ray diffractive chart as shown in Appendix 6, and according to comparison with these result, the kaoline mineral has low crystallinity, even though its peaks partially overlaps with the peak zone of quartz.

- (b) Outcrops RZ-44 (West of the branch point of S. Jenaham and S. Pituman)

The X-ray diffractive analysis detected that it chiefly consists of Kaoline mineral, with some chlorite. Gibbsite is also contained. (Fig. 3-19)

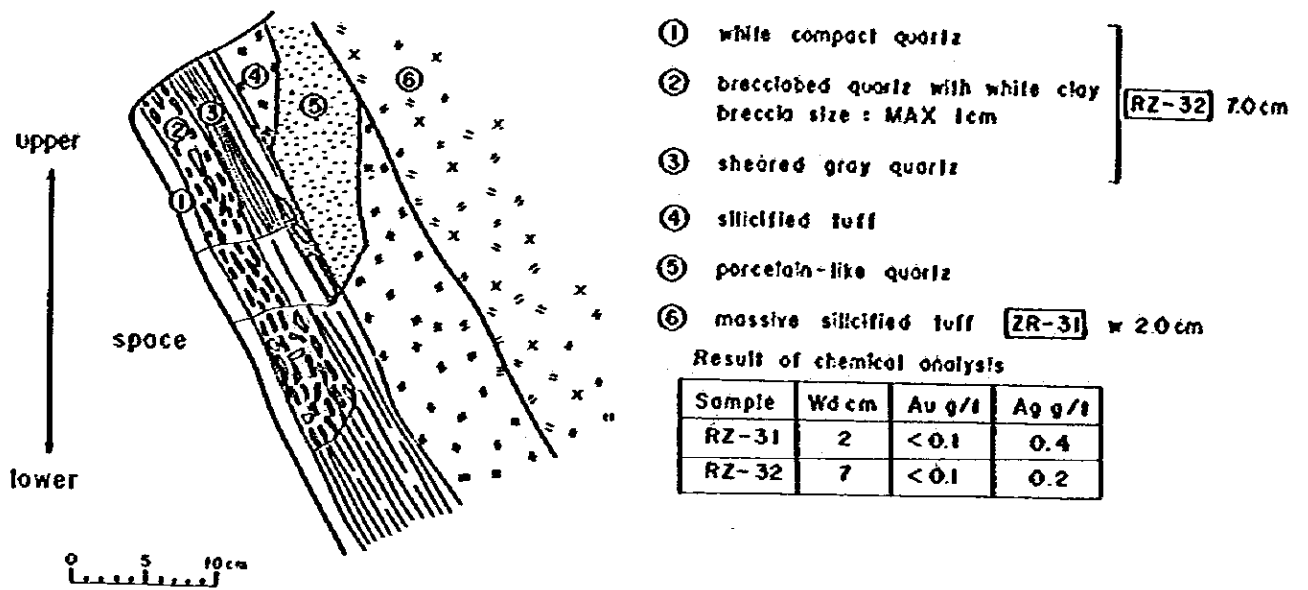
- (c) Outcrop Rx-30 (Upperstream of S. Jenaham)

It is a white clay zone of G. Sebiawak granodiorite exposing for 20 m along S. Jenaham. The X-ray diffractive analysis detected kaoline mineral, sericite and quartz.

- (d) Outcrop Rx-56 (Northern old Panji Village)

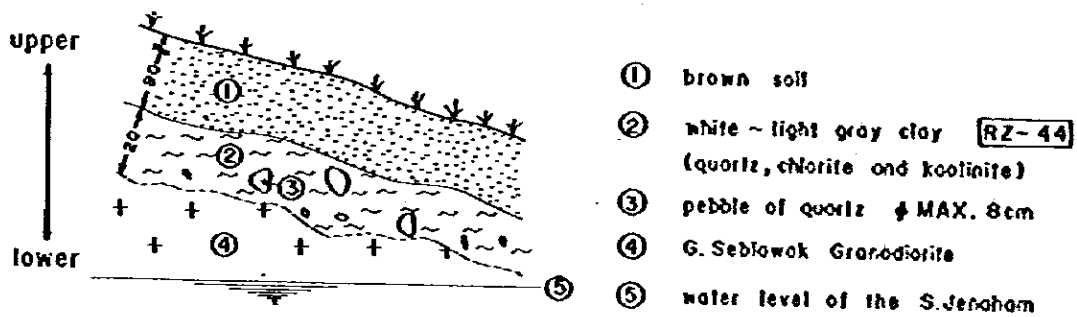
It is white clay, chiefly containing kaoline mineral with some quartz.

All of these clay zones are made of clay chiefly consisting of kaoline mineral (of low crystallinity), partially containing gibbsite. However, since they are not accompanied by any sulphide minerals such as pyrite, chalcopyrite and so on forth, they are considered to be argilization resulting from weathering or low hydrothermal process.



Sketch of mineralization (East of S. Merompöku)

Fig. 3-18 Sketch Map of Mineralization (East of Merampaku) (Panji Area)



Sketch of Alteration zone  
(upper stream of S. Jenahom : 100m west from branch point  
of S. Jenahom and S. Pitunuan)

Fig. 3-19 Sketch Map of Mineralization at West  
of S. Jenahom and S. Pitunan (Panji Area)

### 3-5 Geochemical Survey

#### 3-5-1 Sampling and the Number of Samples Collected

Soil sampling work for the geochemical survey was carried out from B-horizon at the interval of every 200 m along the geophysical survey (IP Survey) line for 20 km (10 lines × 2 km NS) and also selecting five (5) sampling points per km<sup>2</sup> at ridges and summits where having no influence and no contamination from rivers. 196 samples were collected in total, consisting of 110 samples from along IP survey line and 86 samples from other areas. For the pathfinding elements, copper and molybdenum were chosen because disseminated copper ore deposit in granodiorite is expected in Panji area.

#### 3-5-2 Statistical Processing and Interpretation of Analytical Data

In the same way as Selakean area, assay values were standardized by the logarithmic conversion to prepare histogram, and cumulative frequency distribution in order to calculate the mean values, standard deviations and coefficients of correlations of pathfinder elements (Fig. 3-20, 21, 22, 23). Furthermore, the 1st-class anomalous value and the 2nd-class anomalous value were determined from the calculated threshold value (1)  $(M + 2\sigma)$  and threshold value (2)  $(M + \sigma)$  to analyze anomalous areas in the geochemical survey (Table 3-5).

Table 3-5 Value of Mean Standard Deviation and Threshold in Panji Area

Element	n pcs	M ppm	M + $\sigma$ ppm	M + 2 $\sigma$ ppm	Threshold value *ppm	Max ppm	Min ppm
Cu	196	51.1266	137.9785	372.3708	351.5363	514	4
Mo	196	9.3719	16.2552	28.1938	13.0393	123	3

\* Threshold value based on bending point in graph of cumulative frequency distribution.

The threshold value obtained through the cumulative frequency distribution were 351 ppm of copper, according to the Lepeltier method type 1, and 13 ppm of molybdenum according the Lepeltier method type 2.

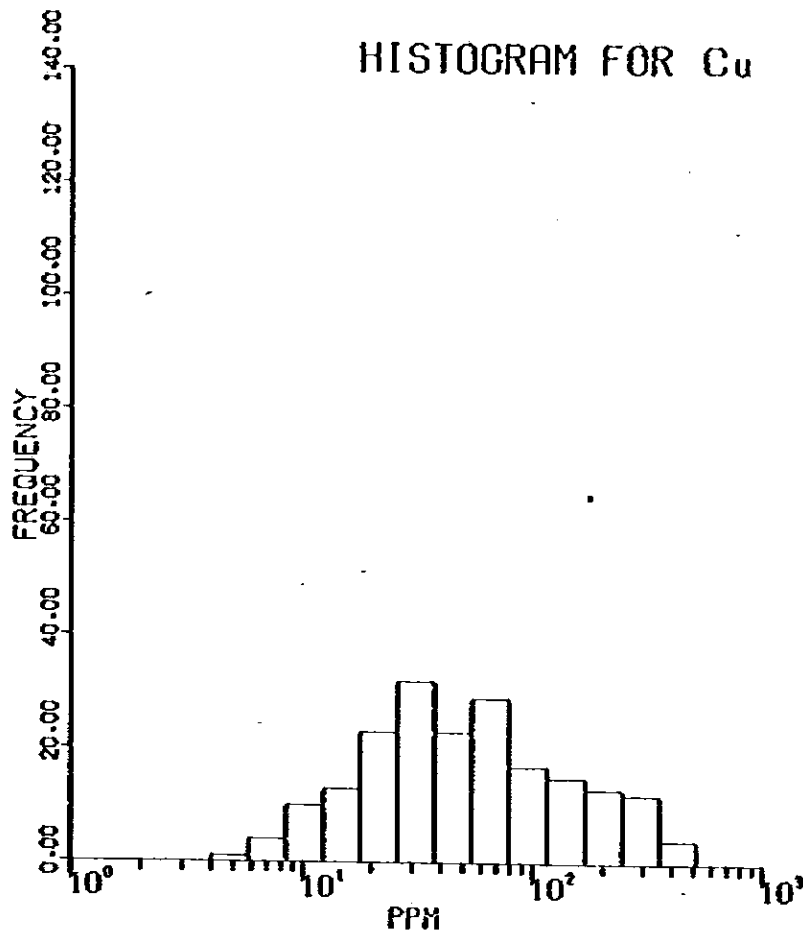
The above assay results indicated the 1st-class copper anomalous area with 350 ppm, the 2nd-class copper anomalous area with 135 ppm, the 1st-class molybdenum anomalous area with 28 ppm and the 2nd-class molybdenum anomalous area with 15 ppm.

The coefficient of correlation is 0.546%. As the result of interpretation of correlation diagram (Fig. 3-23), the correlation between molybdenum and copper is divided into two parent populations of high molybdenum (10~100 ppm) and low molybdenum (under 10 ppm).

### 3-5-3 Anomalous Areas

Distribution of the copper anomalous area (Cu with more than 135 ppm) and the molybdenum anomalous area (Mo with more than 15 ppm) in the geochemical survey are overlapped respectively, and found in the range of 2 km NS and 1.5 km EW in the area where the geophysical survey (IP Survey) was conducted from the midstream of S. Jenaham through the midstream of S. Tapis to the south of S. Jenaham. (Fig. 3-17) This area is within the range which was bordered as tourmaline (copper) mineralization in the geological survey. Especially, the first-class copper anomalous area (Cu with more than 350 ppm) coincides with the first-class molybdenum anomalous area (Mo of more than 28 ppm), occupying the central part in this mineralization range and extending toward NNE ~ SSW lineament. The mean value of copper is 51 ppm and that of molybdenum is 9 ppm but the values of copper and molybdenum of the area when the geophysical survey was conducted are generally higher than mean values in detailed survey area. (PL3-8, PL3-9, Fig. 3-17).





Cu

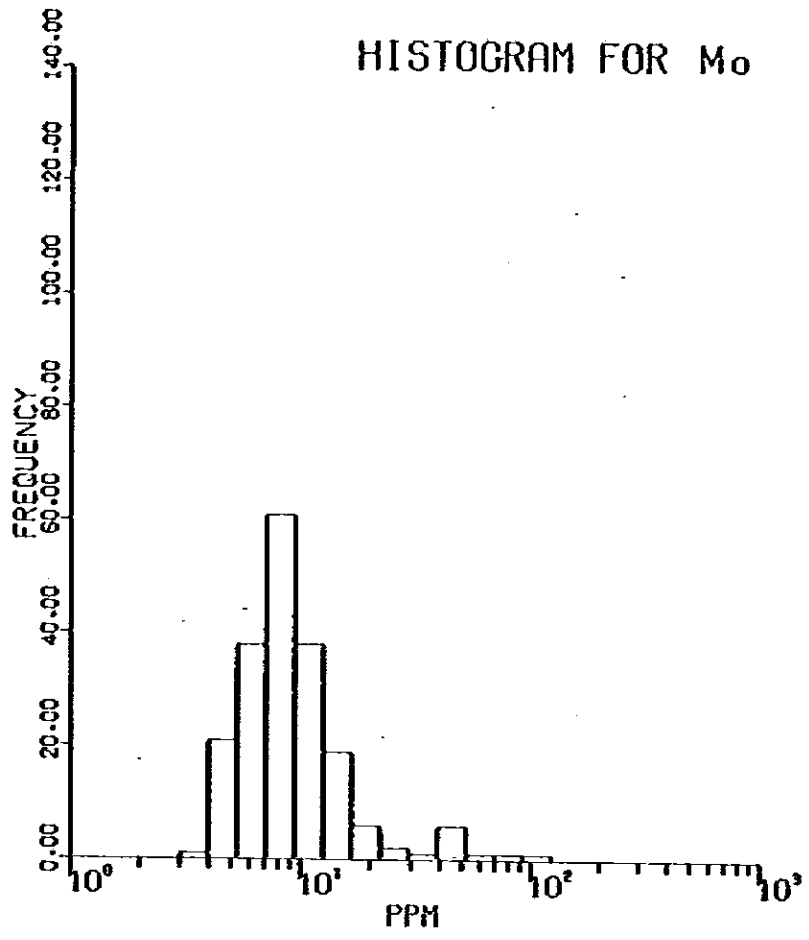
N	CLASS LIMIT		FREQUENCY	CUMULATED FREQUENCY	CUMULATED FREQUENCY IN PER CENT
1	514.0000-	353.7853	4	4	2.04
2	353.7853-	243.5093	12	16	8.16
3	243.5093-	167.6074	13	29	14.80
4	167.6074-	115.3639	15	44	22.45
5	115.3639-	79.4048	17	61	31.12
6	79.4048-	54.6542	29	90	45.92
7	54.6542-	37.6184	23	113	57.65
8	37.6184-	25.8927	32	145	73.98
9	25.8927-	17.8219	23	168	85.71
10	17.8219-	12.2668	13	181	92.35
11	12.2668-	8.4432	10	191	97.45
12	8.4432-	5.8114	4	195	99.49
13	5.8114-	4.0000	1	196	100.00

LOG INTERVAL= .1622233E+00

MEAN= .5112667E+02      STANDARD DEVIATION= .4311640E+00

THRESHOLD(1)= .3723708E+03      THRESHOLD(2)= .1379785E+03

Fig. 3-20 Histogram for Cu of Geochemical Analysis in Panji Area



MO

N	CLASS LIMIT	FREQUENCY	CUMULATED FREQUENCY	CUMULATED FREQUENCY IN PER CENT
1	123.0000-	92.4368	1	.51
2	92.4368-	69.4680	2	1.02
3	69.4680-	52.2065	3	1.53
4	52.2065-	39.2341	6	4.59
5	39.2341-	29.4852	10	5.10
6	29.4852-	22.1587	12	6.12
7	22.1587-	16.6526	18	9.18
8	16.6526-	12.5143	37	18.88
9	12.5143-	9.4051	75	38.27
10	9.4051-	7.0681	136	69.39
11	7.0681-	5.3118	174	88.78
12	5.3118-	3.9919	195	99.49
13	3.9919-	3.0000	196	100.00

LOG INTERVAL= .1240603E+00

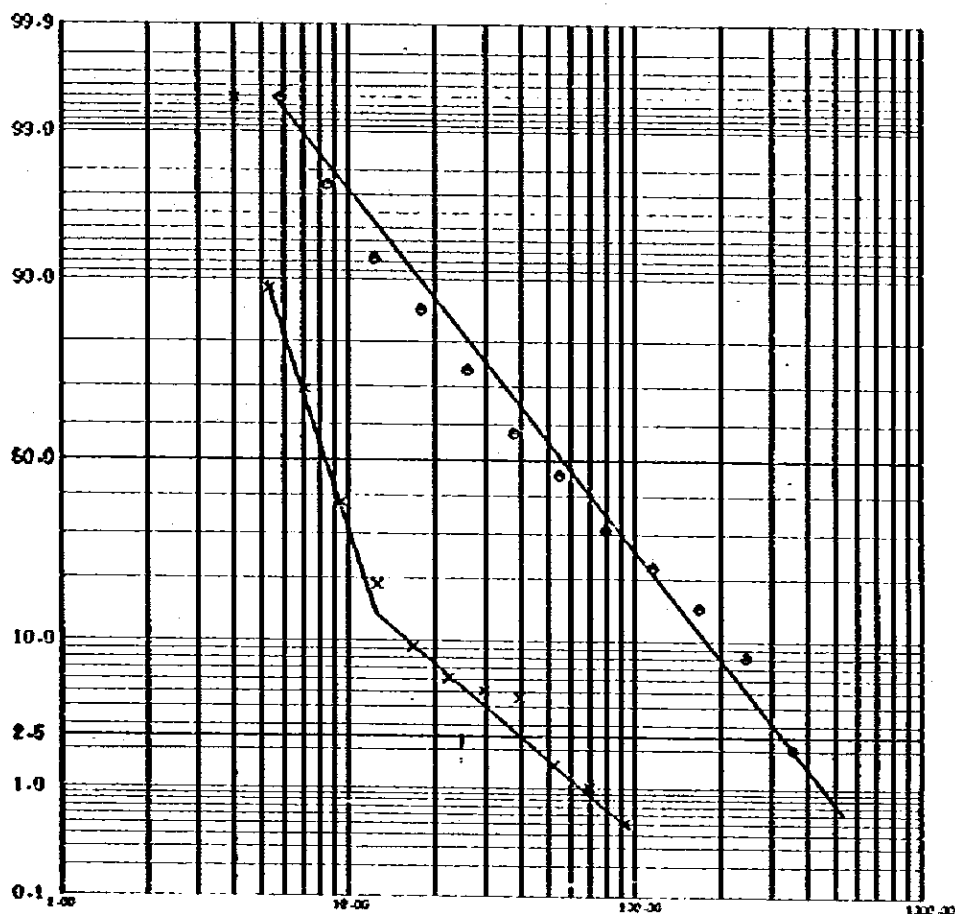
MEAN= .9371938E+01      STANDARD DEVIATION= .2391628E+00

THRESHOLD(1)= .2819389E+02      THRESHOLD(2)= .1625520E+02

Fig. 3-21 Histogram for Mo of Geochemical Analysis in Panji Area

# CUMULATIVE FREQUENCY DISTRIBUTION

o Cu  
x Mo



CU

Y=A+BX

N1= 1      N2=12      A= .1799461E+03      B= -.1194777E+01  
X= .1271821E+03      Y= .2799186E+02  
X= .3813774E+02      Y= .1343800E+03

BACKGROUND= .5329943E+02  
THRESHOLD= .3515363E+03      TYPE= 1

MO

Y=A+BX

N1= 3      N2= 8      A= .9369365E+02      B= -.8694262E+00  
N1= 8      N2=11      A= .2102354E+03      B= -.2855809E+01  
N1=11      N2=12      A= .3045336E+03      B= -.5451096E+01  
X= .8571444E+02      Y= .2517127E+02  
X= .5565128E+02      Y= .5130897E+02  
X= .3633556E+02      Y= .1064710E+03  
X= .2993895E+02      Y= .1410124E+03

BACKGROUND= .8609429E+01  
THRESHOLD= .1303936E+02      TYPE= 2

Fig. 3-22 Cumulative Frequency Distribution for Cu and Mo of Geochemical Analysis in Panji Area

C.C.=0.5467

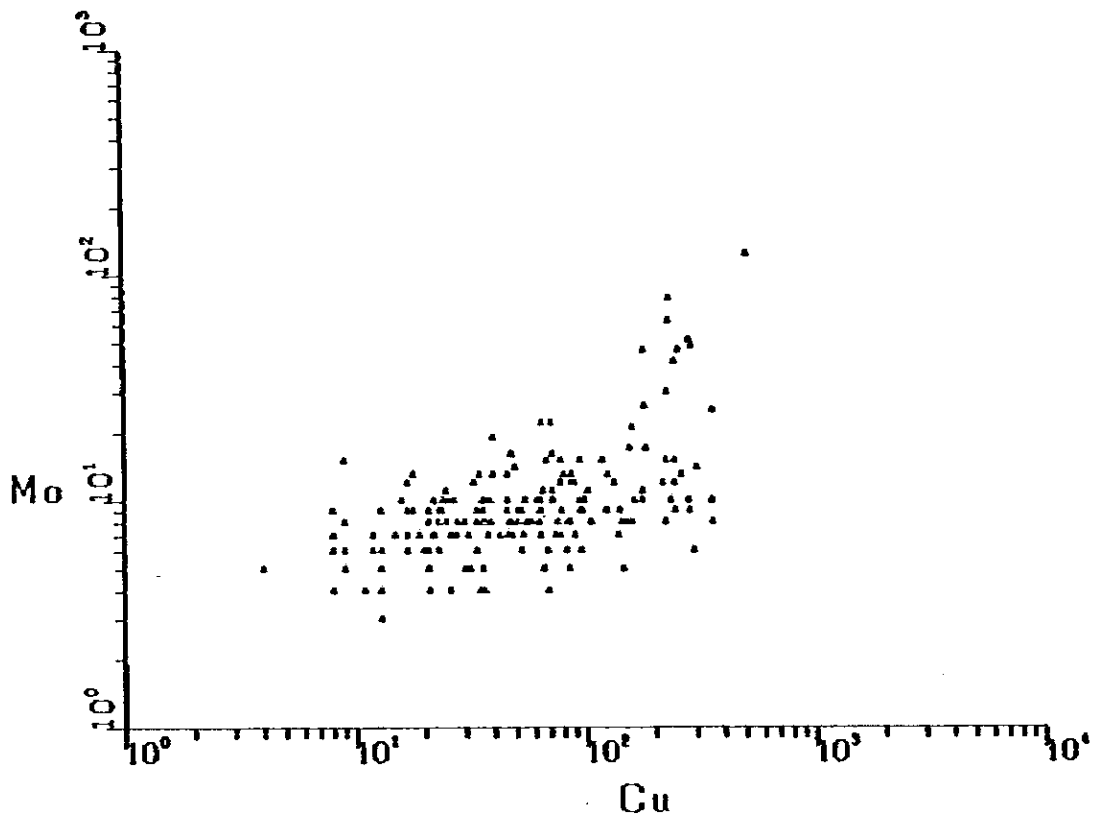


Fig. 3-23 Correlation of Geochemical Elements (Cu and Mo) in Panji Area

### 3-6 Characteristics of Panji Mineralization

Mineralizations distributed in Panji area, copper and molybdenum anomalous areas found in the geochemical survey and interpretation results of the geophysical survey were collectively indicated in Fig. 4-18.

Although the observation of outcrops revealed weak mineralization distribution pattern of Mineralization in Panji area shows a range, extending 2 km EW and 3 km NS, having zoning accompanying pyrite dissemination (S. Napal and S. Menjalin areas and S. Bayung area) outside and tourmaline chalcopyrite mineralization inside, extending NNE ~ SSW direction.

In the central part of this area, rocks are poorly exposed so that no mineralization was discovered except poor pyrite and chalcopyrite disseminations in granodiorite in S. Bagak. However, a copper and molybdenum anomalous areas were found in the geochemical survey situated in the central part of this zone. These anomalous areas are ranging in two directions of NNE ~ SSW and WNW ~ ESE. The tectonic line found in Panji Mineralization is NNE ~ SSW intruding of dolerite dike and dacitic intrusive rocks and interpreted as a lineament by airphotographs, but WNW ~ ESE trend is not clear.

According to the analytical results by the geophysical survey (IP Survey), its anomaly generally coincides with the geochemical survey anomalous areas, especially the northern IP anomaly shows arrangement coinciding with the geochemical survey anomalous area extending WNW ~ ESE. In Panji area, there is a possibility of another latent tectonic line of WNW ~ ESE trend combining with the tectonic line of NEN ~ SWS trend which can be interpreted as a lineament regulating mineralizations in this area.

As a copper (molybdenum) mineralization accompanying tourmaline, there is Banyu area where the second phase survey was conducted in this survey area. Quartz veins accompanying copper and molybdenum are found in G. Bawang, etc. Mineralizations in Panji area are considered to be the same type of mineralization as the above. Therefore, there is a possibi-

lity of younger igneous rocks latently existing, although they were not found in the field survey because of poor rock exposure.

## CHAPTER 4 AGE DATING OF G. IBU GRANITIC ROCKS

### 4-1 G. Ibu Granite

Granodiorite distributed in G. Ibu ~ G. Raya situated 10 km east of Singkawang for 15 km EW and 7 km NS in extensions constitutes a part of granodiorite batholith intruding during Cretaceous period extensively distributed from Central Kalimantan to West Kalimantan.

Chalcopyrite-molybdenum mineralization was found in this area where the Geological Survey of Indonesia conducted a survey of mineral resources under technical collaboration of the Belgium Government in project CTA-19 1974 through 1978. Similar mineralizations are found in areas from Central Kalimantan to West Kalimantan, all of which have been identified, through recent surveys, to have relations with igneous activities during late Cretaceous ~ Tertiary period. The K-Ar absolute age dating was made of younger G. Ibu granodiorite which is deeply concerned with mineralization, in order to examine relationship of mineralization and igneous activities in G. Ibu area.

G. Ibu granodiorites are classified into the following old granodiorites and younger granodiorites in the survey by the Geological Survey of Indonesia (T. Suhandi) (Fig. 3-24).

#### (1) Old granodiorites:

##### (a) Sikancu leucocratic tonalite rock ~ granodiorite

This is medium-grained tonalite rock ~ granodiorite extensively distributed from G. Sijangkung to east G. Ibu.

##### (b) Sendoreng quartz diorite and tonalite rock

This rock is quartz diorite ~ tonalite rock distributed on the southern side of G. Raya.

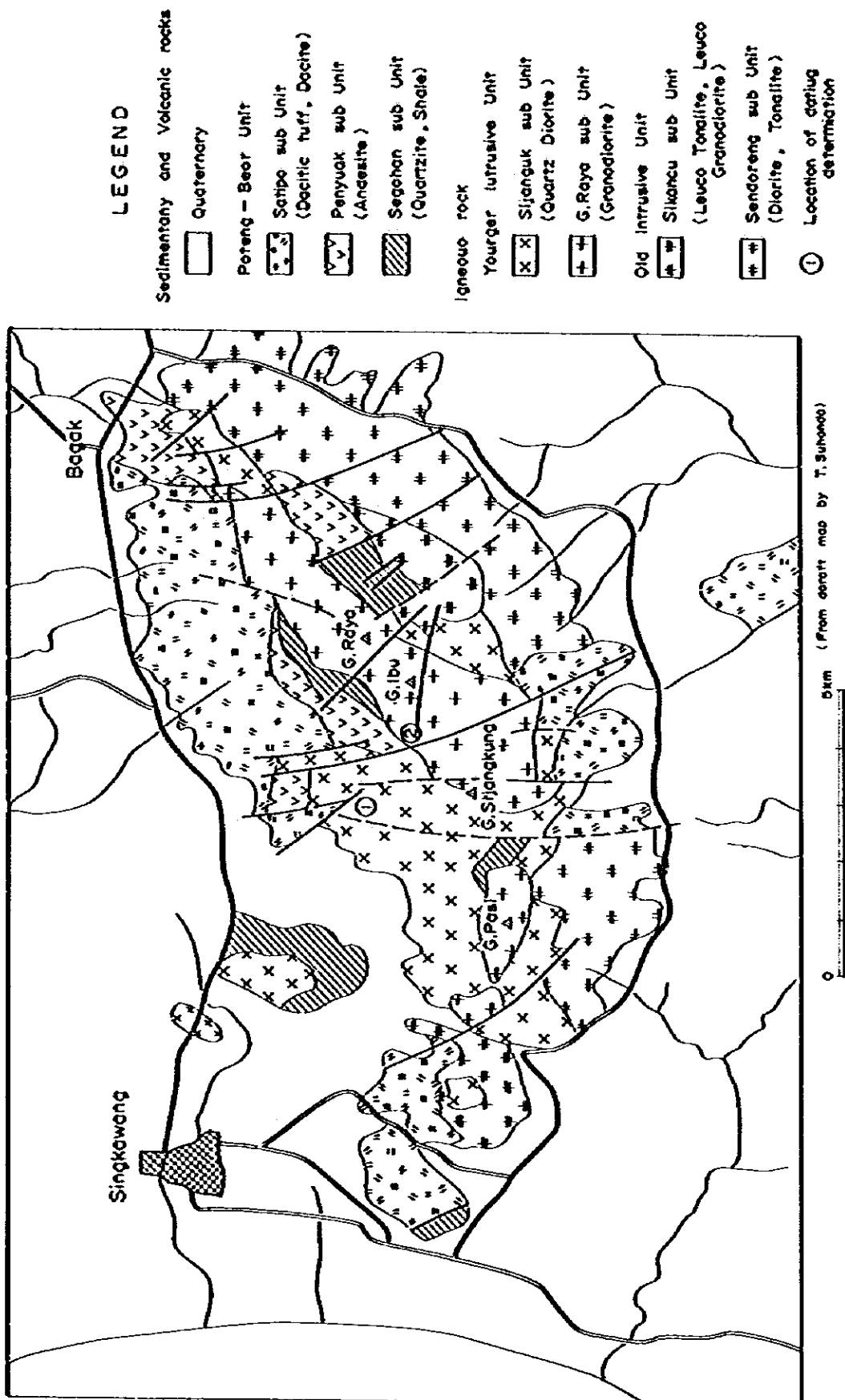


Fig. 3-24 Geological Map of G. Ibu Area

(2) Younger granitic rocks:

This rock is distributed at ridge and on the western side of G. Raya, G. Ibu and G. Sijangkung and classified into the following two rocks by lithology.

(a) Sijanguk quartz diorite

This rock is extensively distributed on the western side of the G. Raya mountain range. Fine grained, holocrystalline 30 of color index. Under microscope (QD-1), the result revealed to consist of plagioclase, quartz, hornblende and sericite, having holocrystalline, equigranular. Hydrothermal alteration zone (sericitization, silicification alteration) is found at the contact with G. Raya granodiorite, of which partial molybdenite chalcopyrite mineralization is recorded (T. Suhandu).

(b) G. Raya granodiorite

This rock covers mountain ridges from G. Ibu to G. Raya and it is considered to be the youngest intrusive rock in this area. It is biotite hornblende granodiorite (GD-1) of medium grain, equigranular holocrystalline and it is lithologically tonalitic rock. (Incidentally, this rock is different from G. Raya granodiorite which was named in West Kalimantan Project CTA-39b).

These granodiorites have intruded into Segohan shale-quartzite Formation, Penuyak andesite Formation and Satipo dacitic Formation (T. Suhandu).

They are considered to be correlative with Bengkayang Group, Jirak Formation, Belango Formation in West Kalimantan project area respectively.

#### 4-2 Chemical Compositions and Age of G. Ibu Granitic Rocks

Modal calculation of G. Ibu granodiorite has been made by the Indoensia-Belgium collaborative geological survey (T. Suhandu). Fig. 3-27 is its quartz-plagioclase-potash feldspar diagram. This trend shows almost the same trend (calc-alkali rock series) as that of modal quartz-plagioclase-potash feldspar diagram (Fig. 3-28).



When the complete analysis result of G. Raya granodiorite, which is classified as the younger granite (GD-1) and Sijanguk quartz diorite is combined with oxide-differentiation index (D-1) variation diagram (Fig. 3-16) and normative quartz-plagioclase-potash feldspar diagram (Fig. 3-15), G. Ibu granodiorite and granodiorites in West Kalimantan survey area are plotted in the same trend. Therefore, they are all considered to belong to the same batholith.

The K-Ar absolute age dating of G. Raya granodiorite (GD-1) and Sijanguk quartz diorite (QD-1) resulted in 30 m.y. both for the former and the latter. Since it intruded approximately the same age as that of Sirih and Banyu tonalites in the West Kalimantan project area and since it is lithologically somewhat close to tonalite from chemical analytical results and microscopic observations, G. Raya granodiorite resembles Sirih and Banyu tonalites.

It is of a great significance for the interpretation of mineralizations in this area that the fact that copper and molybdenite mineralizations found from Central Kalimantan to West Kalimantan resulted from younger igneous activities was confirmed also in the absolute age dating of G. Ibu granodiorite (Fig. 3-25, 26).

The geological relationship of West Kalimantan project area and G. Ibu area is attempted to correlated as Table 3-6.

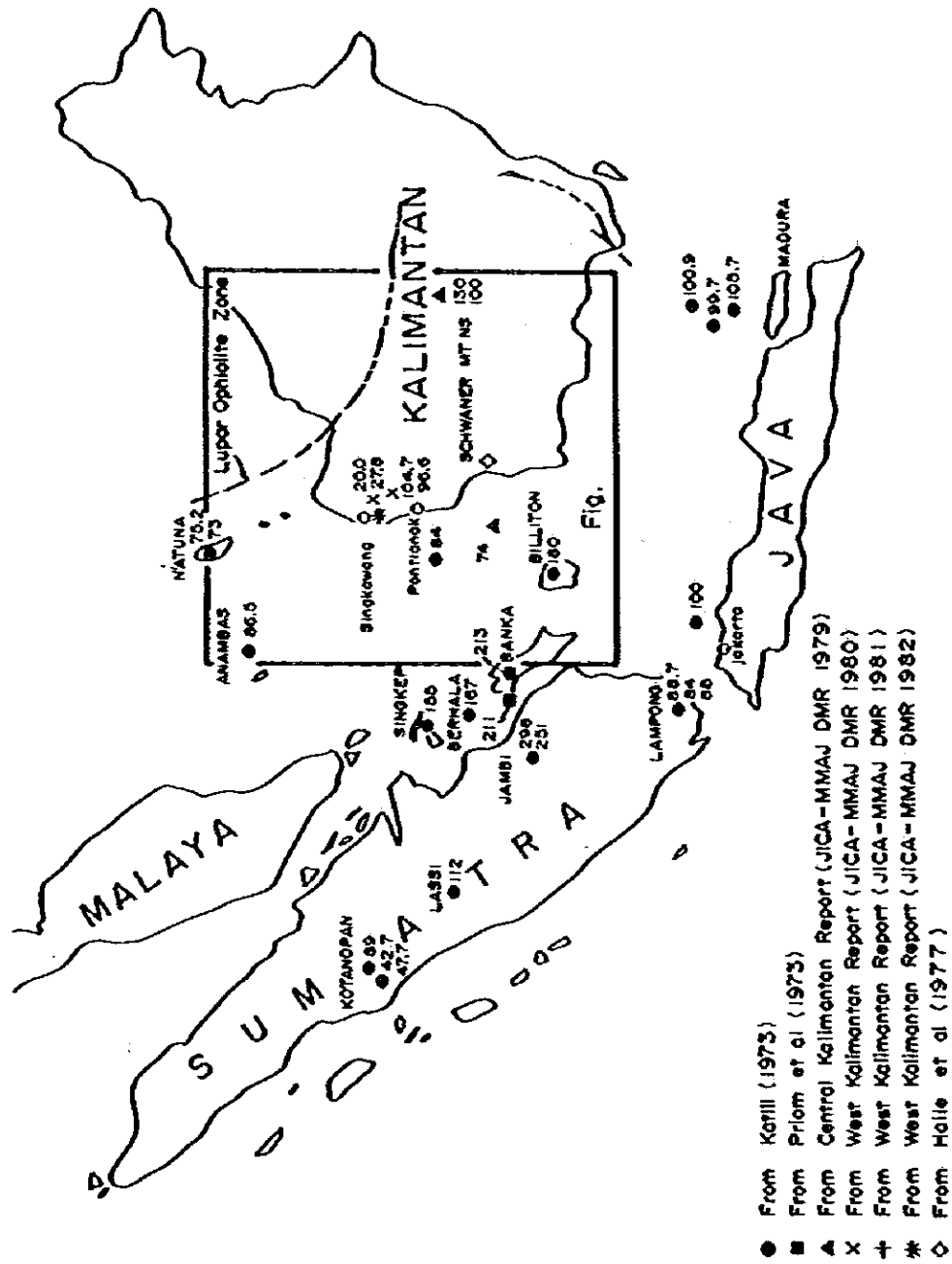


Fig. 3-25 Absolute Age of Granitic Rocks in West Indonesia.

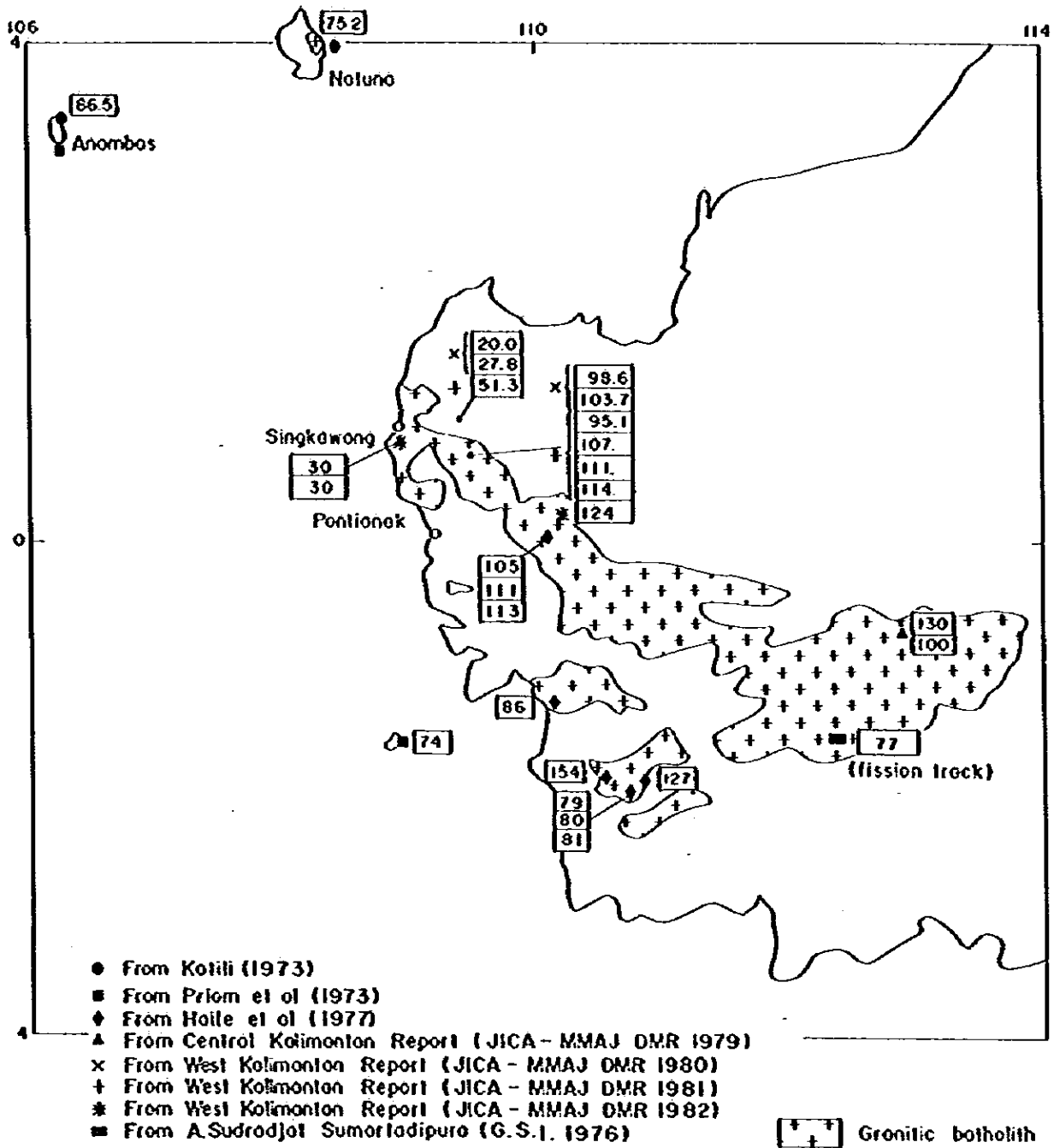


Fig. 3-26 Absolute Age of Granitic Rocks in West Kalimantan

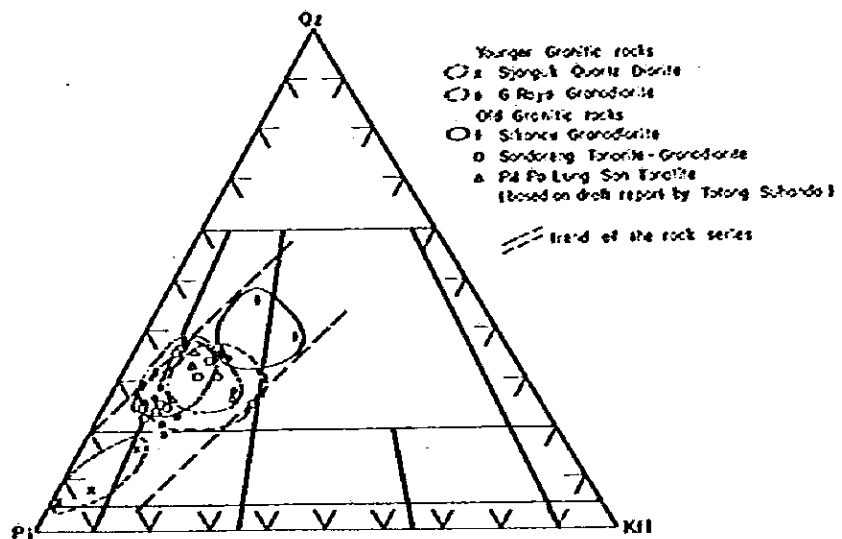


Fig. 3-27 Modal Qz - Pl - Kf1 Diagram of Granitic Rocks in G. Ibu Area

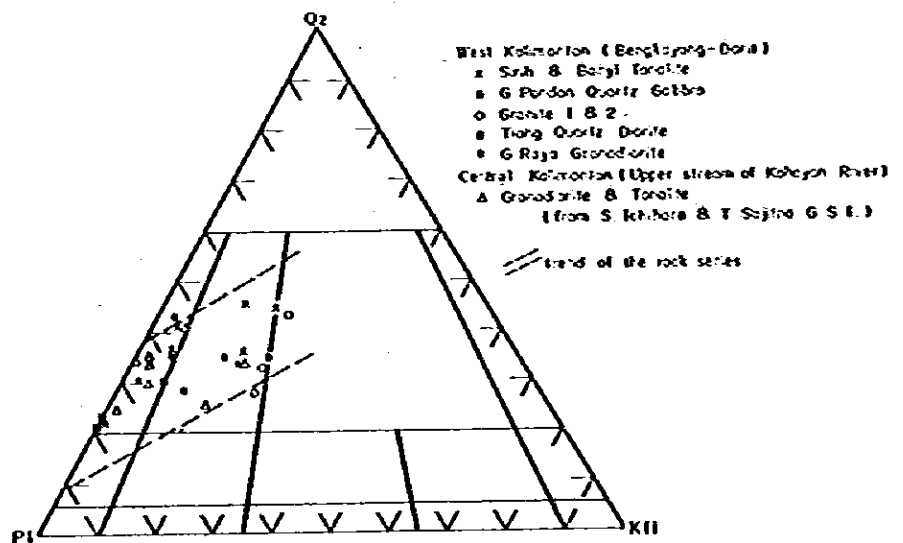


Fig. 3-28 Modal Qz - Pl - Kf1 Diagram of Granitic Rocks in Project Area

Table 3-6 Stratigraphic Correlation of West Kalimantan Area

		West Kalimantan Project Area		G. Ibu Area	
		Formation	Rocks	Formation	Rocks
Quaternary Tertiary Oligocene	Quaternary Banyi & Sirih Tonalite (20 ~ 27 m.y.)	Tonalite		Quaternary Younger intrusive Sijanguk sub Unit (30 m.y.) G. Raya sub Unit (30 m.y.)	Quartz Diorite  Granodiorite-Tonalite
Eocene	Serantak Da- cite & Dacitic pyroclastics (51 m.y.)	Dacite pyroclastic Rocks and Dacite			
Middle- Lower Cretaceous	Tiang Quartz Diorite (95 ~ 98 m.y.)  Raya Grano- Diorite (103 ~ 114 m.y.)  G. Sebiawak Granodiorite (124 m.y.)	Quartz diorite  Granodiorite Tonalite  Granodiorite		Old intrusive Sendoreng sub Unit  Poreng-Beor Unit Sikancu sub Unit	Diorite Tonalite  Tonalite - Granodiorite
Middle- Upper Jurassic	Belango For- mation  Jirak For- mation	Dacitic pyroclastic rocks  Andesite Andesitic pyroclastic rocks		Satipo sub Unit  Penyuak sub Unit	Dacitic tuff, dacite  Andesite
Lower Jurassic Upper Trias- sic	Sungaibetung Formation Riamperaya Formation Kalung Formation Banan Formation	Alternated bed of sandstone, mudstone Sandstone  Black fine sandstone mudstone Tuffaceous sandstone		Segohan sub Unit	Quartzite, shale
		(JICA-MMAJ-DNR project)		(Indonesian and Belgian project)	

**PART IV**

**GEOPHYSICAL SURVEY (IP METHOD)**

## CHAPTER 1 OUTLINE OF GEOPHYSICAL SURVEY

The second phase geological survey in the Panji area has found the chalcopyrite dissemination in a granodiorite, which can presumably be promising for dissemination ore deposits. In the third phase survey, the IP method (induced polarization method) has been conducted to search for the promising ore deposits, as the IP method is one of the most effective methods prospecting for such a type of orebody.

For the purpose of clarifying the lateral extent and the electrical feature of the above-mentioned dissemination zone, the IP survey has been conducted in an area of 3.6 km<sup>2</sup> (1.8 km EW and 2 km NS) south of Old Panji Village. 10 survey lines, 2 km-long in the NS direction and 200 m apart, have been established over there. The separation of the survey stations is 100 m, as shown in PL. 4-1.

In the field IP measurements, apparent resistivities, frequency effects and metal conduction factors have been determined with variable frequencies (0.3 / 3 Hz) in the dipole-dipole configuration and electrode separation coefficients of  $n = 1, 2$  and  $3$ . For interpreting the field IP results, we have measured physical properties of 24 rock specimens sampled in and around the survey area. The rock specimen tests have been completed in Japan together with the analytical work, such as statistical analysis of the IP results, qualitative analysis of plan and section maps and quantitative simulation analysis using high-speed computers.

The computer analysis is applicable to determine the geological structure including mineralized zones by using the IP data obtained along the survey lines. The volume, depth and physical properties can be estimated by computer simulation tests. The thus analyzed results can suggest the possibilities of ore deposits by taking the geological and geochemical results in the survey area into consideration.

## CHAPTER 2 IP METHOD

### 2-1 General

#### 2-1-1 Principles of Measurement

The IP method (Induced polarization method) is one of the most effective direct prospecting methods which are applicable to metal mines, especially sulfide ore deposits. The principle of the IP method is based on the physical fact that the electrical polarization phenomenon is induced in metal ore deposits by the electric current sent into the ground. The IP phenomenon is conspicuously appeared in sulfide minerals such as pyrite and chalcopyrite. The cause of the phenomenon is presumed as polarization induced on the boundary layer between metal ore and included liquid.

There are two types of IP field surveys: time domain method and frequency domain method.

- (1) Time domain method: A square pulse of current is sent into the ground, and then the voltage decay is measured during the no-current period. This method is also called transient method or pulse method.
- (2) Frequency domain method: When a square-wave alternative current is supplied into the ground, the voltage varies with frequencies of the current. The frequency-response variation is measured, so that this method is sometimes called variable frequency method.

For the present survey the latter method has been adopted by using the dipole-dipole electrode configuration with low frequencies of 0.3 and 3 Hz.

#### 2-1-2 Dipole-Dipole Method of Operation

The outline of the dipole-dipole array is shown in Fig. 4-1.

The current electrodes A and B are located on a survey line with a given separation of  $a$ , and the current  $I$  is supplied by the transmitter. On the other hand, the potential electrodes M and N are located on the same



line with a separation of  $a$ . The separation between the nearest current and potential electrodes is chosen to be  $na$  ( $n$ : integer number), as shown in Fig. 4-1. For the first step of measurement,  $n$  is usually taken as 1. The receiver measures the voltage  $V$  between the electrodes M and N. In this case, the voltage is measured at frequencies of 0.3 Hz and 3 Hz, and the correspondent AR and FE are calculated by Eqs. (1) to (3) (refer to 2-1-3). In actual surveys, the FE is indicated directly on a meter of the receiver.

After the first step  $n = 1$  of measurement is finished, the current electrodes A and B are removed, and then the measurements are repeated for the second and third steps  $n = 2$  and 3. After the three steps of measurement are completed, the potential electrodes M and N are transferred to the neighboring stations. Similar measurements from each pair of current electrodes are repeated for the transferred potential electrodes. The electrode separation  $a$  is taken to be 100 m for the present survey.

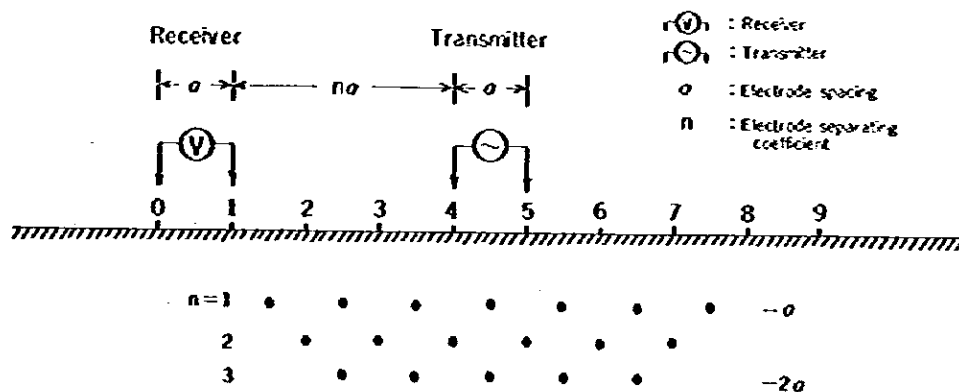


Fig. 4-1 IP Measurements of Dipole-Dipole Configuration

### 2-1-3 IP Characteristics

#### (1) Frequency Effect (FE)

In the frequency domain method, the IP response is expressed by a quantity which is defined as

$$\begin{aligned}
 FE &= \frac{V_{0.3\text{Hz}} - V_{3\text{Hz}}}{V_{3\text{Hz}}} \times 100(\%) \\
 &= \frac{\rho_{0.3\text{Hz}} - \rho_{3\text{Hz}}}{\rho_{3\text{Hz}}} \times 100(\%) \quad (1)
 \end{aligned}$$

Where  $V_{0.3\text{Hz}}$  and  $V_{3\text{Hz}}$  are the voltages (unit: V) at frequencies of 0.3Hz and 3Hz respectively, and  $\rho_{0.3\text{Hz}}$  and  $\rho_{3\text{Hz}}$  the apparent resistivities (unit: ohm-m) at frequencies of 0.3Hz and 3Hz respectively.

**(2) Apparent Resistivity (AR)**

The apparent resistivities at frequencies of 0.3Hz and 3Hz are respectively defined as follows:

$$\rho_{0.3\text{Hz}} = K \frac{V_{0.3\text{Hz}}}{I} \quad (\text{ohm-m}) \quad (2)$$

$$\rho_{3\text{Hz}} = K \frac{V_{3\text{Hz}}}{I} \quad (\text{ohm-m}) \quad (3)$$

In the above formulae,  $I$  is the output current of a transmitter (unit: A) and  $K$  the electrode configuration factor defined by

$$K = n(n+1)(n+2)\pi a$$

where  $n$  is the electrode-separation coefficient and  $a$  the electrode spacing (unit: m).

Equations (1) to (3) show that FE and AR can be determined by measurements of  $I$ ,  $V_{0.3\text{Hz}}$  and  $V_{3\text{Hz}}$ . For the present survey, Eq. (3) is used to calculate ARs.

**(3) Metal Conduction Factor (MF)**

The metal conduction factor is defined as

$$MF = \frac{FE}{\rho} \times 1,000 \quad (4)$$

Most of sulfide ore deposits indicate a high FE and a low AR. In order to emphasize such characteristics, MF is used in most cases as an indicator of metal conduction of ore deposits.

## 2-2 Data Representation

### 2-2-1 Plotting of Results

The values of FE, AR and MF are plotted on cross sections and plan maps. On a cross section as indicated in Fig. 4-2, the results are plotted at the intersection of 45-degree lines from the center point of the current electrodes AB and the center point of the potential electrodes MN. On a plan map, the results are plotted at vertical projection points on the ground surface. In these cases, it should be borne in mind that the plotted results cannot be considered as the electrical properties of rocks at the plotted points.

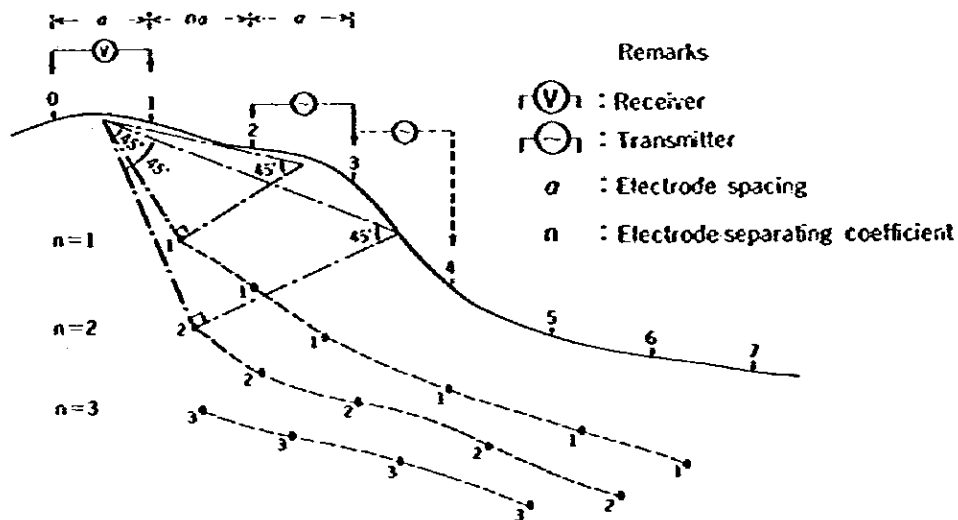


Fig. 4-2 Illustration of IP Measurements

### 2-2-2 Data Processing

The data obtained from field IP measurements and geodetic survey are preliminarily prepared for analyses. To begin with, the values of FE and AR and geodetic survey results described previously on data sheets are punched in data cards. The data cards are provided for computer

analyses. The values of MF are computed from the observed values of FE and AR. The locations of plotting FE, AR and MF on a cross section or a plan map are computed, and then the plotter draws contour maps of the computed results. Histograms are obtained from statistical analyses of values of FE, AR and MF.

In a rugged terrain area, the terrain effect on AR is so sensitive that terrain corrections are necessary for data analyses. However, the terrain effect is not so serious in the present survey, because, for a 2 km-long survey route, the elevation difference amounts to 100 m or less. Therefore, terrain corrections have never been considered.

### 2-2-3 Physical Properties of Rock Specimen

The measurement of physical properties of rock provides us with important information for the interpretation of the field IP results. There are two methods for evaluating IP characteristics of rock: the one is a laboratory measurement of IP characteristics of rock specimens sampled from the survey area and the other is an in-situ measurement. For the present survey, the former method is adopted. An outline of this method is briefly explained as follows:

Fig. 4-3 shows a block diagram of the measuring apparatus. The measurement is made with a rock specimen which is formed into a 3×3×2cm prism. Then the specimen is dipped into water up to a state of water saturation. The specimen is set on the sample holder, and the resistivity is measured with the 3Hz electric current supplied between both the sides of the specimen. For determining resistivity, the following formula is used:

$$\rho = \frac{SV}{lI}$$

S: Sectional area of a specimen (m<sup>2</sup>)

l: Length of a specimen (m)

V: Voltage measured (V)

I: Current supplied (A)

The value of FE is read from a meter by using electric current of 0.3Hz.

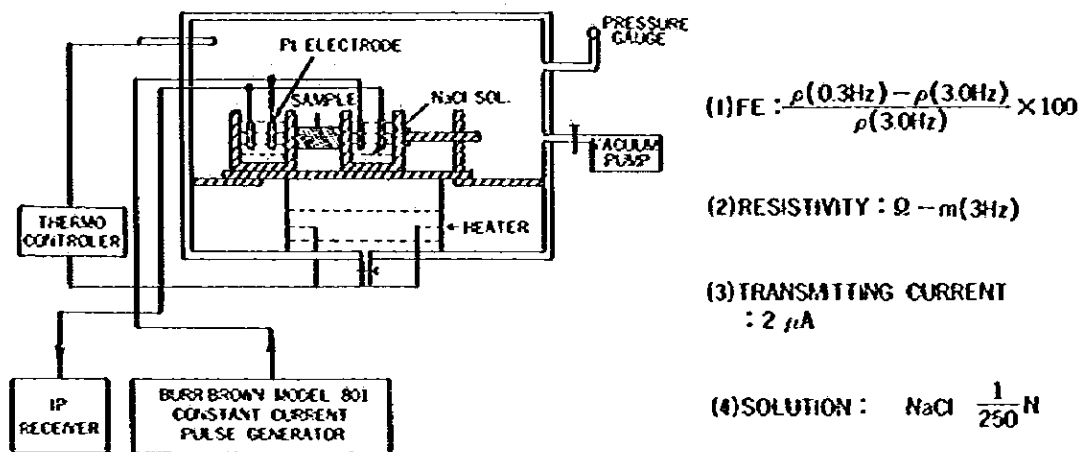


Fig. 4-3 A Block Diagram of the Laboratory Measuring Apparatus

## 2-3 Method of Field Data Analyses

### 2-3-1 Qualitative Analyses

The outlines of geological structure and the distribution of mineralized zones are generally considered by qualitative analyses of IP data on the basis of cross sections and plan maps. The classification of all probable anomaly sources can be made by taking the histograms of FE, AR and MP results into account. As a result, the anomalous zones are extracted from cross sections along survey lines and plan maps at various levels. The spacial dimensions of the anomaly source can be presumed from geological and geochemical data as well as results of rock specimen tests.

### 2-3-2 Quantitative Analyses

The second stage of the analyses is the computer simulation for determining the geological structure, the outlines of which are presumed by the qualitative analyses. Assuming model structures based on the IP field data, the computations are repeatedly made to determine the optimum model by comparing with the field results. Such computer trial-and-error procedures obtain the final determinations of dimension and depth of the anomaly source, which may represent the mineralized bodies.

The following Fig. 4-4 is the flow chart showing the jobs of data processing and analysis.

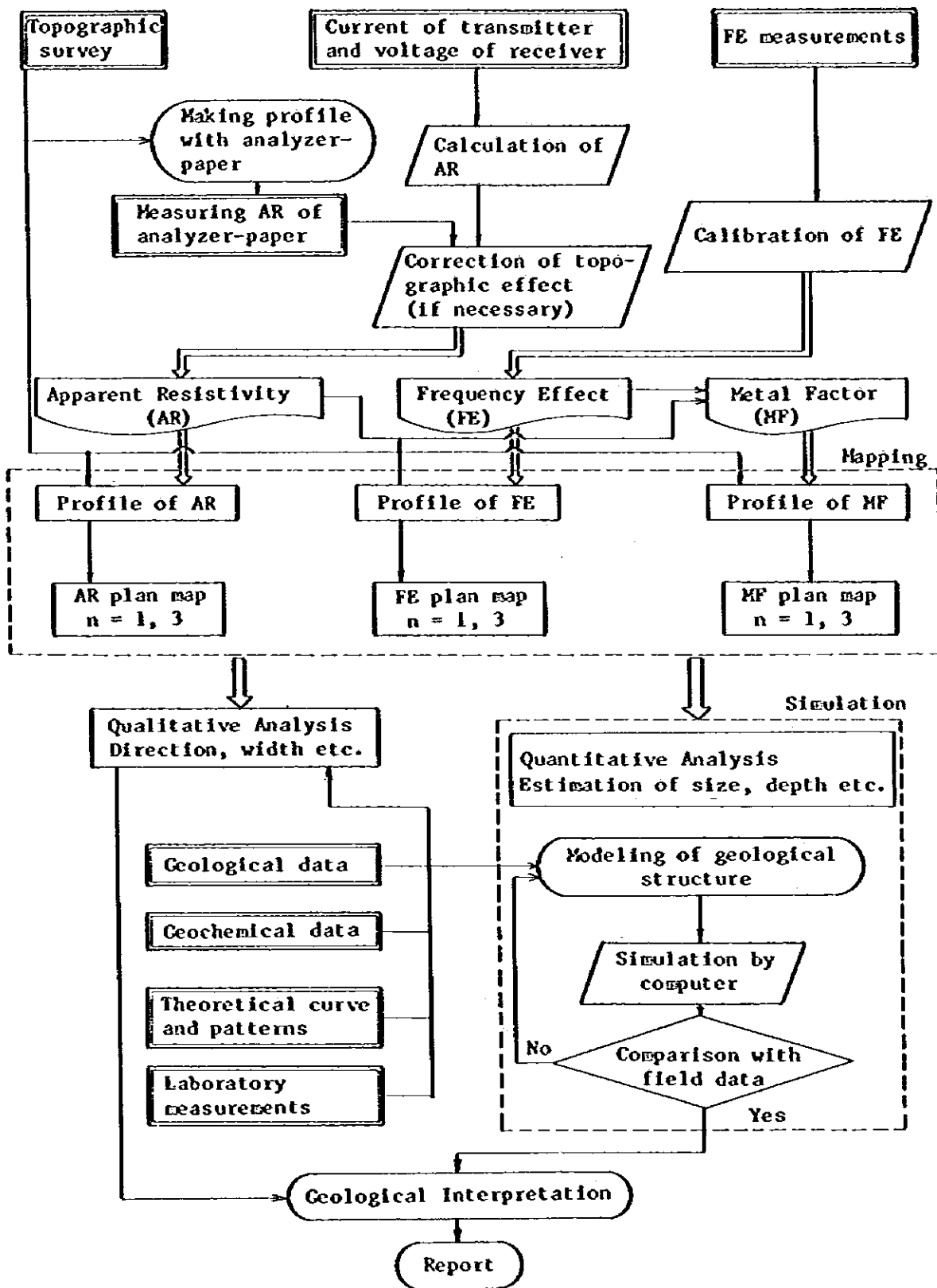


Fig. 4-4 Flow Chart of IP Data Processing and Interpretation

## **2-4 Instruments**

### **2-4-1 Instruments Used for Geophysical Survey**

#### **(1) Transmitter**

**Type:** IP Transmitter Model CH505A and CH505B

**Manufacturer:** Chiba Electronics Laboratory

**Input Voltage and Frequency:** AC 115V  $\pm$  15V, 400Hz

**Output Voltage:** 100 - 800V

**Output Current:** 0.1 - 3A

**Output Frequency:** 0.1, 0.3, 1.0, 3.0 and 10.0Hz

#### **(2) Receiver**

**Type:** IP Receiver Model 7505B

**Manufacturer:** Yokohama Electronics Laboratory

**Input Voltage:** 1, 10, 100, 1000mV and 10V with a 5-range fine adjustor

**Input Frequency:** 0.1, 0.3, 1.0 and 3.0Hz

**Time constant:** 2, 6, 20, 60 and 150sec

**Input Impedance:** 10M $\Omega$

**Power:** Two 15.6V Mercury cells/four 006P-type dry batteries

#### **(3) Engine Generator**

**Type:** IP Generator Model HK-2

**Manufacturer:** McCulloch Hite-E-Lite Inc., U.S.A.

**Output, Output Voltage and Frequency:** 2KW, 115V, 400Hz

#### **(4) Electrodes**

Stainless steel rod

#### **(5) IP Checker**

**Type:** Laboratory IP Transmitter Model YN502

**Manufacturer:** Yokohama Electronics Laboratory

**Transmitting Frequencies:** 0.1, 0.3, 1.0, 3.0 and 10.0Hz

**Accuracy:**  $\pm$ 5%

## 2-4-2 Rock Specimen Testing Instrument

### (1) Transmitter

Type: Laboratory IP Transmitter Model 801

Manufacturer: Burr-Brown Research Corporation

Input Voltage and Frequency: 0.01 - 1100Hz with a 5-range fine adjustor

Output Current: 1 $\mu$ A - 11mA with a 4-range fine adjustor

Input Impedance: 10.5M $\Omega$  - 10.5K $\Omega$

### (2) Receiver

Type: Laboratory IP Receiver Model YDC-434

Manufacturer: Yokohama Electric Research Co.

Input Voltage: 0.3, 1, 3, 10, 30, 100, 300 and 1000mV with a 8-range fine adjustor

Frequencies: 0.1, 0.3, 1 and 3Hz

Time Constants: 2, 6, 15, 60 and 150sec

Input Impedance: 10M $\Omega$

Power: two 15.6V Mercury Cells

## CHAPTER 3 SURVEY RESULTS

### 3-1 Results of Rock Specimen Tests

24 rock specimens were sampled in and around the survey area. As there are a few outcrops suitable for sampling in the survey area, some typical specimens were exceptionally sampled around the survey area. The locations of the sampling are shown in PL. 4-1.

Resistivity and FE tests were conducted for these rock specimens. The results of the tests are tabulated in Table 4-1. The correlation between the resistivity and FE results is also shown in Fig. 4-5.

The results of the rock specimen tests can be summarized as follows:



Table 4-1 Results of Rock Sample Tests

No.	Rock Name	FE (%)	Mean	Resistivity (ohm-m)	Mean	Py (Cpy) <sup>(*)</sup>
1	Granodiorite	2.1		4,254		1
4	Granodiorite	4.0		2,632		1
5	Granodiorite	3.4		6,063		1
7	Granodiorite	6.5		5,099		1
8	Granodiorite	2.2		10,452		1
9	Granodiorite	2.4		5,580		1
11	Granodiorite	2.5		3,362		1
15	Granodiorite	4.0	3.35	5,753	4,789	3
16	Granodiorite	3.4		6,657		2
18	Granodiorite	0.9		6,875		2
19	Granodiorite	7.0		859		4
20	Granodiorite	1.5		5,992		1
21	Granodiorite	2.9		4,338		1
23	Granodiorite	3.6		1,863		2
24	Granodiorite	3.9		2,059		3
6	Diorite	4.9		2,191		1
22	Diorite	103.0		1,052		5
10	Dolerite	10.1		429		3
14	Dolerite	5.8		256		2
2	Dacite	1.1		30,924		1
3	Andesite	1.0		3,500		1
12	Andesite	3.1	2.60	10,087	9,045	1
17	Andesite	3.7		13,548		1
13	Tourmaline	0.0		1,216		1

(\*) Pyrite Content

1. No pyrite grains.
2. 2 to 3 pyrite grains.
3. 5 to 6 pyrite grains.
4. Continuous pyrite grains.
5. Pyrite concentration.

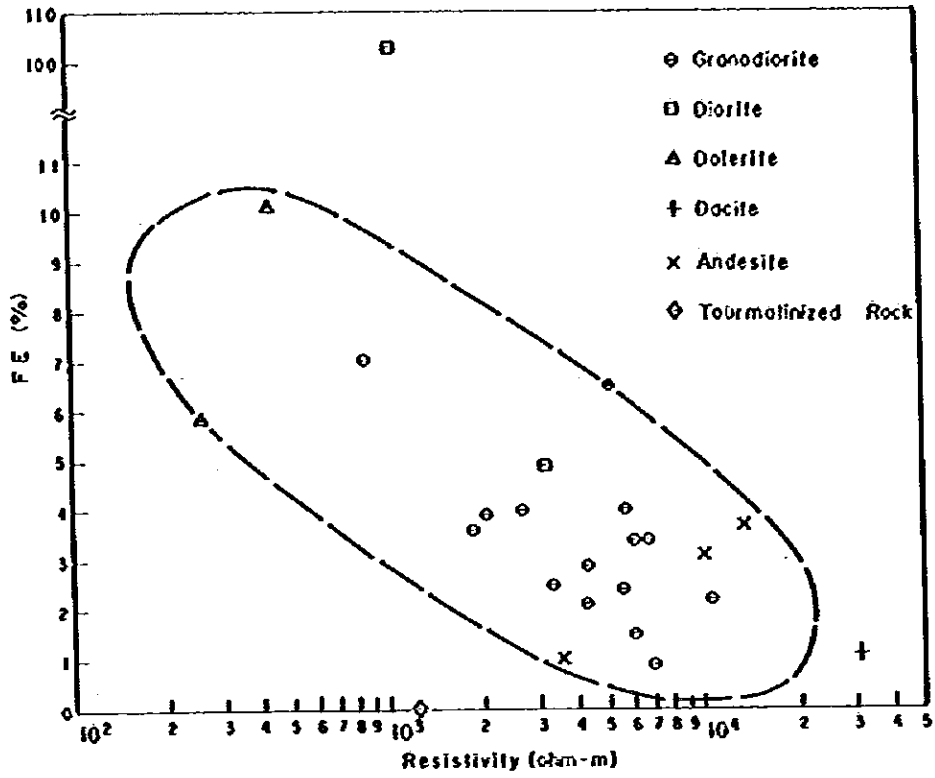


Fig. 4-5 FE-Resistivity Correlation Diagram of Rock Samples

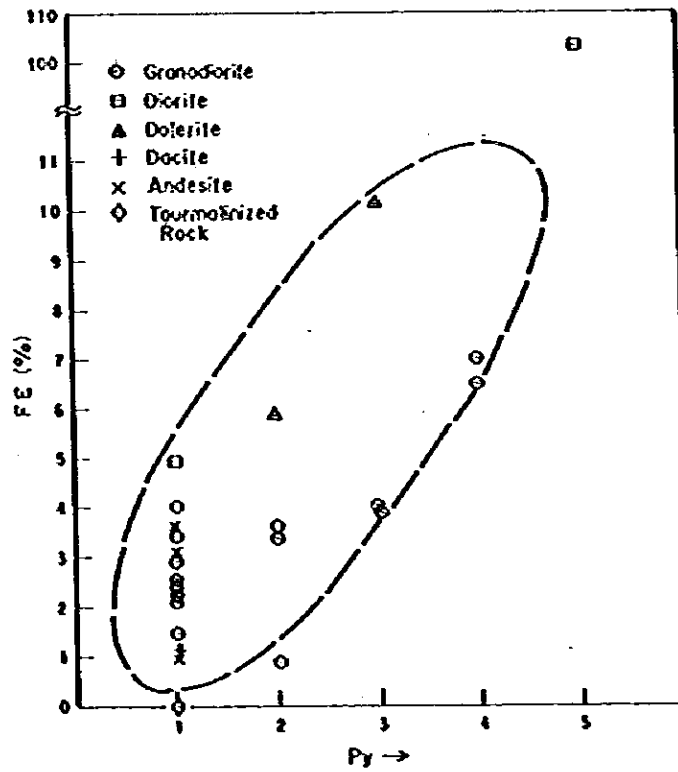


Fig. 4-6 FE-Py Correlation Diagram of Rock Samples

**(1) FE**

The general feature of the FE results can be as follows.

15 specimens of granodiorite, which are distributed over the whole survey area, indicate 0.9 to 7.0% FE values. The mean value is 3.35%. Most of the FE values are relatively near the mean value except for some peculiar specimens.

Two diorite specimens, which are sampled in the northwest of the survey area and in the neighborhood of Station G-12, the central part of the survey area, indicate high FE values of 4.9 and 10.3%, respectively. Two dolerite specimens, which are sampled around Stations A-3 and A-12, also indicate high values of 5.8 and 10.1%, respectively.

In contrast, a dacite specimen sampled in the southwest of the survey area takes a low FE value.

The FE values of three andesite specimens, which are sampled in the north and northwest of the survey area, range from 1.0 to 3.7%. The mean value is 2.6%. A tourmaline-bearing rock specimen sampled around Station B-20, the northern part of the survey area, does not indicate any frequency effect.

**(2) Resistivity**

The resistivity of granodiorite ranges from 859 to 10452 ohm-m. The mean value is 4789 ohm-m. The two diorite specimens have relatively low resistivities of 2191 and 1052 ohm-m. The two dolerite specimens indicate 429 and 256 ohm-m, which is the lowest resistivity obtained in the present tests. The highest resistivity amounting to 30924 ohm-m is found for the dacite specimen. The resistivity of andesite ranges from 3500 to 13548 ohm-m. The mean value is 9045 ohm-m. The tourmaline-bearing rock specimen has a relatively low resistivity of 1216 ohm-m.

**(3) FE-Resistivity Relationship (Fig. 4-5)**

The results of the specimen tests, which are tabulated in Table 4-1, are plotted in Fig. 4-5, logarithmic resistivity in the abscissa

versus FE in the ordinate. This figure indicates a negative correlation between FE and resistivity. The negative correlation can also be recognized for 15 granodiorite specimens, but not for the other kind of rock specimens because the numbers of the specimens are too small to estimate such correlations.

#### (4) FE-Pyrite Content Relationship (Fig. 4-6)

The pyrite contents of the rock specimens are determined by means of a 20-power lens. The contents are classified as follows.

1. No pyrite grains
2. 2 to 3 pyrite grains
3. 5 to 6 pyrite grains
4. Continuous pyrite grains
5. Pyrite concentration

Fig. 4-6 shows the FE-pyrite content relation according to the above rock classification. A positive correlation can be recognized in this figure.

### 3-2 Results of IP Measurements

#### 3-2-1 Plotted Maps

The results of the IP survey are plotted in sections (PL. 4-2~4-11) along Survey Lines A to J. In these sections, frequency effect (FE), apparent resistivity (AR) and metal conduction factor (MF) are indicated. Furthermore, these IP results are also shown in plan maps at some depths. The electrode separation levels chosen for the plan maps are  $n = 1$  and 3.

The contour intervals of the section and plan maps are 1% for FE; 500, 700, 1000, 1500, 2500, 5000 and 7000 ohm-m for AR; and 1 for MF. In these maps, the anomaly distribution is also represented on the basis of the statistical considerations, which will be described in 3-2-2. For example, the dotted lines indicate 4.5% FE, the mean value of FE, which is obtained by the histogram of the FE results as will be mentioned in the forthcoming paragraph.

### 3-2-2 Statistical Considerations

For the purpose of determining the criterion whether an IP value is anomalously high or not, the following statistical treatments are made.

#### (1) Histograms (Fig. 4-7)

The histograms are made for the measured values of FE and AR. It is seen that the histogram of FE results fits well to a normal statistical distribution curve with the mode of 4 to 5%. On the other hand, the histogram of AR values fits well to a log-normal distribution curve. The mode of the histogram has a tendency to increase with n.

#### (2) Cumulative Frequency Distribution (Fig. 4-8)

The cumulative frequency distributions of the FE, AR and MF values are obtained. Let the mean and the standard deviation be denoted by  $\mu$  and  $\sigma$ , respectively. In this report, FE and MF values greater than  $\mu + 2\sigma$  are defined as "anomaly" and those between  $\mu + 2\sigma$  and  $\mu + \sigma$  are defined as "weak anomaly". On the other hand, AR values lower than  $\mu - 2\sigma$  are defined as "anomaly" and those between  $\mu - 2\sigma$  and  $\mu - \sigma$  are defined as "weak anomaly".

#### (3) Determinations of "Anomaly" and "Weak Anomaly"

On the basis of the cumulative frequency distribution curves, values of "anomaly" and "weak anomaly" are determined in the following:

	Anomaly	Weak anomaly	Mean
FE	> 6%	> 5%	4.5%
AR	< 500 ohm-m	< 1000 ohm-m	1500 ohm-m
MF	> 8	> 5	3

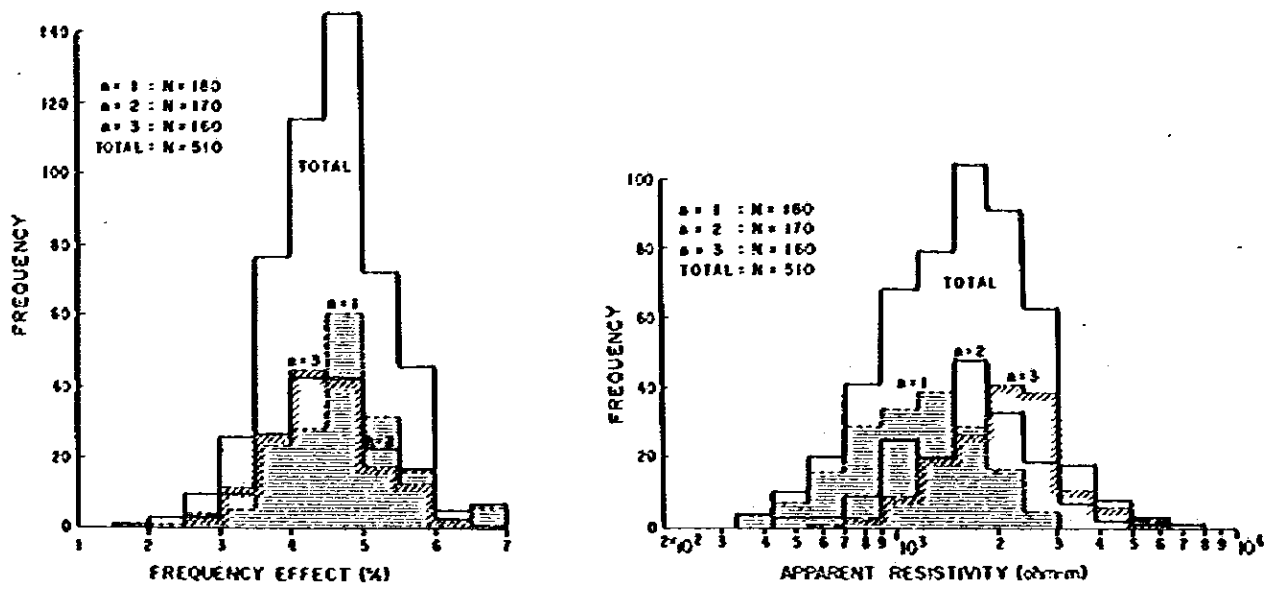


Fig. 4-7 Histograms of FE and AR

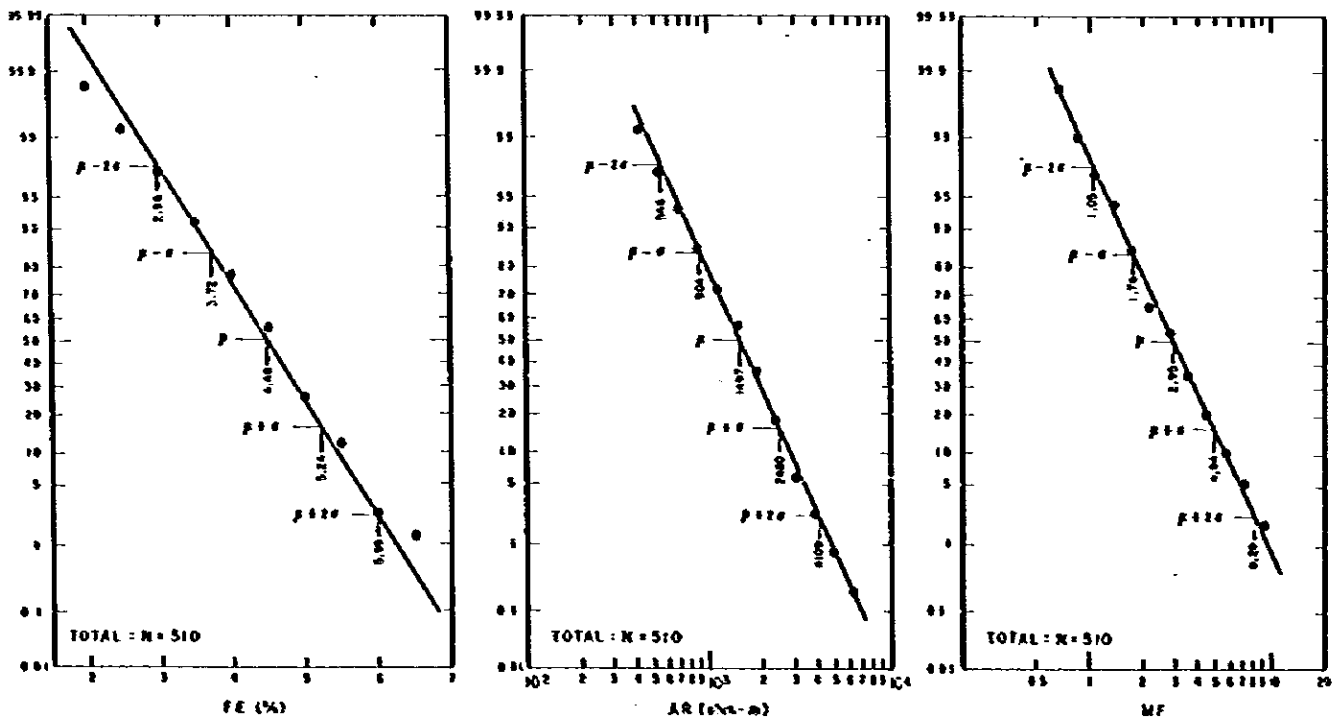


Fig. 4-8 Cumulative Frequency Distributions of FE, AR and MF

(4) Distribution range

The statistical considerations are made for the measured FE and AR. The maximum, minimum and mean values for each survey line and each electrode separation level are tabulated (Table 4-2). The same values are also illustrated in Fig. 4-9.

The highest FE value amounts to 6.8%, which is observed along Line A, while the lowest one becomes 1.8%, which is observed along Line F. The highest AR is 8064 ohm-m along Line C, while the lowest is 329 ohm-m along Line G.

(5) FE-AR correlation (Fig. 4-10)

The correlation between FE and AR is considered as shown in Fig. 4-10, in which FE is taken in the ordinate and log AR in the abscissa. In the following table, the correlation coefficient R is calculated for each of levels  $n = 1, 2$  and  $3$  and the total levels.

	n = 1	n = 2	n = 3	Total
R	0.04	0.28	0.21	0.09

(6) Topographic effect

The topographic effects on FE and AR for  $n = 1$  are considered. Let the topographic elevations of inner electrodes on a  $n = 1$  dipole-dipole configuration (see Fig. 4-1) be denoted by  $H_1$  and  $H_2$ , respectively. The mean elevation  $H_m (= (H_1 + H_2)/2)$  is chosen as a parameter representing the topographic effect (see the footnote of Table 4-3). Thus-obtained correlations between FE and  $H_m$  and between AR and  $H_m$  are tabulated in Table 4-3. As seen in the table, a slightly positive correlation of  $R > 0.5$  between  $H_m$  and FE can be seen along Lines A, C and D, while a similar correlation between  $H_m$  and AR can be seen along Line A. The fact that the  $H_m$ -FE correlation coefficient amounts to  $R = 0.36$  for the total FE values may indicate that FE highs are generally found in high-altitude areas.

Table 4-2 Ranges and Mean Values of IP Measurements

	Frequency effect(%)			Apparent resistivity(ohm-m)			
	Max	Min	Mean	Max	Min	Mean	
Line	A	6.8	3.0	4.80	5916	428	1381
	B	5.0	2.0	4.27	4303	431	1621
	C	6.6	2.0	4.54	8064	341	1453
	D	6.7	3.4	4.67	4823	604	1475
	E	5.5	2.7	4.48	4491	588	1494
	F	5.6	1.8	3.67	3715	384	1209
	G	6.5	3.0	4.76	3580	329	1362
	H	5.8	2.8	4.48	4931	726	1738
	I	5.5	2.7	4.31	3233	681	1569
	J	6.1	3.0	4.62	4039	504	1758
a	1	6.8	1.8	4.62	2954	329	1086
	2	6.2	2.0	4.44	6180	425	1586
	3	6.5	2.6	4.37	8064	674	2021
<b>Total</b>	<b>6.8</b>	<b>1.8</b>	<b>4.48</b>	<b>8064</b>	<b>329</b>	<b>1497</b>	

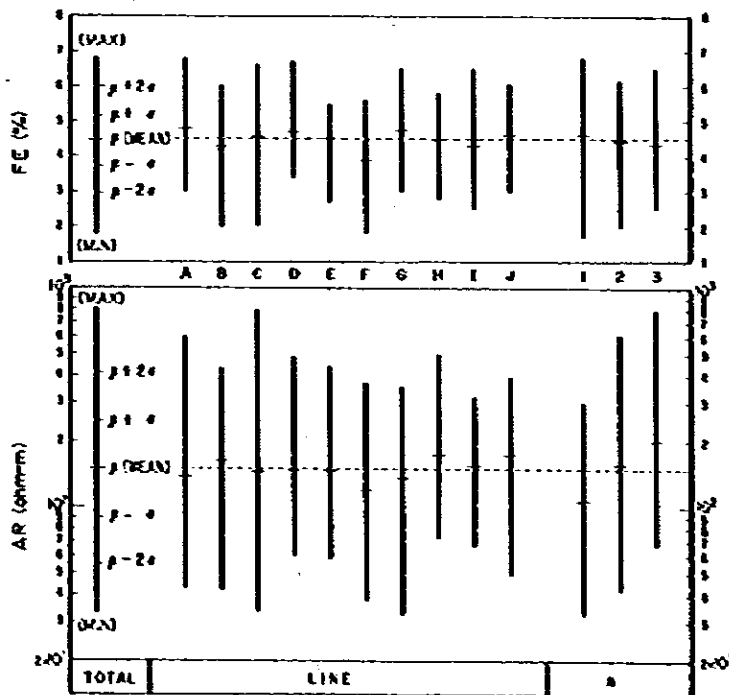
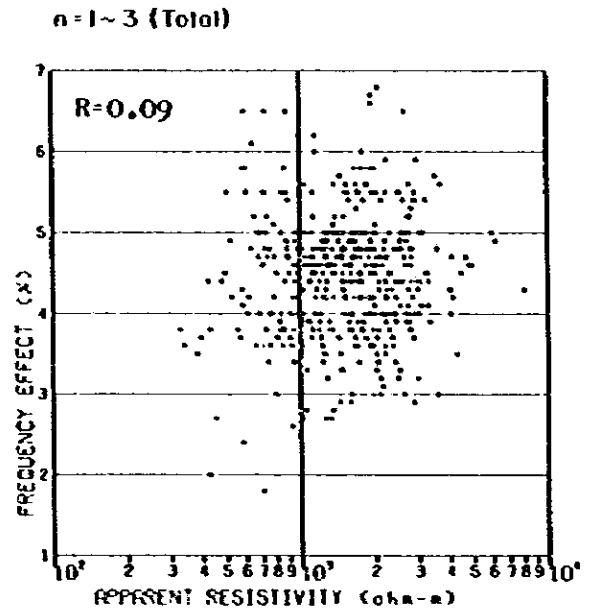
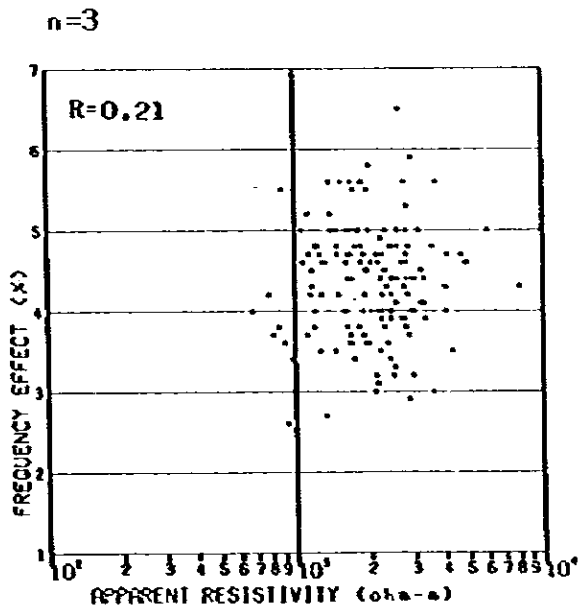
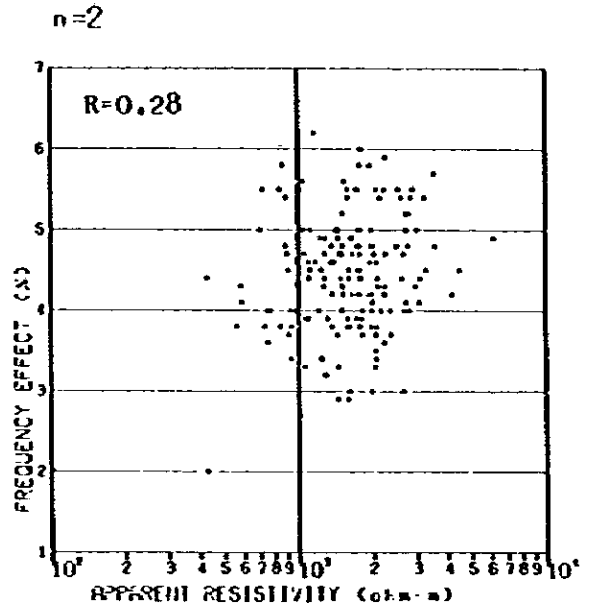
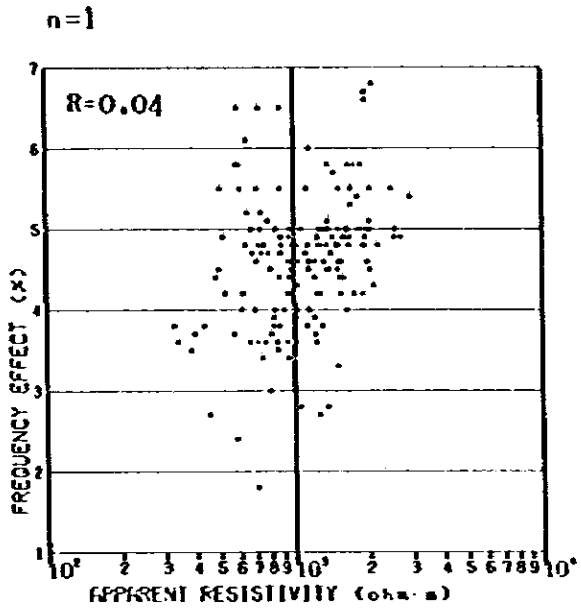


Fig. 4-9 Ranges and Mean Values of FE and AR





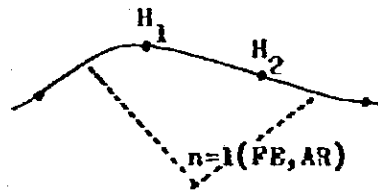
(Note: R=correlation coefficient)

Fig. 4-10 FE-AR Correlation Diagrams of IP Measurements

Table 4-3 Correlation Coefficients between IP Measurements and Topography

Correlation coefficient R for n=1			
	$H_m$ -PE	$H_m$ -AR	
A	0.63	0.55	
B	0.22	0.38	
C	0.75	0.43	
D	0.60	0.04	
Line	E	0.37	0.14
	F	0.28	0.24
	G	0.21	-0.14
	H	0.42	0.15
	I	0.28	-0.15
	J	-0.29	0.08
-----			
Total	0.36	0.18	

Note:  $H_m = \frac{H_1 + H_2}{2}$



In contrast to the above, the  $H_m$ -AR correlation coefficient is relatively low ( $R=0.18$ ). Therefore, it may be concluded that there is no marked topographic effect on AR.

### 3-2-3 IP Anomalies

#### (1) Frequency Effect (FE)

See PL. 4-12, the  $n=1$  plan map. In this map, an anomalously high FE ( $FE > 6\%$ ) is found north of Line A. This anomaly is called "A-16 Anomaly". The other high FE anomalies are seen at Station C-17 (called "C-17 Anomaly") north of Lines C and D and at Station J-13 (called "J-13 Anomaly") north of Line J.

The C-17 Anomaly coincides with the G. Sumiang mountain ridge, whose peak is located about Station C-17. The relatively weak anomaly zone of  $FE > 5\%$  covers widely the surrounding area of the G. Sumiang mountain. In the sections along Lines B to E (PLs. 4-3 ~ 4-6), the C-17 Anomaly is indicated to be a roof-shaped anomaly around Stations C-16 ~ C-17, D-15 ~ D-17, which is a typical indicator promising for a shallow-seated source. But this anomaly does not spread to Lines B and E. Judging from the above observation facts, the C-17 anomaly source may be located at a shallow depth below Stations 15 to 17 along Lines C to D.

The A-16 Anomaly is located around the northwestern corner of the survey area. As seen in the section along Line A (PL. 4-2), this anomaly source is located north of Station A-15. The volume of the source is presumed to be larger than that of the C-17 Anomaly. The northern and western extensions are not so clear, because the A-16 Anomaly is located at the northwestern corner of the survey area.

The J-13 Anomaly is located north of the east side of the survey area. In the section along Line J (PL.4-11), this anomaly is indicated to be a roof-shaped anomaly centering around Stations J-13 ~ J-15 and deeply spreading. The source of this anomaly is presumably shallow-seated below the above mentioned stations.

The G-1 Anomaly is located in the southern part of the survey area. On the basis of the section (PL. 4-8) along Line G, the conductor is presumed to be located south of Station G-3, but its southward extent is not clear. Near Station H-3, we recognize a weak anomaly which is probably related to the G-1 Anomaly. This weak anomaly indicates an explicit roof-shaped pattern (PL. 4-9) which can be presumed as a shallow-seated source.

The plan map of  $n=3$  (PL. 4-13) can be interpreted as follows: There is a weak anomaly zone stretching from Station A-5 to J-12 in the WNW-ESE direction in the northern part of the survey area. In addition, this weak anomaly zone also appears around Stations 16 and 17 along Lines A ~ D as shown in the section maps (PLs. 4-2 ~ 4-11). This fact may imply that this weak anomaly continues to the A-16 and C-17 anomalies. There is another weak anomaly, whose source is shallow, around Station 15 on Lines G to J. The source of the J-13 anomaly, mentioned previously for the case of  $n=1$ , is presumed to extend toward Station 15 on Line G. Furthermore, it is probable that a weak anomaly zone seen on Line E continues to the C-17 anomaly. The source may be shallow-seated below Stations E-12 and 13.

Small-scale weak anomalies occupy predominantly the central and southern parts of the survey area except for the southern tip of Line G, but these anomalies are not regularly arranged. The sources of these anomalies are distributed shallowly under Stations A-2 ~ 3, C-9 ~ 10, G-4 ~ 6 and G-8 ~ 9.

## (2) Apparent resistivity (AR)

In the plan map (PL. 4-14) of  $n=1$ , we see four areas of AR anomaly ( $AR < 500 \text{ ohm-m}$ ): C-14 Anomaly north of Lines B and C, C-2 Anomaly south of Line C, F-17 Anomaly north of Lines F and G, and G-11 Anomaly around the midpoint of Line G.

The general feature of weak anomalies ( $AR < 1000 \text{ ohm-m}$ ) in the survey area is the zonal arrangement. The most predominant one is found in the northern part of the survey area. It involves the C-14 and F-17 anomalies trending in the WSW-ESE direction.

There is no anomalous area in the plan map (PL. 4-15) of  $n=3$ . The mean value of AR in this map is 1500 ohm-m or higher. The exceptions are small-scale weak anomalies found in the northwestern part and the southern part of the survey area.

In the sections (PL. 4-2 ~ 4-11), we see many low-resistivity zones, for example, at Stations 13 ~ 15 on Lines A ~ D, Stations E-17, F-15 ~ F-18, G-17 ~ G-19, J-13 ~ J-16, C-2 ~ C-4, F-11 ~ F-13, G-11 ~ G-13 and F-2 ~ F-3. Most of them have roof-shaped patterns which, in general cases, evidence shallow-seated bodies of low resistivity. The low AR area is trending in the WSW-ENE direction north of Stations 13 on Lines A ~ G. This fact indicates that it forms a large-scale zone of low resistivity including the C-14 and F-17 anomalies.

### (3) Metal conduction factor (MF)

In the plan map (PL. 4-16) of  $n=1$ , we recognize many anomalous areas of  $MF > 8$ : C-14 Anomaly on Lines A ~ D in the northwestern part of the survey area, F-16 Anomaly north of Lines F and G, C-10 Anomaly in the central part of Line C, G-11 Anomaly in the central part of Line G, G-6 Anomaly south of Line G and J-14 Anomaly north of Line J.

The distribution of these MF anomalies is almost equal to that of the AR anomalies. A similar tendency can be seen in the plan map of  $n=3$  and sections. As already stated in details in 3-2-2 (5), Chapter 3, the distribution of MF reflects greatly that of AR in the survey area. This fact may imply that the location of promising ore deposits can not be suggested by the distribution of MF.

### 3-3 Simulation

For estimating shapes of the IP anomaly sources and their physical properties on the basis of the survey results, the computer simulation technique is applied to the two IP sections; i.e., the northern part of Line C (C-10~C-20) and the northern part of Line (J-9~J-19). The models adopted here are based on the results of qualitative analyses stated

previously. The models and the outline of the simulation analyses are summarized as follows:

### 3-3-1 Line C models (Fig. 4-11)

The top of Fig. 4-11 shows the measured result, and the bottom shows the simulated result.

#### (1) Model C-1

IP properties are assumed as the following table. The computation results are given in Fig. 4-11 (a).

Code	FE (%)	Resistivity (ohm-m)
1	3.5	3000
2	3.5	2000
3	3.5	1500
5	3.5	300
10	7.0	1500

A comparison of the computed results of FE, AR and MF with the measured ones suggests the following speculations:

- i) The computed roof-shaped pattern of weak FE anomalies agree well with that of observed data. But the computed pattern is somewhat sharper and the computed FE values are lower in both the sides of the pattern.
- ii) A good agreement can be seen between the locations of the observed weak AR anomalies and the computed ones. But in general, the computed values are slightly higher than the observed ones in shallow places.
- iii) The computed MF pattern is different from the measured one, probably because the roof-shaped pattern of MF is much affected by that of AR in the survey area.

**(2) Model C-2**

Model C-1 is revised to a new model shown in Fig. 4-11 (b), in which ranges of high FE and low AR become wider. Such a revision makes good agreements with the observed FE and AR patterns especially in the southern side of the survey area.

The assumed parameters in this model are as follows.

Code	FE (%)	Resistivity (ohm-m)
2	3.5	2000
3	3.5	1500
4	3.5	400
8	6.0	800
9	7.0	3000
10	7.0	1500

The computed results can be summarized:

- i) The computed pattern agrees much better with the observed one. The range of high FE becomes wider in this model. But the computed anomaly of FE is somewhat intensified in the northern side of the roof-shaped pattern.
- ii) The range of the computed AR anomaly becomes wider, so that its roof-shaped pattern agrees much better with the observed one.
- iii) The computed MF values are still slightly lower than the observed ones, but as a whole the mutual agreement becomes better.

**(3) Model C-3**

This is the final model to be adopted. In this model, the background values of FE in the north side are somewhat changed. Fig. 4-11 (c) shows the computed results.

The following table gives the adopted values of IP properties.

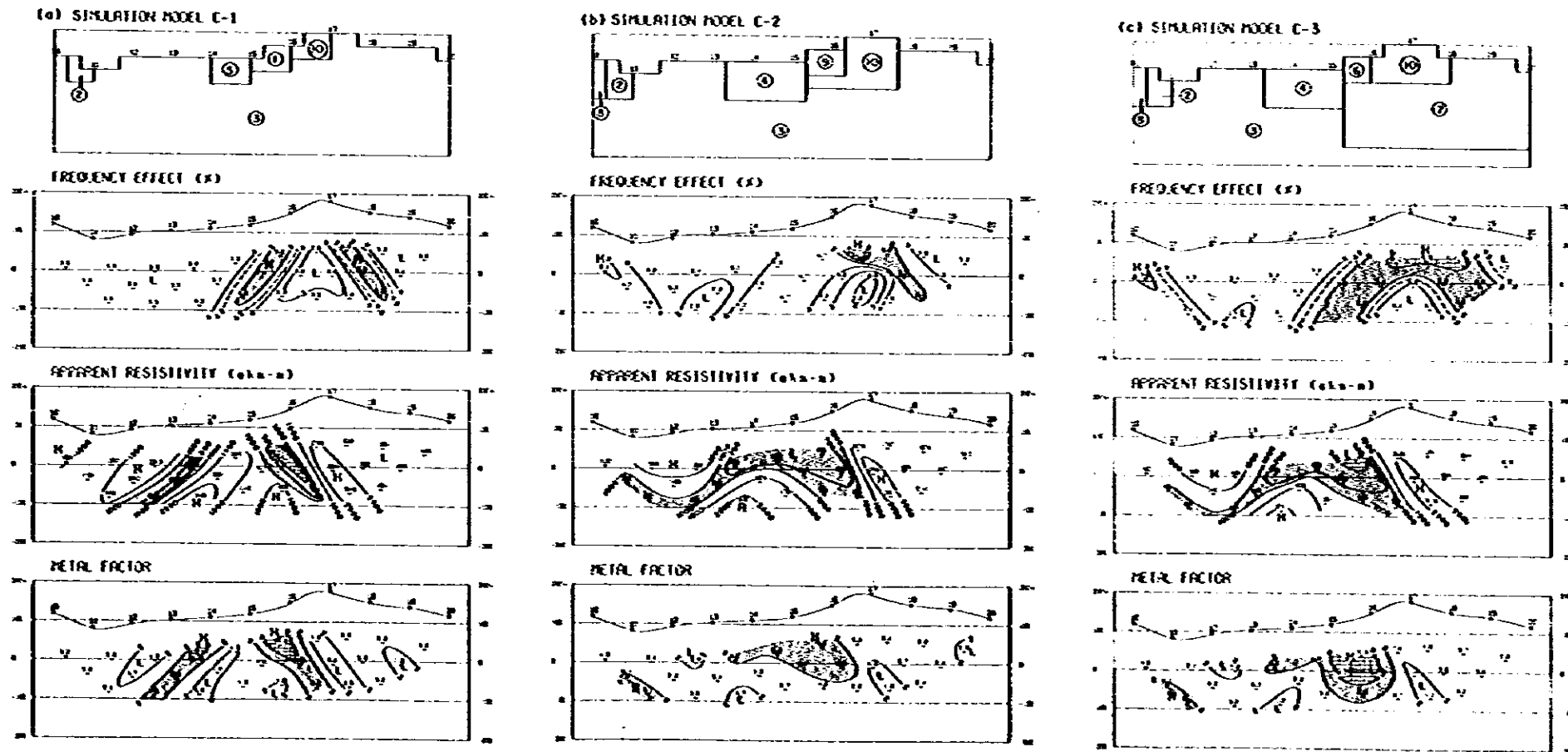
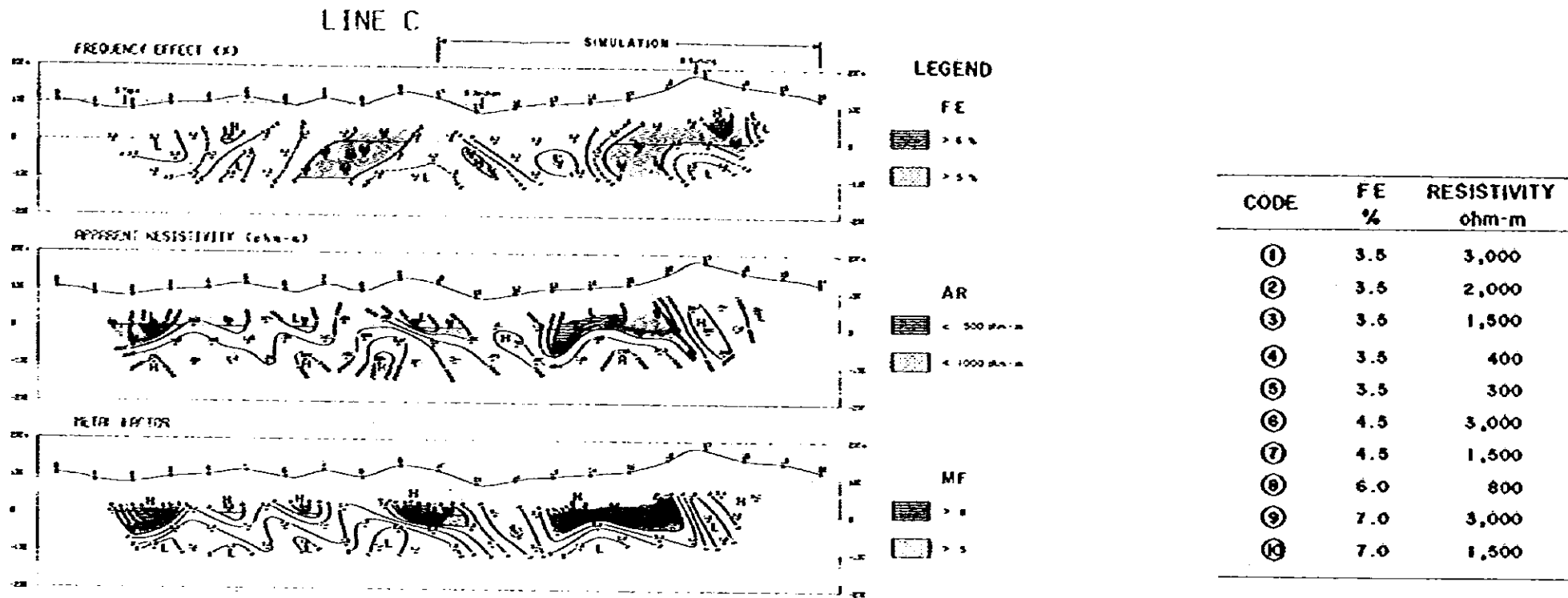


Fig. 4-11 IP Pseudo-sections and Simulated Models for Line C



Code	FE (%)	Resistivity (ohm-m)
2	3.5	2000
3	3.5	1500
4	3.5	400
6	4.5	3000
7	4.5	1500
8	6.0	800
10	7.0	1500

On the basis of the computed results, we can conclude as follows:

- i) The computed pattern of weak FE anomalies match well the observed ones.
- ii) The AR values in this model are the same as those in the C-2 model, except for Code 6. Accordingly, the computed result here is almost similar to that in the C-2 model.
- iii) The computed range of MF anomaly becomes wider than those in the previous models. This is caused by adopting higher values of FE and shortening the range of Code 6.

#### (4) Conclusion

As mentioned above, the model has been changed to match the observed results of FE, AR and MF. C-3 Model is the final one, where we see a good agreement between the computed results and the observed ones.

#### 3-3-2 Line J Models (Fig. 4-12)

The observed result and the computed one are shown in the top and the bottom of Fig. 4-12, respectively.

##### (1) Model J-1

The assumed IP properties are given in the following table. The computation results are given in Fig. 4-12 (a).

Code	FE (%)	Resistivity (ohm-m)
1	4.5	2000
3	4.5	500
5	6.0	2000
7	6.0	500

The computed results in this stage can be summarized as follows:

- i) The location and shape of the computed pattern are similar to those of the observed one except for the high anomaly zone.
- ii) The computed range of the distribution of weak AR anomaly is still narrower than the observed one. As a whole, the computed values are higher than the observed ones.
- iii) The computed MF values are lower than the observed ones because the computed AR values are higher. The distribution range of the high MF anomaly becomes narrower.

(2) Model J-2

The IP parameters adopted in the previous model are changed to match better the observed results. In this model, we increase a little depths of the high FE sources and assume a high FE source in the south side of the profile. Furthermore, we decrease background values of AR as a whole, and the locations of low AR sources are removed downwards in the northern part of the survey area and southwards in the southern part. The Model J-2 is shown in Fig. 4-12(b).

The IP parameters adopted in this model are given by the following table:

Code	FE (%)	Resistivity (ohm-m)
2	4.5	1500
3	4.5	500
4	5.0	1500
6	6.0	1500
7	6.0	500



We can summarize the computed results as follows:

- i) The computed pattern of FE is almost similar to that in Model J-1. This shows that the procedure of deepening the FE sources is not effective.
- ii) The distribution range of weak AR anomaly agrees well with that of the observed one, but the AR values are still small in the marginal areas.
- iii) The computed MF pattern is well approximated to the observed one. The range of the high MF anomaly becomes wider.

(3) Model J-3

The IP parameters are further changed again in order to obtain a best-fitting model. In this model, the FE values are increased around the midpoint of the model, but the other values are remained similarly to the values in Model J-1. Furthermore, we increase the background values of AR in the deeper places. The Model J-3 is shown in Fig. 4-12 (c).

The IP parameters adopted here are given by the following table.

Code	FE (%)	Resistivity (ohm-m)
1	4.5	2000
2	4.5	1500
3	4.5	500
6	6.0	1500
8	6.5	1500
9	6.5	500

The summary of the results obtained by this model computation is as follows:

- i) The high FE anomaly appears in this model result. As a whole, the distribution pattern of the computed values is very similar to the that of the observed ones.

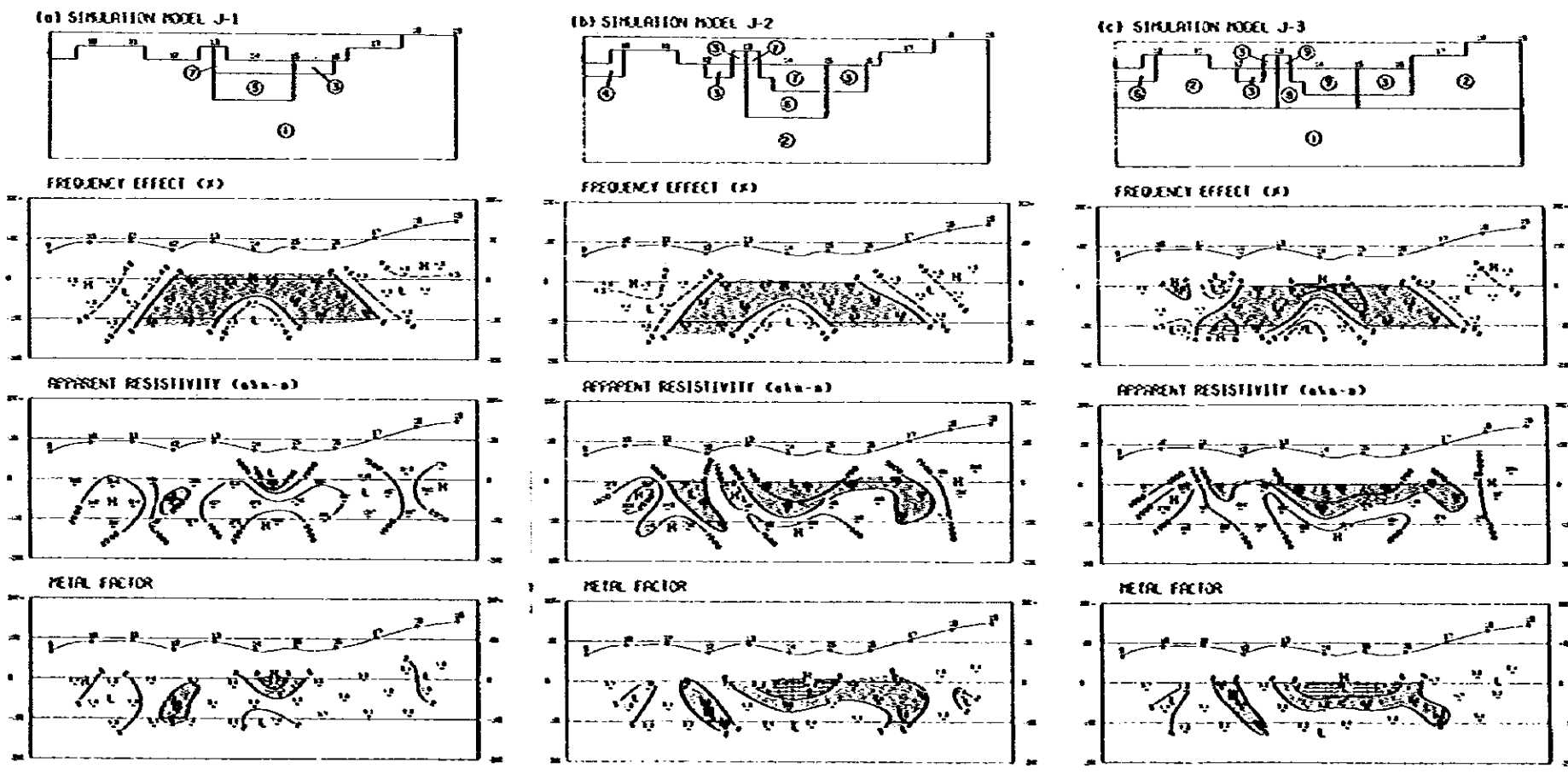
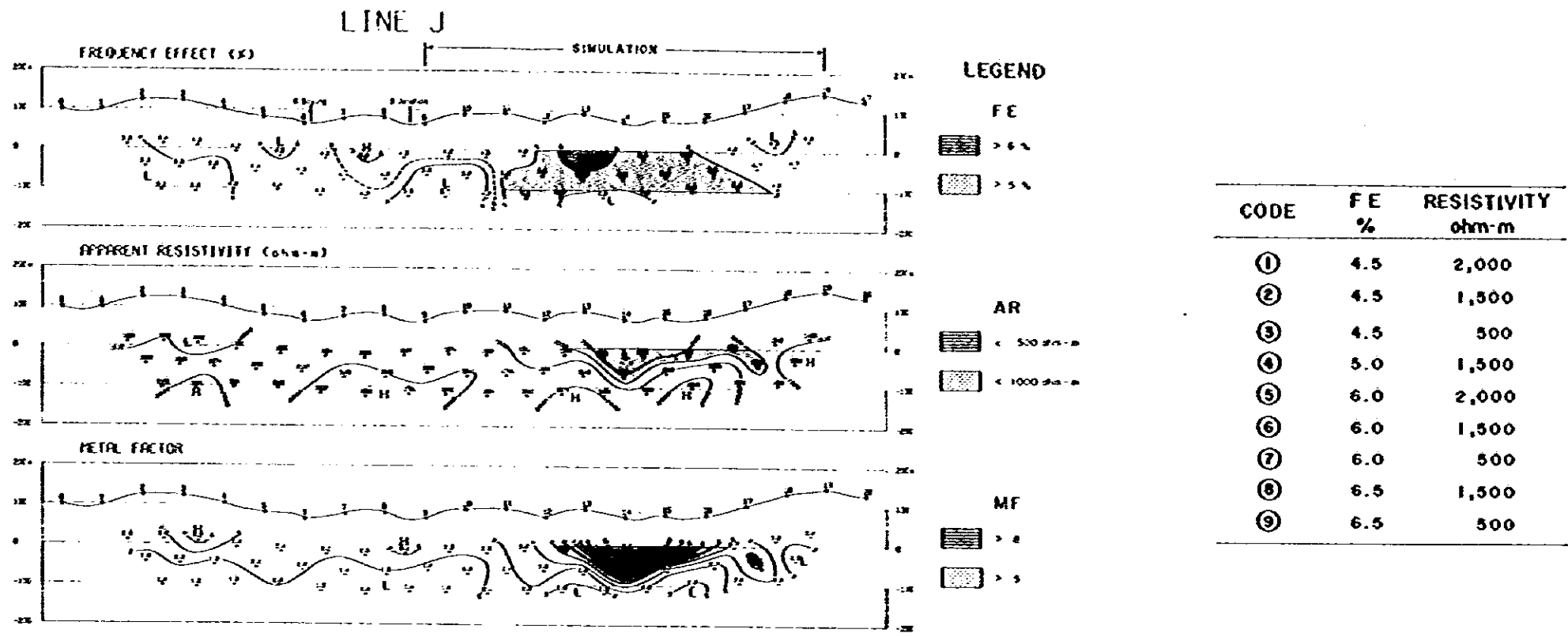


Fig. 4-12 IP Pseudo-sections and Simulated Models for Line J

ii) A good agreement is recognized between the computed AR pattern and the observed one.

iii) A good agreement is also recognized in the case of MF.

#### (4) Conclusion

It is concluded that Model J-3 can well approximate the observed results of FE, AR and MF. Both the patterns agree well each other.

### 3-4 Discussion

The geophysical feature of the survey area, such as physical properties of rock, anomaly distribution, etc., is considered by taking the geological and geochemical survey results into account.

#### 3-4-1 IP Properties of Rock

24 rock specimens are sampled in and around the geophysical survey area for the purpose of testing their IP properties.

The laboratory tests are made to 15 (4) granodiorite, 2 (1) diorite, 2 (1) dolerite, 1 dacite, 3 andesite and 1 tourmalinized rock specimens. Here ( ) denotes the number of specimens sampled in the survey area.

The main part of the geological survey area is occupied by granodiorite trending in the EW direction. The present geophysical survey was carried out in the east part of the granodiorite area. The FE values obtained by the laboratory tests are estimated as 2~3% for specimens, in which the pyrite-dissemination is not observed, and as higher than 6% for continuously disseminated specimens (Table 4-1, Fig. 4-6). Most of the specimens have resistivities of 5000 ohm-m on average (Table 4-1). There is a negative correlation between FE and resistivities, but it is not so marked. (Fig. 4-5).

There are small-scale diorite outcrops near Station G-12 and in the southern tips of Lines D~F, and a small-scale dolerite outcrop near Station A-12. They have relatively high FE values of 4.9~103% but low AR ones of 256~2191 ohm-m. Dacite and andesite are distributed over

the north and the south of the survey area, respectively. They have low FEs ranging from 1.1 to 3.7% but high resistivities ranging from 3500 to 30924 ohm-m.

#### 3-4-2 IP Results

The statistical analyses of the IP data obtained here result in the followings.

The observed values of FE range from 1.8 to 6.8% and those of AR from 329 to 8064 ohm-m (Table 4-2).

The histogram of the total observation data of FE fits well to a normal distribution curve. The histograms of the FE values for each electrode separation level also fit well to other normal distribution curves. The mean values of FE in these histograms are not so different one another. On the other hand, the histograms of AR values fit to log-normal distribution curves, but there are much differences between the histograms for each electrode separation levels (Fig. 4-7). The AR has a tendency to increase with  $n$ . This fact may indicate that the resistivity increases with depth in the survey area.

The criterion of "anomaly" can be decided by the cumulative frequency distribution curve. It enables us to judge whether an observed value is anomalous or not. As a result, the values of FE > 6% and AR < 500 ohm-m are defined as "anomaly", and those of 5% < FE < 6% and 500 ohm-m < AR < 1000 ohm-m are as "weak anomaly". The mean value of FE is 4.5%, and that of AR is 1500 ohm-m (Fig. 4-8).

The FE-AR correlation coefficients are small for the present case. This shows that the values of MF can not be used for an indicator of the mineralization (Fig. 4-10).

In some parts of the survey area, we find the positive correlation between the observed IP and the topographic height of the observed point. This may indicate that the related mountainous area partially contains disseminated bodies. However, there is no conspicuous relation between AR and topographic height (Table 4-3).





### 3-4-3 Distribution of Anomalies

Some typical anomalies are extracted from the IP plan maps and cross sections to undergo computer simulation tests. The volume and depth of an anomaly can be estimated by such simulation analyses. The results thus computed are used for drawing up Fig. 4-13.

The best-fitting models of the observed FE and AR on Lines C and J are determined by the simulation test. As a result, it is verified that the anomalies correspond to a FE higher than 6% and a resistivity lower than 500 ohm-m on the best-fitting model. Similarly, the best-fitting models are also determined for the other anomalies.

In order to make a comprehensive interpretation of the IP results of quantitative analyses, bird's-eye views of (a) the total FE distribution for a electrode separation coefficient of  $n=1$ , (b) the distribution of FE larger than its mean value and (c) the distribution of FE larger than the weak anomaly standard are given in Fig. 4-14 (a), (b) and (c) respectively.

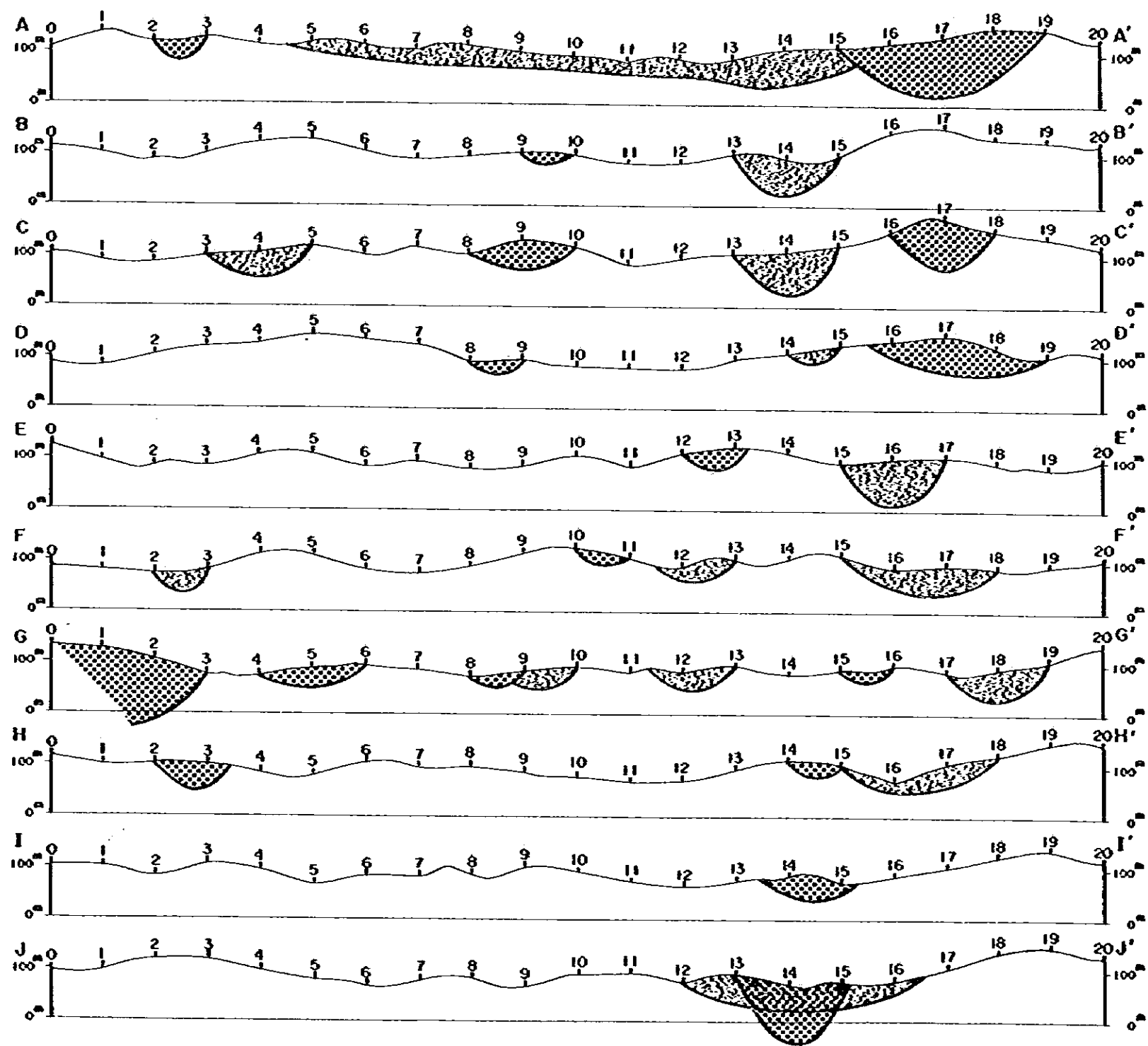
### 3-4-4 Consideration of Mineralization

In order to clarify the relation between the obtained IP results and the distribution of the disseminated deposits, the IP results are compared with the geological and geochemical data obtained in the survey area. PL. 4-18 is a comprehensive map, in which the IP anomalies are illustrated together with the geological structure including the disseminated zones and copper anomalies obtained by the geological and geochemical surveys.

In this map, the FE anomalies are represented in distinction from the AR anomalies, but the MF anomalies are not represented because they are presumed to be independent of the mineralization.

#### (1) FE anomalies

The FE anomalies, which are denoted by M-1 ~ M-7 in the map, are related with the mineralization. The depth of the anomaly sources is estimated to be shallower than 100 m below the ground surface.



**LEGEND**

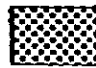

 Interpreted anomalous FE zones related to mineralizations  
 Interpreted anomalous AR zones related to low resistivity rocks

Fig. 4-13 Results of Quantitative Analysis of IP Anomalies

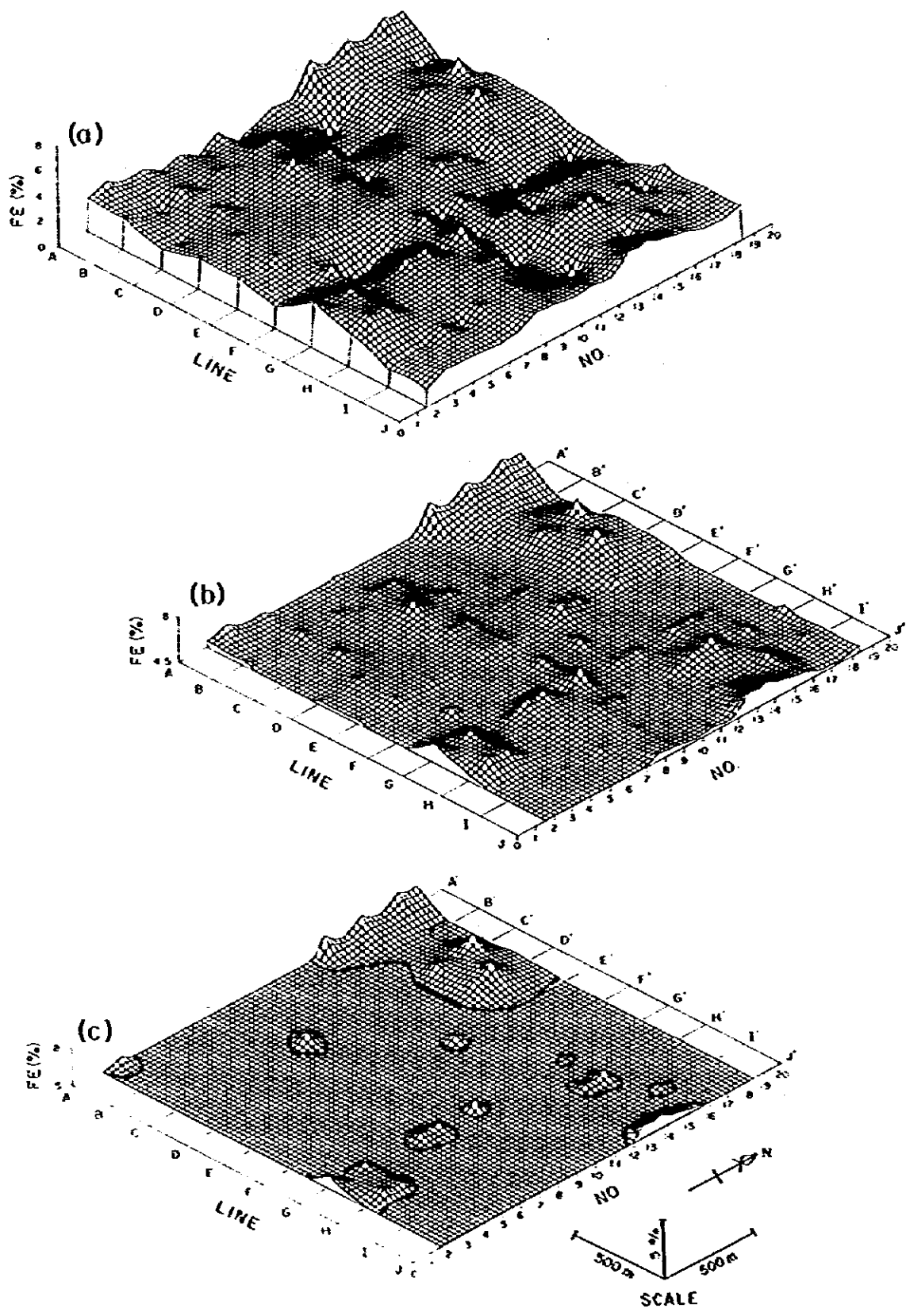


Fig. 4-14 Bird's-eye View of FE Values for n=1  
 (a) FE > 1.8%, (b) FE > 4.5%, (c) FE > 5.0%

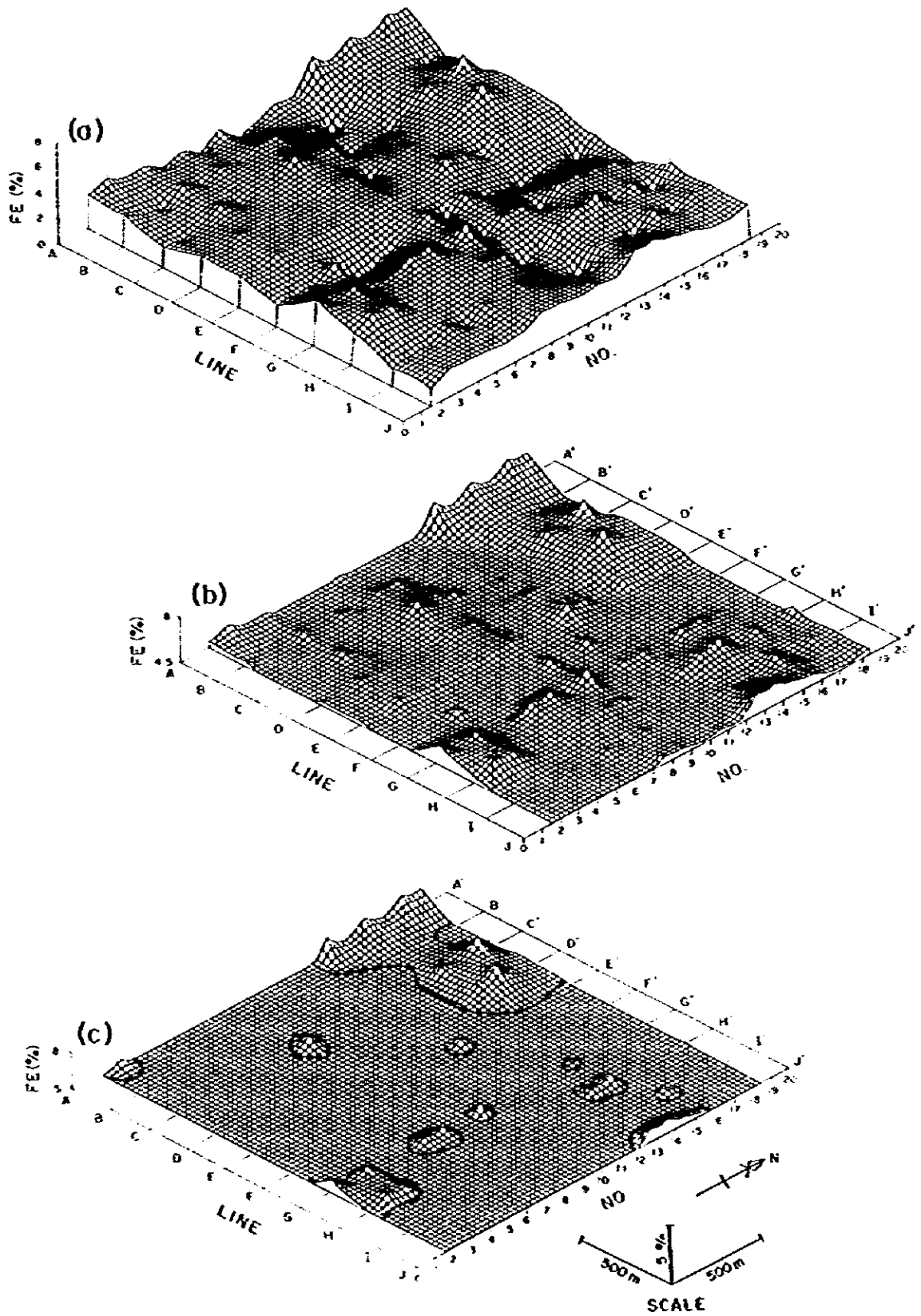


Fig. 4-14 Bird's-eye View of FE Values for  $n=1$   
 (a)  $FE > 1.8\%$ , (b)  $FE > 4.5\%$ , (c)  $FE > 5.0\%$

The FE anomalies such as M-1 (northern part of Lines C and D), M-3 (northern part of Lines G~J), M-4 (the midpoints on Lines B~D), M-5 (the midpoints on Lines E~G), and M-6 (southern part of Lines G and H) coincide with the copper anomalies obtained by the geochemical survey. They may be evidences for the chalcopyrite dissemination.

On the other hand, some of the conspicuous FE anomalies do not coincide with geochemical copper anomalies, for example, M-1 (northern part of Line A), east end of M-3 (on Line J), and southern part of M-6 (south end of Lines G and H). They are presumably caused by the pyrite dissemination.

The FE anomalies M-1, M-2 and M-3 are linearly arranged in the WNW-ESE direction. Their extension is parallel to the geochemical copper anomaly zone in the northern part of the survey area. Meanwhile, the FE anomalies M-1, M-2, M-5 and M-6 are seemed to be arranged on a circular arc. However, the FE arrangement system is not generally explicit.

The M-2 and M-4 FE anomalies coincide with the NNE-SSW trending copper anomaly zone in the western part of the survey area. But it is probable that both the FE anomalies are independent each other.

## (2) AR anomalies

The AR anomalies are represented as R-1 ~ R-5 in the map. They are generally caused by low resistivity layers.

One of the most marked AR anomalies in the survey area is R-1 Anomaly, which trends in the WSW-ENE direction with a width of about 200 m across Lines A ~ H. This anomaly neither coincides with the FE anomaly nor the geochemical copper anomaly. This fact may indicate that the R-1 anomaly does not correspond to a low resistivity zone related with the mineralization. A similar conclusion can be made for the AR anomalies R-2, R-4 and R-5.

These anomalies can be interpreted as low resistivity parts of granodiorite which are located at a depth of less than 50 m below the ground surface. However, their location and volumes do not

correspond to those of clay systems which are confirmed by the geological survey. As the matter of fact, the causes of these low-AR anomalies are still unknown.

The fact that the R-3 anomaly coincides partially with the FE anomaly may suggest the possibility of a low resistivity zone due to the pyrite dissemination in granodiorite. Otherwise, the low resistivity here may be caused by the river water permeation into the superficial parts of granodiorite, because this low resistivity is located in a branch of S. Bاده River.

### (3) Mineralized zones

The geological survey has previously disclosed several mineralized zones in an area of 2 km eastwest and 3 km northsouth including the Old Panji Village. These zones are trending in the NNE-SSW direction with a zonal arrangement of the pyrite dissemination in the outer zone and the chalcopyrite disseminated tourmalinized rock in the inner zone. The geochemical anomalies (copper and molybdenum), in general, coincide with the central parts of these disseminated zones. The number of the IP anomalies amount to seven (M-1 ~ M-7) in the Panji dissemination zones.

The FE anomalies M-1, M-2 and M-3 are linearly arranged in the WNW-ESE direction. The extension of this arrangement is parallel to the trend of the geochemical copper anomalies in the northern part of the survey area. Such a parallelism may be caused by a simultaneous mineralization in the Panji area. Judging from the above, these anomalies M-1, M-2 and M-3 indicate probably mineralized zones. Especially, the M-2 anomaly is one of the most outstanding FE anomalies. This is located at the geochemically anomalous area near the Old Panji mineralization zone actually confirmed by the geological survey. These facts may show that the M-2 anomaly is one of the most promising anomalies in the survey area. The computer simulation analysis of this anomaly concludes that the related mineralized zone of 7% FE has a length of 400 m trending in the EW direction, a width of 200 m and a thickness of

100 m. Its depth is very shallow. Such a value of FE is obtained by continuously pyrite/chalcopyrite disseminated specimens according to the laboratory tests. On the basis of the above facts, it can be concluded that the X-2 anomaly corresponds to a disseminated zone in the superficial part of granodiorite.

# APPENDICES



Appendix-1 List of Rock and Ore Samples Tested

Sample No.	Rock Name	Thin Section	Polished Specimen	X-Ray Analysis	K-Ar Dating	Rock Chemical Analysis	Chemical Analysis
<b>(Selakean area)</b>							
Rx- 2	ore						0
4	andesitic tuff	0					
6	" "	0					
9	" "	0					
11	" "	0					
RY- 6	ore		0				
7	andesitic tuff	0					
8	andesite	0					
12	andesitic tuff	0					
RZ- 5	" "	0					
10	granodiorite	0					
12	ore, clay		0	0			0
14	ore, clay			0			0
<b>(Panjl area)</b>							
Rx-21	granodiorite	0					0
23	altered tuff	0					
28	granodiorite	0					
30	clay			0			
33	granodiorite porphyry	0					
34	"	0					
36	"	0					
37	quartz diorite	0					
49	" "	0					
50	dolerite	0					
51	dacite	0					
53	granodiorite	0			0	0	
54	(quartz) andesitic tuff	0					
55	granodiorite	0					
56	clay			0			
58	Tourmaline quartz		0				0
RY-21	clay, ore	0		0			0
22	quartz andesitic tuff	0					
23	granodiorite	0					
26	"	0					

Sample No.	Rock Name	Thin Section	Polished Specimen	X-Ray Analysis	K-Ar Dating	Rock Chemical Analysis	Chemical Analysis
27	quartz andesitic tuff	0				0	
31	dolerite	0					
35	granodiorite	0					
39	Tourmaline quartz	0	0				0
RZ-21	quartz andesitic tuff	0					
23	granodiorite	0					
24	"	0				0	
28	"	0					
30	quartz andesitic tuff	0					
31	acidic tuff	0					0
32	silicified rock						0
33	" "						0
34	andesitic tuff	0					
35	quartz andesitic tuff	0					
42	clay			0			
44	clay			0			
47	dolerite	0					
49	quartz diorite	0					
51	quartz diorite	0					
52	quartz andesitic tuff	0					
(G. Ibu area)							
QD- 1	quartz diorite	0			0	0	
QD- 2	granodiorite	0			0	0	
<b>Total</b>		<b>44</b>	<b>4</b>	<b>7</b>	<b>3</b>	<b>5</b>	<b>10</b>

## Appendix-2 Microscopic Observation of Thin Sections

Selakau Area

Sample No.	Rock Name	Texture	Grain/Fragment						Groundmass/Matrix						Secondary Mineral						Remarks								
			Q	Kf	Pl	Bt	Hb	Au	Op	Tou	Lich	Q	Kf	Pl	Bt	Py	Op	Q	Sa	Ch		Bt	K	Xe	Ep	Sp	Ca		
Jirak Formation																													
RY-4	And-tf	Pyroclastic																											
6	"	"																											
9	"	"																											
11	"	"																											
KY-7	"	"																											
8	And	"																											
12	And-tf	"																											
PZ-5	"	"																											
G. Ray Granodiorite																													
PZ-10	Granodiorite	HOL CRY																											

Abbreviation

Mineral

- Q: quartz
- Kf: kaly feldspar
- Pl: plagioclase
- Bt: biotite
- Hb: hornblende
- Au: augite
- Op: opaque mineral
- Tou: tourmaline
- Lich: lichen fragment

Rock

- py: pyrite
- Se: sericite
- Ch: chlorite
- X: kaoline
- Her: hematite
- Epi: epidote
- Sp: sphene
- Zr: zircon
- Act: actinolite
- hyp: hypersthene

Texture

- Hol cry: holocrystalline
- Other
- Se alt: sericite alteration
- Q v: quartz vein
- ⊙: abundant
- : Common
- : rare

Fauji Area

Sample No.	Rock Name	Texture	Grain/Fragments													Groundmass/Matrix										Secondary Mineral								Remarks		
			Q	Kf	Pl	Bc	Hb	Au	Op	Tou	Lic	Q	Kf	Pl	Bc	Py	Op	Q	Se	Ch	Bc	X	He	Ep	Sp	Ca										
Belango Formation																																				
RX-23	almond cf	Porphyritic	•?					•																												Argillization phenocrysts - clay matrix Se alt
RX-54	Q and cf	Pyroclastic	•					•																											g v. v. ch. ch	
RY-22	"	"	•					•											and															Acc.		
RY-26	Q and	Porphyritic	•					•																												
RY-27	Q "	"	•					•																												
RZ-21	Q and cf	Pyroclastic	•					•?																												
RZ-30	"	"	•					•											dc and															Other clay		
RZ-31	Acidic cf	"	•					•											ms																	
PZ-34	Dac cf	"	•					•?											and																	
PZ-35	and cf	"	•					•																										Se alt		
PZ-52	Q and cf	"	•					•											and																	
C. Sablavak Granodiorite																																				
RX-21	Granodiorite	Nal Crx	•					•																												
RX-53	"	"	•					•																										myrmekite		
RX-55	"	"	•					•																												
RY-23	"	"	•					•													Zr															
RY-35	"	"	•					•																												
RZ-23	"	"	•					•?														Zr														
RZ-24	"	"	•					•																												
RZ-28	"	"	•					•														Zr														
RY-28	"	"	•					•																										Porphyritic		



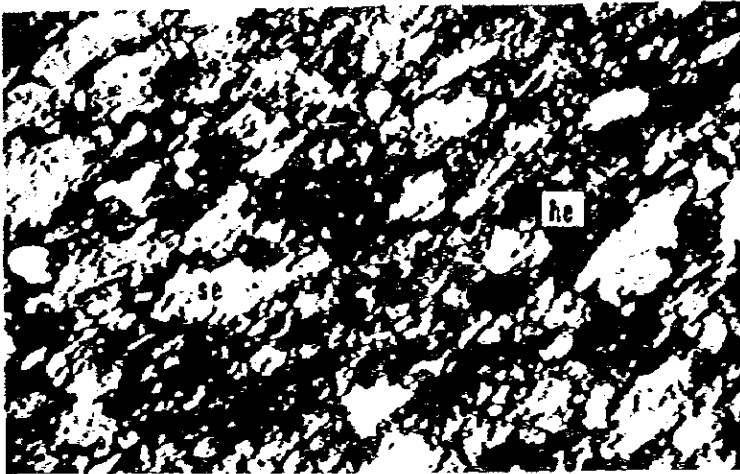
Sample No.	Rock Name	Texture	Grain/Fragments								Groundmass/Matrix								Secondary Mineral								Remarks
			Q	Kf	Pl	Be	Rb	Au	Op	Tou	Kfsch	Q	Kf	Pl	Be	Py	Op	Q	Se	Ch	Hc	K	Mg	Zp	Sp	Ca	
	G. 12w Area																										
QB-1	Quartzite	Not cry	○	○	○	○	○	●		Zi								●									
GB-1	Granodiorite	"	○	○	○	○	○	●										○					●	●			

Appendix-3 Microscopic Observation of Polished Specimen

Area	Sample No.	cp	cov	sph	py	arpy	Description
Selakcan	RY-6	○	●	○		⊙	Arsenopyrite >> chalcopyrite ± sphalerite >> covellite Pyrite is cube in shape, and arsenopyrite is coarse grain in shape. Chalcopyrite occurs as exsolution dot in sphalerite, or with pyrite and sphalerite in gangue mineral. Chalcopyrite is maximum 0.8 mm in size, sphalerite is maximum 0.7 mm in size.
	RZ-12	●	●			○	Pyrite and arsenopyrite are scattered in gangue mineral. Fine grained covellines occur around arsenopyrite in gangue or in fine vein.
Panji	RY-39	○	●				Irregular grained chalcopyrites are less than 4mm in size, associa- ting covellite. Gangue minerals are tourmaline and quartz.
	RX-58	○	●		○		Pyrites in irregular form are less than 1.5 mm in size, and are scattered in gangue mineral. Chalcopyrite also occurs in gangue mineral, associating with small amount of covellite and very fine grained mineral (may be sphalerite). Gangue minerals are tourmaline and quartz.

⊙ abundant ○ common ● rare cp: chalcopyrite cov: covellite sph: sphalerite py: pyrite arpy: arsenopyrite

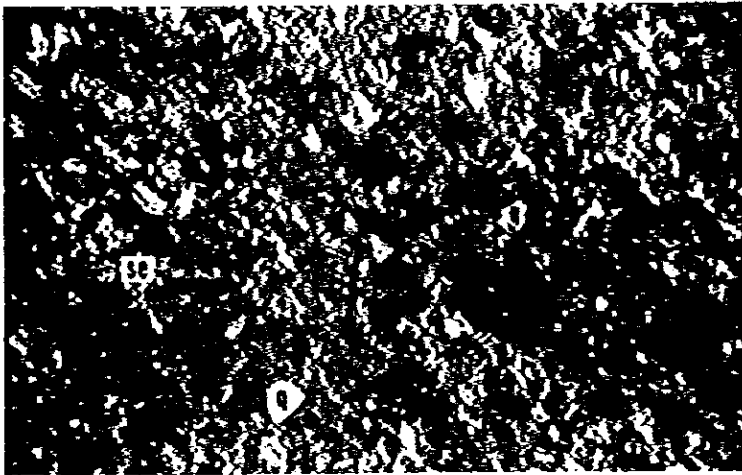
Appendix-4 Microscopic Photographs of Thin Section



Sample No.: RX-4  
Locality : Slakean  
Rock Name : Andesitic red tuff  
(Jirak Formation)

se: sericite  
he: hematite

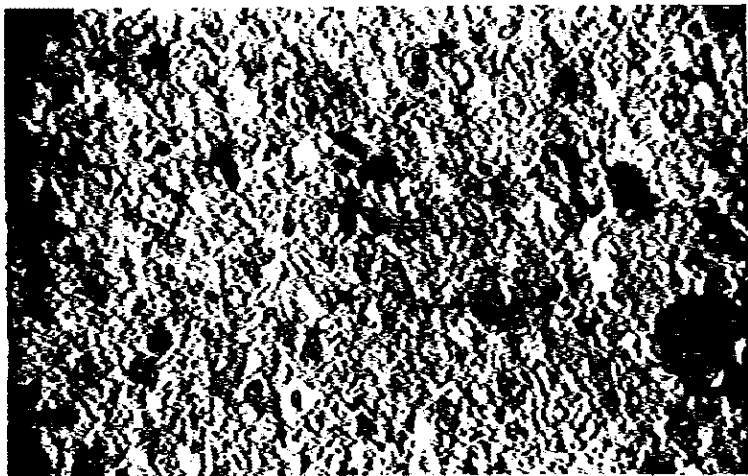
Open nicol  
0.5 mm



Sample No.: RY-7  
Locality : Slakean  
Rock Name : Quartz andesitic tuff  
(Jirak Formation)

se: sericite  
q : quartz

Crossed nicols  
0.5 mm

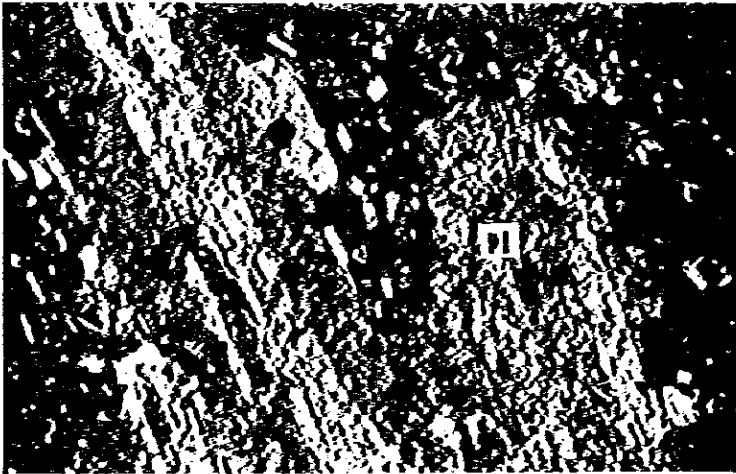


Sample No.: RY-7  
Locality : Slakean  
Rock Name : (Quartz) Andesitic  
tuff  
(Jirak Formation)

se: sericite  
q : quartz

Open nicol  
0.5 mm

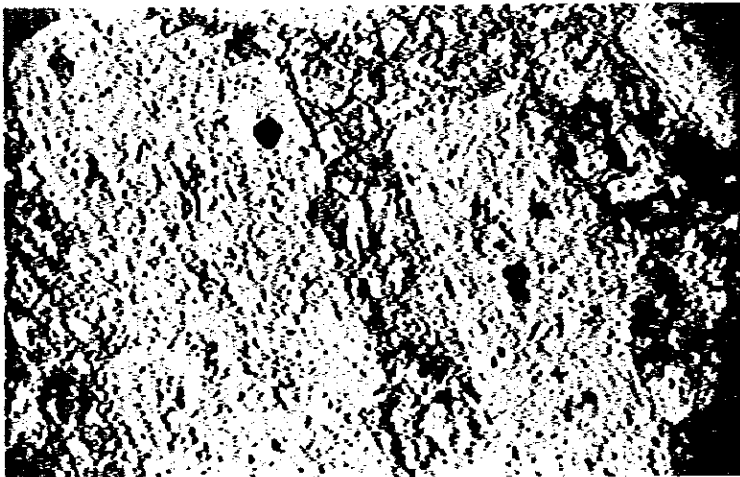




Sample No.: RY-8  
Locality : Slakean  
Rock Name : Andesite  
(Jirak Formation)

pl: plagioclase  
se: sericite

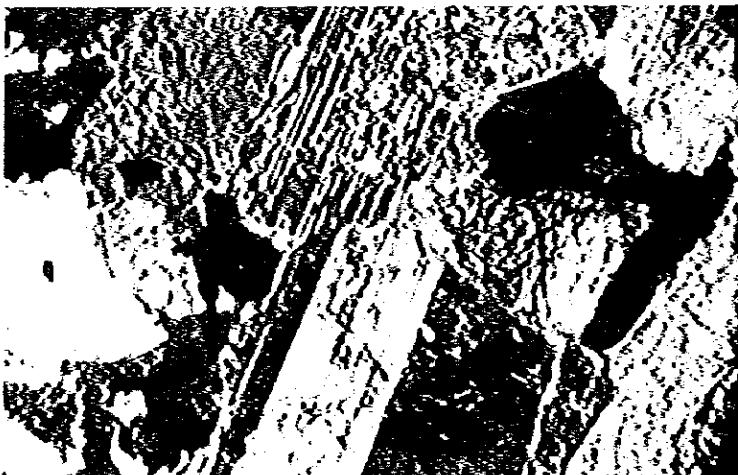
Crossed nicols  
0.5 mm



Sample No.: RY-8  
Locality : Slakean  
Rock Name : Andesite  
(Jirak Formation)

pl: plagioclase  
plagioclase is partly altered  
to sericite

Open nicol  
0.5 mm

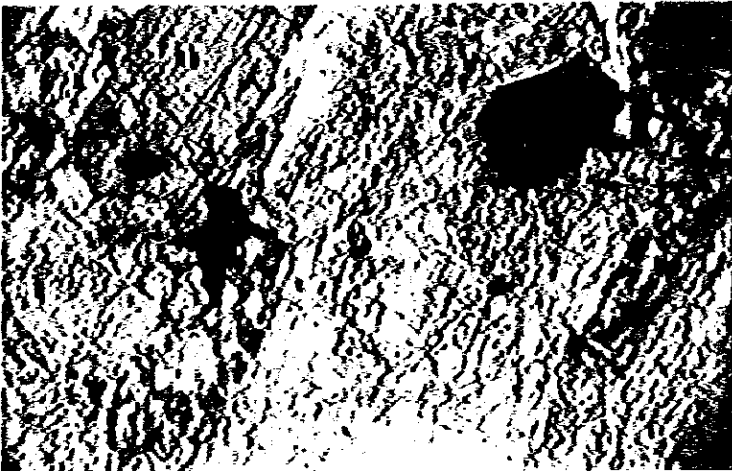


Sample No.: ZR-10  
Locality : Slakean  
Rock Name : G. Raya granodiorite

pl: plagioclase  
hb: hornblende

plagioclase is partly altered  
to sericite

Crossed nicols  
0.5 mm



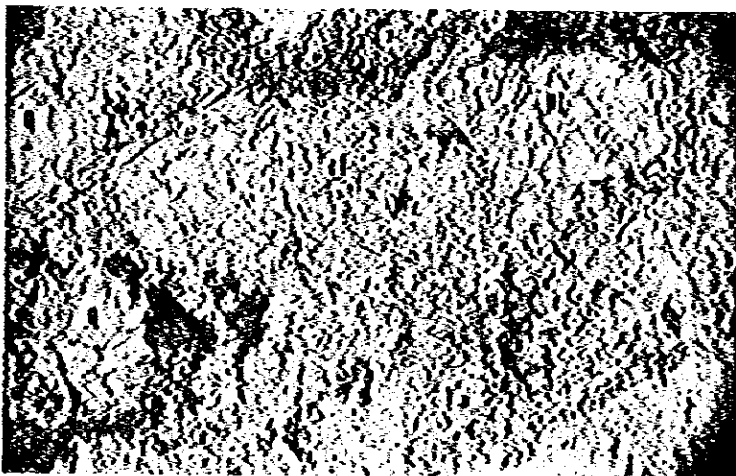
Sample No. : ZR-10  
Locality : Slakean  
Rock Name : G. Raya granodiorite  
q : quartz  
se: sericite  
hb: hornblende

Open nicol  
0.5 mm



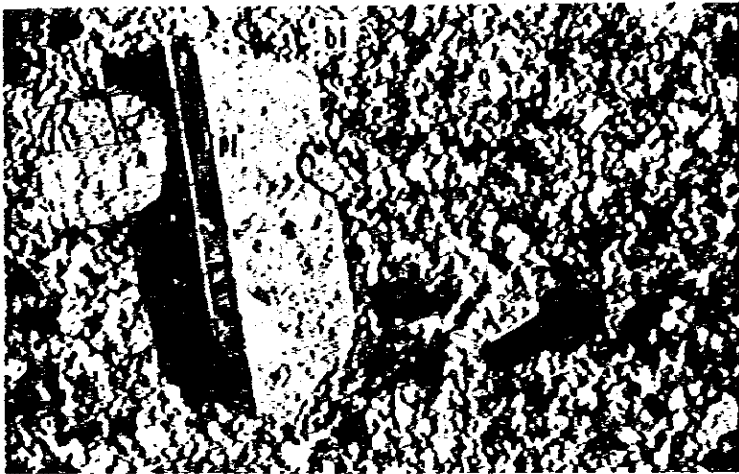
Sample No. : RY-22  
Locality : Panji  
Rock Name : Quartz andesitic tuff  
(Belango Formation)  
pl: plagioclase  
q : quartz  
rf: rock fragment

Crossed nicols  
0.5 mm



Sample No. : RY-22  
Locality : Panji  
Rock Name : Quartz andesitic tuff  
(Belango Formation)  
pl: plagioclase  
q : quartz  
rf: rock fragment

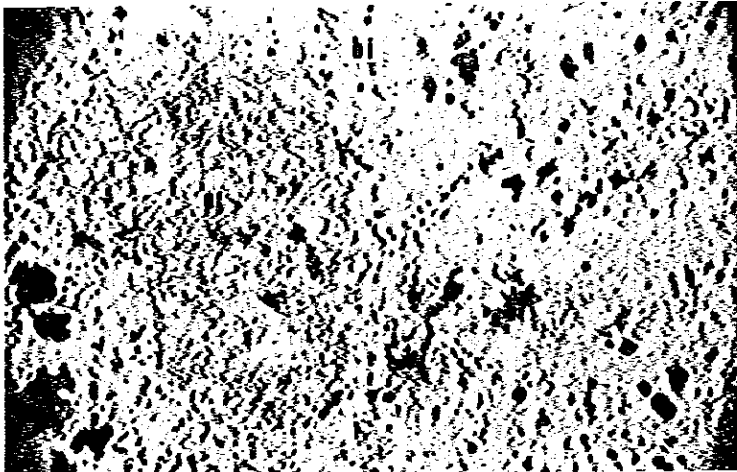
Open nicol  
0.5 mm



Sample No.: RY-26  
Locality : Panji  
Rock Name : Quartz andesite  
(Belango Formation)

q : quartz  
pl: plagioclase  
bi: biotite

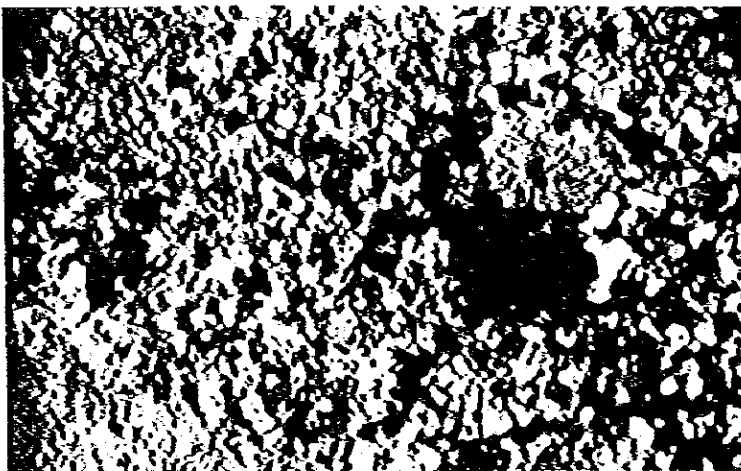
Crossed nicols  
0.5 mm



Sample No.: RY-26  
Locality : Panji  
Rock Name : Quartz andesite  
(Belango Formation)

q : quartz  
pl: plagioclase  
bi: biotite

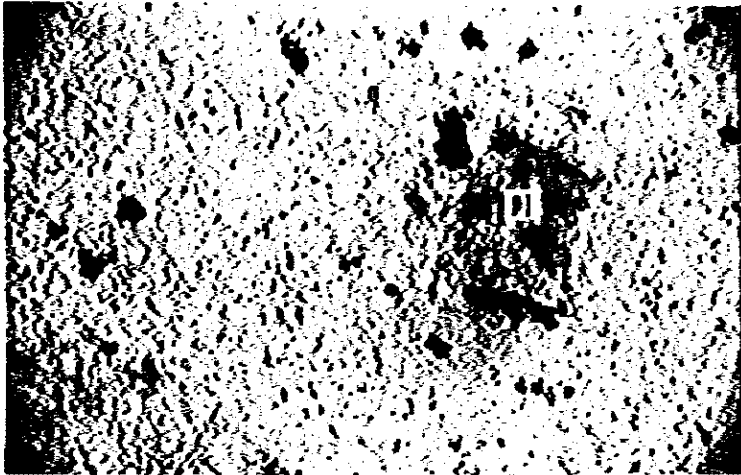
Open nicol  
0.5 mm



Sample No.: RY-27  
Locality : Panji  
Rock Name : (Quartz) andesite  
(Belango Formation)  
(hornfelsic)

q : quartz  
pl: plagioclase

Crossed nicols  
0.5 mm



Sample No.: RY-27  
 Locality : Panji  
 Rock Name : Quartz andesite  
 (Belango Formation)  
 (hornfelsic)  
 q : quartz  
 pl: plagioclase

Open nicol  
 0.5 mm



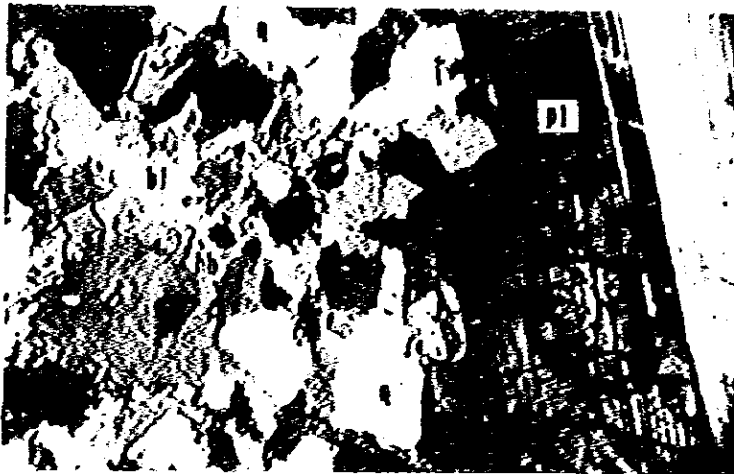
Sample No.: RZ-34  
 Locality : Panji  
 Rock Name : Dacitic tuff  
 (Belango Formation)  
 q : quartz  
 ch: chlorite  
 rf: rock fragment

Crossed nicols  
 0.5 mm



Sample No.: RZ-34  
 Locality : Panji  
 Rock Name : Dacitic tuff  
 (Belango Formation)  
 q : quartz  
 ch: chlorite  
 rf: rock fragment

Open nicol  
 0.5 mm



Sample No.: RX-53  
Locality : Panji  
Rock Name : G. Sebiawak  
Granodiorite

q : quartz  
pl: plagioclase  
bi: biotite  
hb: hornblende

Crossed nicols  
0.5 mm



Sample No.: RX-53  
Locality : Panji  
Rock Name : G. Sebiawak  
Granodiorite

q : quartz  
pl: plagioclase

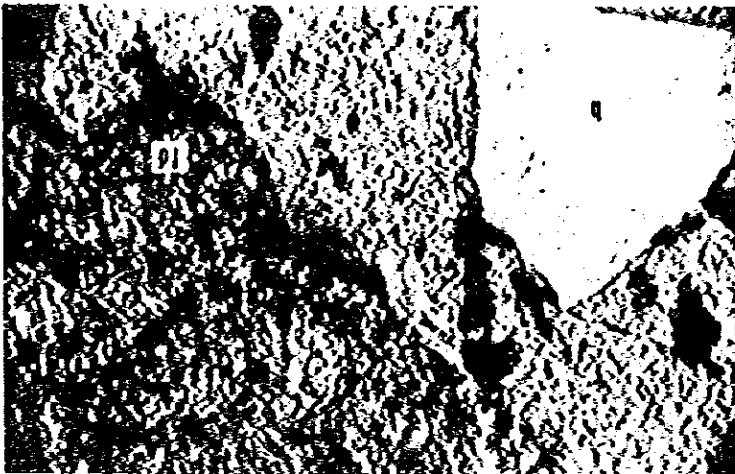
Open nicol  
0.5 mm



Sample No.: RX-51  
Locality : Panji  
Rock Name : Dacite porphyry

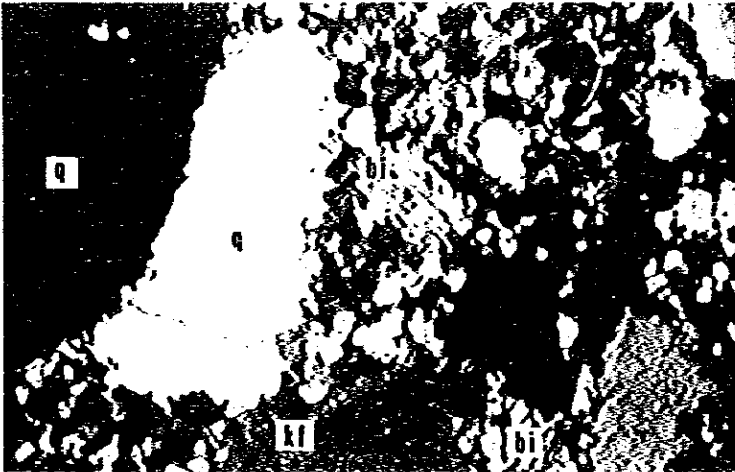
q : quartz  
pl: plagioclase

Crossed nicols  
0.5 mm



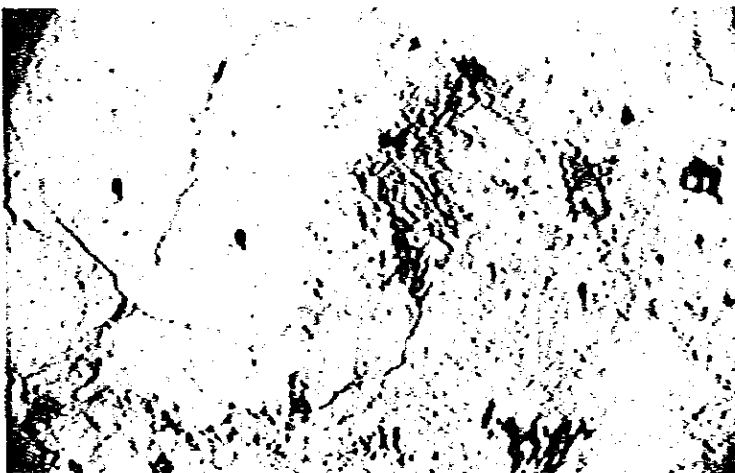
Sample No.: RX-51  
Locality : Panji  
Rock Name : Dacite porphyry  
q : quartz  
pl: plagioclase

Open nicol  
0.5 mm



Sample No.: RX-34  
Locality : Panji  
Rock Name : Quartz porphyry  
q : quartz  
kf: kalifeldspar  
bi: biotite

Crossed nicols  
0.5 mm



Sample No.: RX-34  
Locality : Panji  
Rock Name : Quartz porphyry  
q : quartz  
kf: kalifeldspar  
bi: biotite

Open nicol  
0.5 mm



Sample No.: RZ-47  
Locality : Panji  
Rock Name : Dolerite

pl: plagioclase  
hb: hornblende

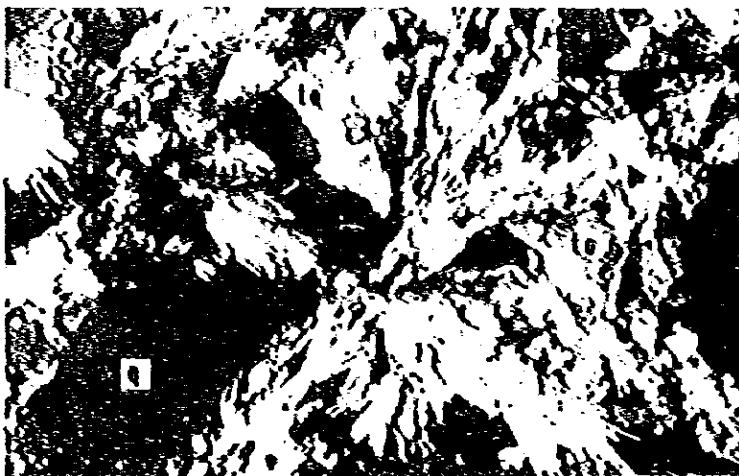
Crossed nicols  
0.5 mm



Sample No.: RZ-47  
Locality : Panji  
Rock Name : Dolerite

pl: plagioclase  
hb: hornblende

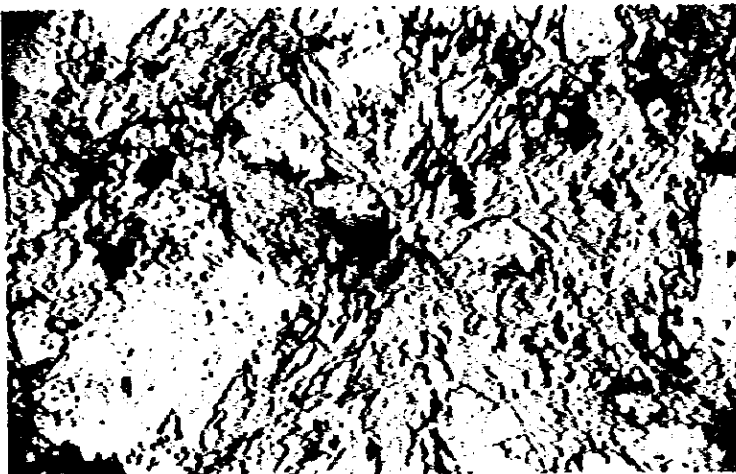
Open nicol  
0.5 mm



Sample No.: RX-58  
Locality : Panji  
Rock Name : Tourmaline quartz  
rock

q : quartz  
to: tourmaline

Crossed nicols  
0.5 mm



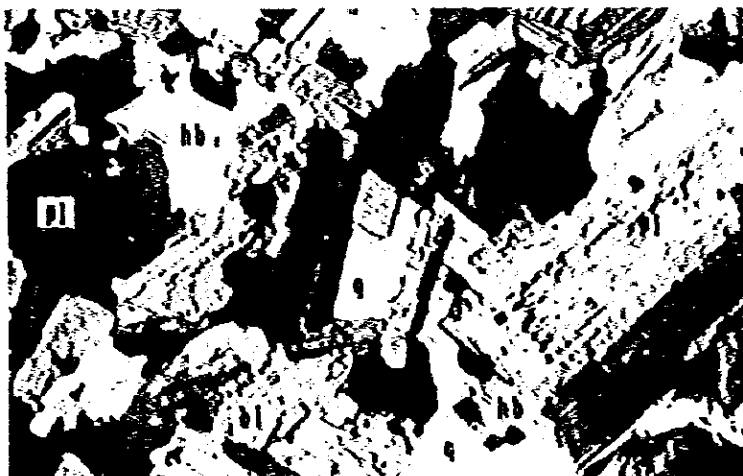
Sample No.: RX-58  
Locality : Panji  
Rock Name : Tourmaline quartz  
rock  
q : quartz  
to: tourmaline

Open nicol  
0.5 mm



Sample No.: RY-39  
Locality : Panji  
Rock Name : Tourmaline quartz  
rock  
q : quartz  
to: tourmaline

Crossed nicols  
0.5 mm



Sample No.: QD-1  
Locality : G. Ibu  
Rock Name : Quartz diorite  
q : quartz  
pl: plagioclase  
hb: hornblende  
bi: biotite

Crossed nicols  
0.5 mm

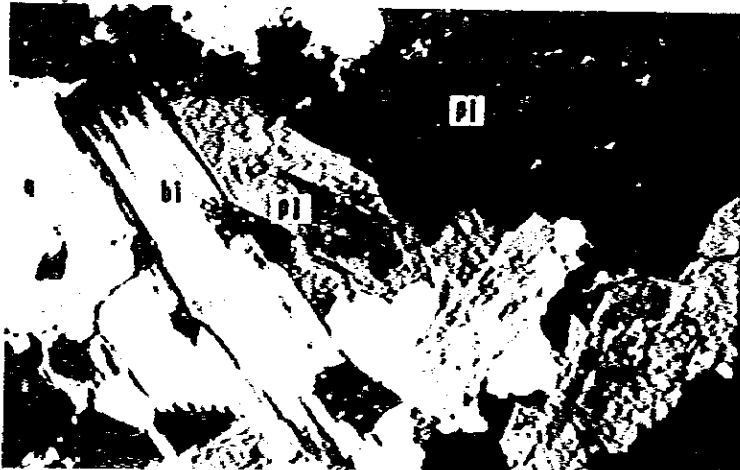




Sample No.: QD-1  
 Locality : G. Ibu  
 Rock Name : Quartz diorite

q : quartz  
 pl: plagioclase  
 hb: hornblende

Open nicol  
 0.5 mm



Sample No.: GD-2  
 Locality : G. Ibu  
 Rock Name : Granodiorite

q : quartz  
 pl: plagioclase  
 bi: biotite

Crossed nicols  
 0.5 mm



Sample No.: GD-2  
 Locality : G. Ibu  
 Rock Name : Granodiorite

q : quartz  
 pl: plagioclase  
 bi: biotite

Open nicol  
 0.5 mm

Appendix-5 Microscopic Photographs of Polished Specimen



Sample No.: RY-6

Exsolution dots and lamellas of chalcopyrite in sphalerite.

cp : Chalcopyrite  
sph: Sphalerite

0 0.2 mm



Sample No. : RY-6

Locality : Selakean

Name of Ore: Cp-Sph-Asp Ore

cp : Chalcopyrite  
sph: Sphalerite  
asp: Arsenopyrite

Chalcopyrite occurs as exsolution dot in sphalerite.

0 0.2 mm



Sample No. : RY-6

Locality : Selakean

Name of Ore: Cp-Sph-Asp Ore

cp : Chalcopyrite  
py : Pyrite  
sph: Sphalerite  
asp: Arsenopyrite

0 0.2 mm



Sample No. : RZ-12

Locality : S. Entagok, Selakean

Name of Ore: Cu-Asp Ore

cov: Covellite  
asp: Arsenopyrite

covellite is found around arsenopyrite.

0 0.2 mm



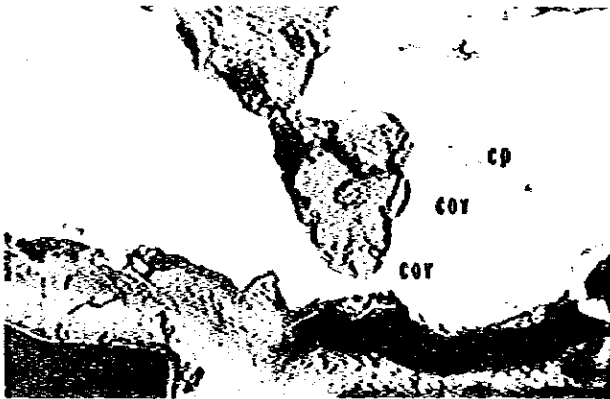
Sample No. : RY-39

Locality : Panji

Name of Ore: Chalcopyrite dissemination  
in tourmaline

Covellite is found around chalcopyrite

0 0.2  $\mu$ m



Sample No. : RX-58

Locality : Panji

Name of Ore: Chalcopyrite dissemination  
in tourmaline quartz

cp : Chalcopyrite  
cov: Covellite

0 0.2  $\mu$ m



Sample No. : RX-58

Locality No.: Panji

Name of Ore : Pyrite dissemination in  
tourmaline quartz

0 0.2  $\mu$ m

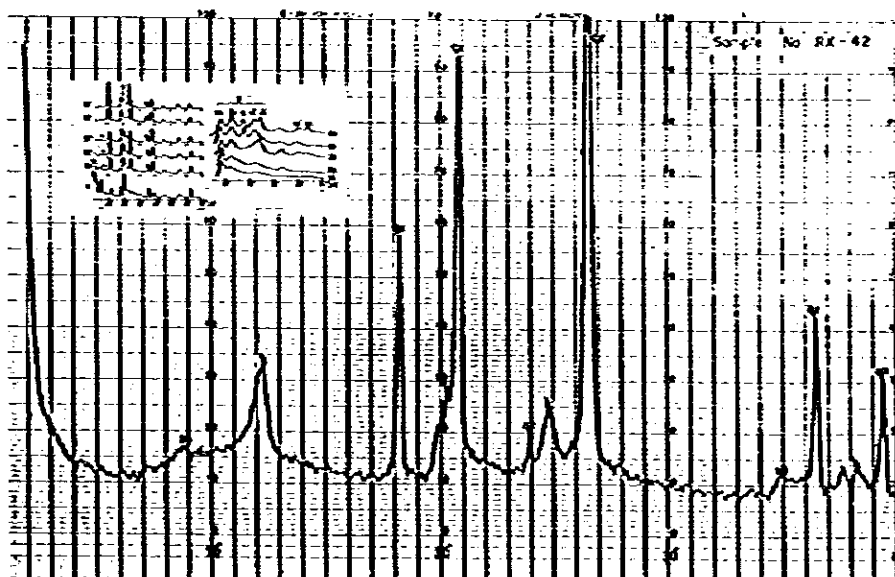
Appendix-6 Chart and List of X Ray Diffractive Analysis of Clay Mineral

Sample No.	Location	Q	Se	K	Ch	Pl	La	Ac	Cb	Ca	Aspy	Py
Selakeem												
RZ-12	S. Entagak	⊙	○					?d=5.64			○	
RZ-14	S. Melanci				●	⊙	⊙			?		○
Panji												
RX-21	S. Karonang											
RX-30	up st. of S. Jendaham	⊙	○	●								
RX-56	East of old panji	⊙		⊙								
RZ-42	S. Jendaham, S. Pegan	⊙	○	●								
RZ-44	S. Pitunam	⊙		●	○?				●			

Q: Quartz    Se: Sericite    K: Kaoline mineral    Ch: Chlorite  
 Pl: Plagioclase    La: Laumontite    Ac: Analcite    Cb: Gibbsite  
 Ca: Calcite    Aspy: Arsenopyrite    Py: Pyrite    ⊙: Abundant  
                   ○: Common  
                   ●: Rare

Condition  
 Target             Cu             Divergency slit     1°  
 Filter             Ni             Scatter                1°  
 Voltage            30 kv        Receiving slit      0.3 mm  
 Current            15 mA       Chart speed         2 cm/min  
 Scanning speed   2°/min      Full scale            1,000 cps  
 Time constant    2 second







Appendix-7 Assay Result of Geochemical Sample

Serial No.	Sample No.	Chemical Assay		Serial No.	Sample No.	Chemical Assay	
		Cu ppm	Pb ppm			Cu ppm	Mo ppm
(Selakean)				(Panji)			
1	TX- 1	31	27	32	TX-21	31	5
2	2	73	21	33	22	17	6
3	3	29	29	34	23	21	6
4	4	40	24	35	24	28	8
5	5	53	26	36	25	13	6
6	6	83	22	37	26	34	9
7	7	62	38	38	27	25	8
8	8	29	24	39	28	51	9
9	TY- 1	70	29	40	29	34	8
10	2	79	41	41	30	36	4
11	3	61	34	42	31	12	6
12	4	48	26	43	32	9	8
13	5	44	24	44	33	13	5
14	6	40	17	45	34	23	6
15	7	24	19	46	35	69	4
16	8	27	33	47	36	13	3
17	9	48	28	48	37	21	4
18	10	55	23	49	38	28	8
19	11	41	30	50	39	85	5
20	TZ- 1	73	33	51	40	96	6
21	2	75	30	52	41	87	13
22	3	84	46	53	42	64	10
23	4	58	44	54	43	36	9
24	5	58	23	55	44	21	9
25	6	41	23	56	45	46	9
26	7	44	26	57	46	53	6
27	8	41	23	58	TY-21	23	9
28	9	44	35	59	22	66	11
29	10	36	51	60	23	46	13
30	11	126	26	61	24	9	8
31	12	50	35	62	25	9	6
				63	26	38	10
				64	27	21	9



Serial No.	Sample No.	Chemical Assay		Serial No.	Sample No.	Chemical Assay	
		Cu ppm	Pb ppm			Cu ppm	Mo ppm
65	TY-28	9	8	102	32	27	7
66	29	13	4	103	33	8	7
67	30	9	5	104	34	46	7
68	31	4	5	105	35	8	4
69	32	26	7	106	36	8	9
70	33	30	8	107	37	15	7
71	34	17	7	108	38	11	4
72	35	17	9	109	39	81	13
73	36	17	12	110	40	36	5
74	37	9	8	111	41	49	7
75	38	43	7	112	42	19	7
76	39	30	5	113	43	36	10
77	40	32	5	114	44	78	12
78	41	126	13	115	45	47	7
79	42	40	13	116	46	63	10
80	43	17	9	117	47	54	7
81	44	38	7	118	TA- 0	119	15
82	45	26	10	119	2	65	22
83	46	123	9	120	4	66	11
84	47	125	9	121	6	79	9
85	48	53	9	122	8	97	9
86	49	74	7	123	10	147	5
87	50	12	7	124	12	76	8
88	51	25	11	125	14	63	8
89	52	71	22	126	16	18	9
90	53	86	12	127	18	21	5
91	TZ-21	50	14	128	20	13	9
92	22	8	6	129	TB- 0	182	46
93	23	23	8	130	2	103	11
94	24	36	8	131	4	183	26
95	25	47	8	132	6	228	30
96	26	59	8	133	8	244	15
97	27	46	10	134	10	226	15
98	28	53	9	135	12	142	9
99	29	78	15	136	14	68	15
100	30	34	9	137	16	35	13
101	31	26	4	138	18	18	13

Serial No.	Sample No.	Chemical Assay		Serial No.	Sample No.	Chemical Assay	
		Cu ppm	Pb ppm			Cu ppm	Mo ppm
139	20	95	15	176	6	48	16
140	TC- 0	185	17	177	8	48	8
141	2	158	17	178	10	55	8
142	4	233	62	179	12	61	10
143	6	235	78	180	14	27	10
144	8	256	46	181	16	152	8
145	10	246	41	182	18	140	7
146	12	161	8	183	20	83	8
147	14	99	10	184	TC- 0	21	8
148	16	357	10	185	2	55	10
149	18	224	8	186	4	286	51
150	20	28	8	187	6	40	19
151	TD- 0	64	9	188	8	69	6
152	2	66	5	189	10	72	11
153	4	284	51	190	12	72	16
154	6	161	21	191	14	292	48
155	8	361	25	192	16	179	11
156	10	135	12	193	18	78	7
157	12	514	123	194	20	94	10
158	14	296	6	195	TH- 0	34	8
159	16	284	9	196	2	20	6
160	18	178	10	197	4	32	5
161	20	106	8	198	6	9	15
162	TD-E0	35	4	199	8	37	4
163	2	83	6	200	10	34	6
164	4	56	8	201	12	153	8
165	6	263	13	202	14	236	10
166	8	95	9	203	16	307	14
167	10	90	7	204	18	90	12
168	12	247	9	205	20	149	8
169	14	72	10	206	TI- 0	22	7
170	16	282	10	207	2	64	7
171	18	359	8	208	4	31	7
172	20	86	8	209	6	28	7
173	TF- 0	36	8	210	8	22	7
174	2	57	8	211	10	33	12
175	4	37	8	212	12	219	12



Serial No.	Sample No.	Chemical Assay		Serial No.	Sample No.	Chemical Assay	
		Cu ppm	Pb ppm			Cu ppm	Mo ppm
213	14	243	12				
214	16	165	10				
215	18	24	10				
216	20	22	10				
217	TJ- 0	24	9				
218	2	22	7				
219	4	51	8				
220	6	58	8				
221	8	39	8				
222	10	22	7				
223	12	37	10				
224	14	16	10				
225	16	39	10				
226	18	25	10				
227	20	17	12				